FINAL REPORT

A Field Method to Quantify Chlorinated Solvent Diffusion, Sorption, Abiotic and Biotic Degradation in Low Permeability Zones

SERDP Project ER-2533

JUNE 2021

Richelle M. Allen-King
University at Buffalo

Michelle Lorah
U.S. Geological Survey-MD

Daniel Goode
U.S. Geological Survey-PA

Thomas Imbrigiotta
U.S. Geological Survey-NJ

Claire Tiedeman
U.S. Geological Survey-Menlo Park

Allen Shapiro
U.S. Geological Survey-Reston

SERDP
DOD ▪ EPA ▪ DOE

REPORT DOCUMENTATION PAGE

Form Approved
OMB No. 0704-0188

1. REPORT DATE *(DD-MM-YYYY)*	**2. REPORT TYPE**	**3. DATES COVERED** *(From - To)*
30-06-2021	SERDP Final Report	9/15/2015 to 9/15/2020

4. TITLE AND SUBTITLE
A Field Method to Quantify Chlorinated Solvent Diffusion, Sorption, Abiotic and Biotic Degradation in Low Permeability Zones

5a. CONTRACT NUMBER
W912HQ-15-C-0056

5b. GRANT NUMBER

5c. PROGRAM ELEMENT NUMBER

6. AUTHOR(S)
Richelle M. Allen-King, University at Buffalo
Michelle Lorah, U.S. Geological Survey-MD
Daniel Goode, U.S. Geological Survey-PA
Thomas Imbrigiotta, U.S. Geological Survey-NJ
Claire Tiedeman, U.S. Geological Survey-Menlo Park
Allen Shapiro, U.S. Geological Survey-Reston

5d. PROJECT NUMBER
ER-2533

5e. TASK NUMBER

5f. WORK UNIT NUMBER

7. PERFORMING ORGANIZATION NAME(S) AND ADDRESS(ES)

SUNY Research Foundation on behalf of University at Buffalo, 126 Cooke hall, Buffalo, NY, 14214

US Geological Survey Offices: Pennsylvania Water Science Center; Menlo Park; Maryland-Delaware -DC Water Science Center; New Jersey Water Science Center

8. PERFORMING ORGANIZATION REPORT NUMBER
ER-2533

9. SPONSORING / MONITORING AGENCY NAME(S) AND ADDRESS(ES)

SERDP Program Office
4800 Mark Center Drive,
Suite 16F16
Alexandria VA 22350-3600

10. SPONSOR/MONITOR'S ACRONYM(S)
SERDP

11. SPONSOR/MONITOR'S REPORT NUMBER(S)
ER-2533

12. DISTRIBUTION / AVAILABILITY STATEMENT
DISTRIBUTION STATEMENT A. Approved for public release: distribution unlimited.

13. SUPPLEMENTARY NOTES

14. ABSTRACT

The objective of this project is to develop a method, including tools and protocols, for determining the site-specific transport properties of chlorinated volatile organic compounds (CVOCs) in low permeability matrix of fractured sedimentary rock aquifers. In order to achieve the project objective, we developed and tested: 1) a packer tool, 2) a specialized sampling apparatus, 3) a dosing tool (for tracer introduction), 4) a practicable test protocol, and 5) a numerical model capable of simulating the field data.

In an uncased portion of a well, a dual packer system isolates a low permeability test interval that has been exposed to CVOCs. The monitoring data supplies the record of historical exposure of the matrix rock to contamination in the borehole. We initiate a field test by replacing the contaminated groundwater in the test interval with groundwater with the contaminants removed and tracers added. The concentrations of the CVOCs, including degradation products (DPs), and tracers are monitored over time. Simulations are used to estimate the diffusion and sorption coefficients in the matrix, and the biodegradation rate coefficients in the borehole, for the contaminants and DPs.

We present the results of two successful tracer tests in adjacent vertical intervals of the same borehole; the similarity of the parameters estimated indicates good reproducibility for the field conditions of the tests. The parameters estimated from the field tests are also reasonably consistent with supporting laboratory measurements and literature data, verifying the test protocol. A single test provides information equivalent to at least three sets of research-quality independent laboratory tests of the rock properties (a diffusion test, a sorption study, a biodegradation study).

15. SUBJECT TERMS
Diffusion, Sorption, Degradation, Biodegradation, Field test, Diffusion test, Trichloroethene, *cis*-1,2-dichloroethene, Trichlorofluoroethene

16. SECURITY CLASSIFICATION OF:			**17. LIMITATION OF ABSTRACT**	**18. NUMBER OF PAGES**	**19a. NAME OF RESPONSIBLE PERSON**
a. REPORT	**b. ABSTRACT**	**c. THIS PAGE**			Richelle M. Allen
UU	UU	UU	UU	114	**19b. TELEPHONE NUMBER** *(include area code)* 716-777-1461

Table of Contents

List of Tables iii
List of Figures iv
Lists of Acronyms, Chemicals, Dimension, and Mathematical Variables vii
Acronyms vii
Chemical Abbreviations viii
Units and Dimensions viii
Mathematical Variables ix
Keywords x
Acknowledgements x
Abstract 1
Executive Summary (ES) 2
ES: Introduction 2
ES: Method 3
ES: Results 4
ES: Implications and recommendations 6
ES: Contributions to training the next generation of professionals 7
Objective 8
Technical Approach 9
Background 11
Materials and Methods 14
Field site 14
Downhole straddle packer system 20
Hydraulic test 24
Field sampling methods 24
Closed-loop sampling device 24
Closed-loop device sampling procedure 24
Borehole geochemical sampling 25
Tracer test initiation 28
Tracer test completion 30
Contaminant and tracer analysis 31
Simulation method 31
Supporting Laboratory Experiments 35
Sorption 35
Aerobic abiotic TCE:TCFE degradation rate comparison 35
Biodegradation rate measurements 35
Microbial community analyses 37

Results 38
Supporting Laboratory Experiments 38
TCE and TCFE sorption 38
Aerobic abiotic TCE:TCFE degradation rate comparison 40
Biodegradation rate measurements 41
Microbial communities 55
Field Test Results 58
Field Tests in 71BR at 85 and 87 ft depths 58
Parameters estimated 64
Concentration and mass profiles 65
Anaerobic abiotic degradation in matrix 67
Abiotic degradation of sorbed phase 67
Abiotic degradation of dissolved phase 68
Calibrations with abiotic degradation 68
Discussion 71
Comparison between field and independently determined parameters 71
Comparisons between tests: reproducibility 72
Anecdotal comparison to 2015 field observation 74
TCFE tracer 74
Comparing TCE masses and mass transfer rates to potential abiotic degradation rates 74
Conclusions 77
Implications for Implementation/Future Research 78
Contributions to Training the Next Generation of Professionals 79
Literature Cited 81
Appendix A. Supporting Data 87
Appendix A.1: Results of the 07BR-49 test 88
Appendix A.2: Data from the 71BR-87 test 93
Appendix B. List of Scientific/Technical Publications 97
Refereed Journal Articles 97
Technical Reports, including Peer Reviewed Theses and Data Releases 97
Peer-reviewed conference presentations with published abstract 97
Appendix C: Interim Review Questions 99

List of Tables

Table 1. TCE sorption isotherm coefficients for NAWC mudstone samples from the Lockatong. The units on K_f are $((\mu g/kg)/(\mu g/L)^n)$ 38
Table 2. Estimated first-order rate constants and half-lives ($t_{1/2}$) for degradation of TCE and TCFE in microcosms constructed for well sites (a) 07BR and (b) 68BR with groundwater only or groundwater plus the microbial community passively collected by incubation on crushed rock or sand, and with or without the addition of lactate. TCE and TCFE were added together in these microcosms to give combined initial concentrations of 10 to 20 mg/L. 45
Table 3. Estimated zero-order rate constants (ψ) for degradation of TCE and TCFE and first-order rate constants (λ) for production of cDCE in microcosms constructed for well site 71BR with groundwater only or groundwater plus the microbial community passively collected by incubation of sand at a packed interval depth of either 85 ft (71BR-85) or 87 ft (71BR-87) depth. 50
Table 4. Concentrations (in µM) for daughter compounds analyzed at 55 days in triplicate 71BR-87 microcosms amended with TCE and TCFE. Analyses were conducted to assess production of terminal biodegradation products; TCE, TCFE, cDCE, and the DCFEs were not analyzed in these samples. 54
Table 5. Historical and pre-test average concentrations for the 71BR-85 and 71BR-87 tests. 61
Table 6. Simulation and estimated parameters (bold) of the 71BR-85 and 71BR-87 tests are listed. Sorption coefficients for VOCs are estimated by a fixed ratio to the estimated TCE K_d 65
Table 7. Calibrated results (parameters estimated) for cases with abiotic degradation of TCE in the matrix. 69
Table 8. Comparison between parameters for the matrix estimated from the 71BR-85 test and values in published studies for gray mudstones from the NAWC 71
Table 9. Students that participated in project related research at UB. 80

List of Figures

Figure 1. Conceptual diagrams illustrating diffusive mass transfers before (a,b) and during (c) the field test (Allen-King et al. In revision). 9
Figure 2.Selected wells and lithologic unit contacts projected to land surface between major stratigraphic units that dip to the northwest, and line of section A-A' at the field site. Map created by A. Fiore for this report. 15
Figure 3. Cross section along A-A' showing dipping mudstone strata, locations of wells (blue lines), and gamma-ray logs (red lines) for wells 24BR, 07BR, and 71BR. Locations of field tests at 07BR-49 and 71BR-85 are indicated by blue squares. Lacombe (2000) presented the initial NAWC stratigraphy (Lithologic units), and the refined stratigraphy was presented by Lacombe and Burton (2010). The individual unit labels (e.g. GryMas-234) are taken from (Tiedeman et al. 2018). Figure created by A. Fiore for this report. . 16
Figure 4. Geophysical Log data for 07BR. 17
Figure 5. 71BR composite logs. 18
Figure 6. The configuration of packed off intervals in 71BR prior to our tracer tests that were conducted in Zone E, below the deepest packer. Also shown are transmissivity tests for selected borehole intervals. 19
Figure 7. Photographs of selected rock core from 68BR. Blue box in (a) marks in GryMas-234 strata equivalent to the 71BR-85 test interval and red box in (b) marks rock core that are in GryMas-263 strata equivalent to the 07BR-49 test interval. Numbers represent approximate depths of core in situ, in feet. Image created by A. Fiore for this report. 20
Figure 8. Custom-manufactured packer system being lowered into borehole for field testing. A microbial sampler (stainless-steel mesh bag containing inert sand support) is fixed in the test interval between the packers. 22
Figure 9. Photograph and identification of components of downhole test-interval equipment prior to installation in 71BR. The yellow and orange indicate ¼-inch tubes used in the injection of water and tracers and the red and blue are 1/8-inch tubes used to sample. Although Bot-1/8-Red is ¼-inch OD in the test interval, it is 1/8-inch OD from above the top packer to ground surface. 23
Figure 10. Configuration of the closed-loop sampling manifold attached to packer tool (a) and photograph of the sampling device (b). The peristaltic pump is on and the "Center Valve" is open during circulation. The valve is closed during sampling, and the peristaltic pump is run at low speed to fill the sample syringe. The valve separates the manifold into two distinct flow paths: to the left is the replacement side, where sparged makeup water (red) is injected to the bottom of the test interval via Bot-1/8-Red; to the right is the sampling side, where test interval water (blue) is collected from Mid-1/8-Blue. The sample syringe 3-way valve directs flow either from the pump into the sample syringe or from the sample syringe to the sample port. 26
Figure 11. Closed-loop sampling manifold and peristaltic pump during field testing. 27
Figure 12. Nitrogen gas was used to remove VOCs from borehole water in a vented glass 'sparge vessel' cooled with an ice jacket. This water was flushed through the test interval to replace the *in situ* water. 28
Figure 13. Tracer solution in a foil-lined gas-sampling bag. 29
Figure 14. Dosing test interval without volume change by simultaneous injection of concentrated tracer solution into continuous flow (circulation from the test interval) and withdrawal of return flow. 30

Figure 15. Schematic of processes simulated to interpret the field test (a) before and (b) during the field test. Created by Paul Hsieh. 32
Figure 16. Sorption isotherms for TCE for representative samples of NAWC lithologies from 68BR. The sample numbers are the depth, in ft. The sorbed concentrations are normalized by f_{oc}.. The reference line is as described in the text. From Brotsch (2017). 39
Figure 17. The TCE and TCFE sorption isotherms for 68BR-131 are shown. Data are not f_{oc} normalized. Data for TCE from Brotsch (2017) and TCFE from Pugnetti (2018). Solid symbols are used for the TCFE isotherm fit for comparison as described in the text. 40
Figure 18. Concentrations of (a) TCE and (b) TCFE in microcosms constructed with groundwater and the in situ microbial community obtained from passive samplers containing crushed rock incubated in well site 07BR. 44
Figure 19. Estimated first-order rate constants for degradation of TCE compared to those for degradation of TCFE in microcosms constructed with the in situ microbial community and groundwater from the indicated well sites. Attached in situ microbial communities were obtained from passive samplers containing crushed rock, except for a second microcosm for well site 07BR constructed with incubated sand. 46
Figure 20. Concentrations of (a) TCE and (b) TCFE in microcosms constructed for well site 71BR with groundwater only or groundwater plus the microbial community passively collected by incubation of sand at a packed interval depth of 85 ft (71BR-85). 51
Figure 21. Concentrations of (a) DCE and (b) DCFE in microcosms constructed for well site 71BR with groundwater only or groundwater plus the microbial community passively collected by incubation of sand at a packed interval depth of 85 ft (71BR8571BR-8571BR85). 52
Figure 22. Possible anaerobic biodegradation products of TCFE (after Hageman et al. 2001) ... 53
Figure 23. TCFE degradation in microcosms amended with the groundwater and microbial community passively collected by incubation on sand at a depth of 87 ft in 71BR. TCFE concentrations (in triplicate bottles) decreased (purple) as degradation product compounds concentrations increased (combined *z*DCFE and *e*DCFE concentration shown, green). Yellow line shows production of 1,1CFE and *z*CFE combined. TCFE in killed controls is shown in blue. The error bars are 1σ. Initial concentrations of TCFE and (*z*+*e*)DCFE are estimated. The initial (*z*+*e*)DCFE is the concentration measured 24 hr before the second addition of TCFE. The initial TCFE concentration is estimated as the sum of the observed concentrations of TCFE, *z*DCFE and *e*DCFE at 18 hour, the first measurement following the second TCFE addition. Measurement of the CFEs began at 72 hr. 54
Figure 24. Microbial community composition at the order level in passive microbial samplers incubated in borehole 07BR, including samplers containing crushed rock and sand samplers that were placed adjacent to one another above the packed interval and a third sampler containing sand that was incubated within the packed interval. 56
Figure 25. Microbial community composition at the family level in a sand microbial sampler incubated in the packed interval during the field test in 71BR-87 (in situ) compared to compositions over time in microcosms constructed with sand from the 85 ft depth in 71BR-87 and amended with (a) moderate concentrations of TCE and TCFE and (b) high concentrations of TCE and TCFE at day 0. The microcosm treatments correspond to 71BR-85-SA-TCFE and 71BR-85-SA-highTCFE in Table 3. 57

Figure 26. The TCE and DPs concentrations for borehole 71BR-E (zone E) from drilling to the start of the test at 87 feet. Note that the pre-test concentration for the 71BR-85 test is nearly double that of the 71BR-87 test. The periods used for the reported average concentrations and periods when the P&T pump in 15BR was off are also noted. After (Allen-King et al. In revision)..... 60
Figure 27. Nonreactive Br tracer concentrations with time during the a) 71BR-85 and b) 71BR-87 tests, respectively. 62
Figure 28. Sorbing and biodegradable tracer TCFE concentrations during test 71BR-85. Discussion about the degradation product is later in the text. 63
Figure 29. The TCE, cDCE and VC concentrations during the a) 71BR-85 and b) 71BR-87 test. Note the difference in TCE concentration scale between panels..... 64
Figure 30. Simulated TCE and DP concentration profiles in the matrix at the start (t=0 days) of each of the two tests: (a) 71BR-85, (b) 71BR-87. Note the difference in vertical axis scale. Panel (a) from (Allen-King et al. In revision)..... 66
Figure 31. Simulated abiotic degradation product accumulation during test 71BR-85. In the D or S case, abiotic degradation of only the dissolved or sorbed phases occurs, respectively. The maximum concentration of ADP for dissolved degradation is 1.0µg/L. 70
Figure 32. The TCE degradation rate during the 71BR-87 test. 73
Figure 33. The simulated VOC matrix mass (a) and rate of mass diffusion from the matrix (into the borehole) (b) during the 71BR-85 test. All quantities are calculated for the entire borehole interval and surrounding matrix. In panel (b), negative numbers indicate diffusion into the matrix from the borehole. 76

Lists of Acronyms, Chemicals, Dimension, and Mathematical Variables

Acronyms

ADP	Abiotic degradation products of TCE produced under anaerobic conditions; these are ethene, ethane, and acetylene
BAT^3	Multifunction bedrock-aquifer transportable testing tool
Bot	Bottom of the test interval
cm	Centimeter
CVOC	Chlorinated volatile organic compound (for example TCE, cDCE, VC)
DELCD	Dry electrolytic conductivity detector (GC)
DNA	Deoxyribonucleic acid
DO	Dissolved oxygen
DOC	Dissolved organic carbon
DP	Degradation products
EPA	United States Environmental Protection Agency
ER	Environmental Restoration
FID	Flame ionization detector (GC)
foc	Fraction organic carbon
GC	Gas chromatograph
GC/MS	Gas chromatograph mass spectrometer
LHG	Light hydrocarbon gas
Mid	Middle of the test interval
NA	Natural attenuation
NAWC	Naval Air Warfare Center
NJ	New Jersey
OD	Outer diameter
PEST	Code for model-independent parameter estimation and uncertainty analysis
PVC	Polyvinyl chloride
SERDP	Strategic Environmental Research and Development Program
SRI	SRI Instruments (www.srigc.com)
SS	Stainless steel
UB	University at Buffalo, The State University of New York
USGS	United States Geological Survey

VOC	Volatile organic compound (for example, TCE, cDCE, VC)
WBC-2	Mixed culture of anerobic bacteria and methanogens

Chemical Abbreviations

Br	Bromide
cDCE	*cis*-1,2-dichloroethene
CO_2	Carbon dioxide
DCFE	Dichlorofluoroethene
*e*CFE	(*E*)-1-chloro-2-fluoroethene
*e*DCFE	(*E*)-1,2-chloro-2-fluoroethene
FE	Fluoroethene (vinyl fluoride)
N_2	Nitrogen
rRNA	Ribosomal ribonucleic acid
TCE	Trichloroethene
TCFE	Trichlorofluoroethene
VC	Vinyl chloride
*z*DCFE	(Z)-1,2-chloro-2-fluoroethene

Units and Dimensions

µg	Microgram
µL	Microliter
µM	Micromolar
ft	Feet
kg	Kilogram
l	Length
L	Liter
m	Meter
M	Molar
mg	Milligram
min	Minute
mL	Milliliter
s	Seconds

Mathematical Variables

A	Zeroth order biodegradation rate
B	Production rate of a species
C	Dissolved concentration in the rock matrix
C^*	Dissolved concentration in the borehole
C_s	Sorbed concentration
D	Effective diffusion coefficient
D^o	Free water diffusion coefficient
h	Height of the test interval
i	Subscript indicates chemical species
K_d	Sorption distribution coefficient, C_s/C
K_f	Freundlich sorption coefficient
K_{oc}	Sorption distribution coefficient normalized by the f_{oc}
n	Freundlich isotherm slope
r	Radial distance from the center of the borehole
R	Retardation factor
r_w	Radius of borehole
t	Time
V	Volume of water in the borehole interval
θ	Matrix porosity
λ	First-order biodegradation rate
Λ	first-order abiotic degradation rate constant for the dissolved phase
$\overline{\Lambda}$	first-order abiotic degradation rate constant for the sorbed phase
ρ_b	Bulk density of the rock matrix
τ	Tortuosity factor
ψ	Zeroth order biodegradation rate coefficient

Keywords

Diffusion, Sorption, Degradation, Biodegradation, Field test, Diffusion test, Trichloroethene, *cis*-1,2-dichloroethene, Trichlorofluoroethene

Acknowledgements

We appreciate the laboratory and experimental support supplied by the following former UB undergraduate students: Hannah Annunziata, Matt Buzzeo, Rory Dishman, Kassandra Kimmie, Virginia Cistaro, and Katie Tresino. USGS student interns Carol Morel and Jessica Teunis provided much appreciated assistance with microcosm experiments. We appreciate support in sample collection and/or packer installation from USGS interns Christopher L. Leach, Savannah A. Miller, Jeremy R. Patterson, Rebecca A. Talbot, and Matthew A. Pronshinske. We received assistance to install the packers from USGS employee Rob Rosman. We had helpful discussions about the experiment design and sampling methods with USGS employees Gary Curtis and Karl Hasse. The efforts of all of these USGS staff are greatly appreciated.

Abstract

Introduction and Objectives. The objective of this project is to develop a method, including tools and protocols, for determining the site-specific transport properties of chlorinated volatile organic compounds (CVOCs) in low permeability zones in fractured sedimentary rock aquifers.

Technical Approach. In an uncased portion of a well, a dual packer system isolates a low permeability test interval that has been exposed to CVOCs. The monitoring data supplies the record of historical exposure of the matrix rock to contamination in the borehole. We initiate a field test by replacing the contaminated groundwater in the test interval with groundwater with the contaminants removed and tracers added. The concentrations of the CVOCs, including degradation products (DPs), and tracers are monitored over time. Simulations are used to estimate the diffusion and sorption coefficients in the matrix, and the biodegradation rate coefficients in the borehole for the contaminants and DPs.

In order to achieve the project objective, we developed and tested: 1) a packer tool, 2) a specialized sampling apparatus, 3) a dosing tool (for tracer introduction), 4) a practicable test protocol, and 5) a numerical model capable of simulating the field data. We completed laboratory experiments on individual processes (e.g. sorption, biodegradation) against which to evaluate the parameters estimated from the field test.

Results. We present the results of two successful tracer tests in adjacent vertical intervals of the same borehole; the similarity of the parameters estimated indicates good reproducibility for the field conditions of the tests. The parameters estimated from the field tests are also reasonably consistent with supporting laboratory measurements and literature data, verifying the test protocol.

Benefits. The test simultaneously determines CVOC transport parameters needed to model back diffusion from low permeability sedimentary rock in situ. The information gained is suitable for both enhancing site conceptual models and conducting simulation analysis of field conditions. A single test provides information equivalent to at least three sets of research-quality independent laboratory tests of the matrix properties (a diffusion test, a sorption study, a biodegradation study). Further development of the test procedure is needed to broaden its applicability; this is best achieved through application to additional field site(s) with contrasting field properties to the test site.

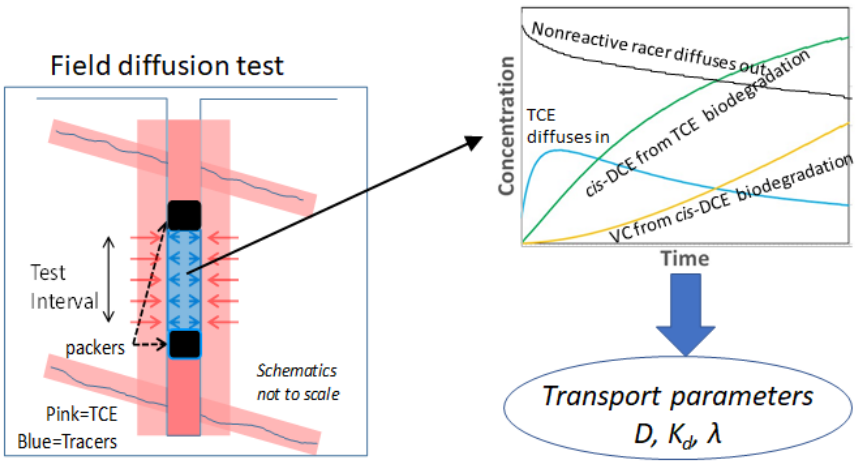

Executive Summary (ES)

ES: Introduction

The objective of this project is to develop a method, including tools, protocols and interpretive method, to determine the site-specific transport properties of chlorinated volatile organic compounds (CVOCs) in low permeability zones in fractured sedimentary rock aquifers. The field and interpretive method responds to the ER-15 Statement of Need (SON) in three ways:

1. The field method determines diffusion coefficients and sorption coefficients in low-permeability zones for use in long-term simulations and predictions of the fate of contaminants. This addresses a limitation in the current state of practice that focuses on characterization that is biased towards high-permeability zones, while long-term attenuation will be ultimately controlled by release of contaminants from low-mobility zones. These parameters can be used in commonly-used models of natural attenuation.
2. Direct measurement at the field scale of back diffusion, including retardation by desorption, in low-mobility zones during testing of the field method will improve current understanding of these processes without the confounding effects of mixing induced by high-permeability zones.
3. The numerical simulation tools that we develop and specifically design to interpret parameters from the field tests are documented and available for application.

In an uncased portion of a well, a dual packer system isolates a low permeability test interval that has been exposed to CVOCs. The monitoring data supplies the record of historical exposure of the matrix rock to contamination in the borehole. We initiate a field test by replacing the contaminated groundwater in the test interval with groundwater with the contaminants removed and tracers added (Figure ES- 1). The concentrations of the CVOCs, including degradation products (DPs), and tracers are monitored over time. Simulations are used to estimate the diffusion and sorption coefficients in the matrix, and the biodegradation rate coefficients in the borehole for the contaminants and DPs.

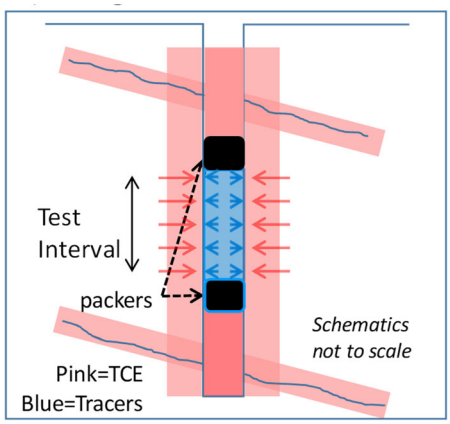

Figure ES- 1 Conceptual diagram illustrating diffusive mass transfers during the field test (from Allen-King et al. In revision). TCE is trichloroethene.

ES: Method

In order to achieve the project objective, we developed and tested: 1) a packer tool (Figure ES- 2), 2) a specialized sampling apparatus, 3) a dosing tool (for tracer introduction), 4) a practicable test protocol, and 5) a numerical model capable of simulating the field data. We completed laboratory experiments on individual processes (e.g., sorption, biodegradation) against which to evaluate the parameters estimated from the field test.

Figure ES- 2. Custom-manufactured packer system being lowered into borehole for field testing. The tool is fabricated to minimize reaction between the contaminants and test materials; all tubing is stainless steel and the packer bladders are constructed of viton. A microbial sampler (stainless-steel mesh bag containing inert sand support) is fixed in between the packers and will be exposed in the test interval.

We interpret the test data using a numerical model specifically created for this project. The processes simulated by the model are illustrated in Figure ES- 1. Transport in the matrix is governed by radial diffusion with retardation from linear, equilibrium sorption. Biodegradation occurs from the well-mixed borehole water. It is necessary to simulate the historical exposure period, characterized by monitoring data, when the matrix takes up the contaminants, as well as

the test period. Parameter estimation uses inverse modeling to provide a best fit of the model to the data including the monitoring data and the test results.

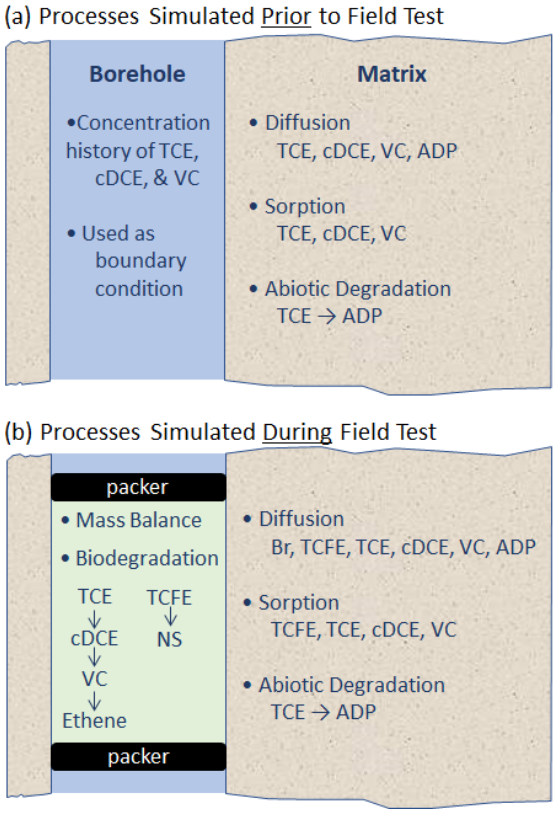

Figure ES- 3. Schematic of processes simulated to interpret the field test (a) before and (b) during the field test. Created by Paul Hsieh.

ES: Results

The data from test 71BR-87 (borehole 71BR at 87 feet below ground surface) are shown in Figure ES- 4. This is one of three sets of test results presented in the report. The borehole was drilled approximately 11 years prior to the test and the matrix rock in the test interval was exposed to a historical average trichloroethene (TCE) concentration of 10,700 µg/L. To start the test, we remove the CVOC from the test interval water and added the nonreactive tracer, bromide (Br). The Br concentration declined during the test. (Data shown in main text). The TCE concentration increased during the initial 10 days of the test, then declined following an approximately 10-day long plateau. The TCE plateau concentration near 2000 µg/L is only 20% of the concentration in the pre-test water samples that are collected from the test interval prior to the test. The *cis*-1,2-dichloroethene (cDCE) concentration is increasing throughout the test and surpasses the historical and pretest concentrations of approximately 2,000 µg/L in approximately one month (30 days). The cDCE concentration rises throughout the test to >4,000 µg/L at the end (136 days). The vinyl chloride (VC) concentration is also increasing, but is orders of magnitude lower than the cDCE concentration. In addition to diffusion from the matrix to the borehole, rapid TCE biodegradation is an important process in the test. This along with slow cDCE biodegradation leads to cDCE accumulation in the borehole.

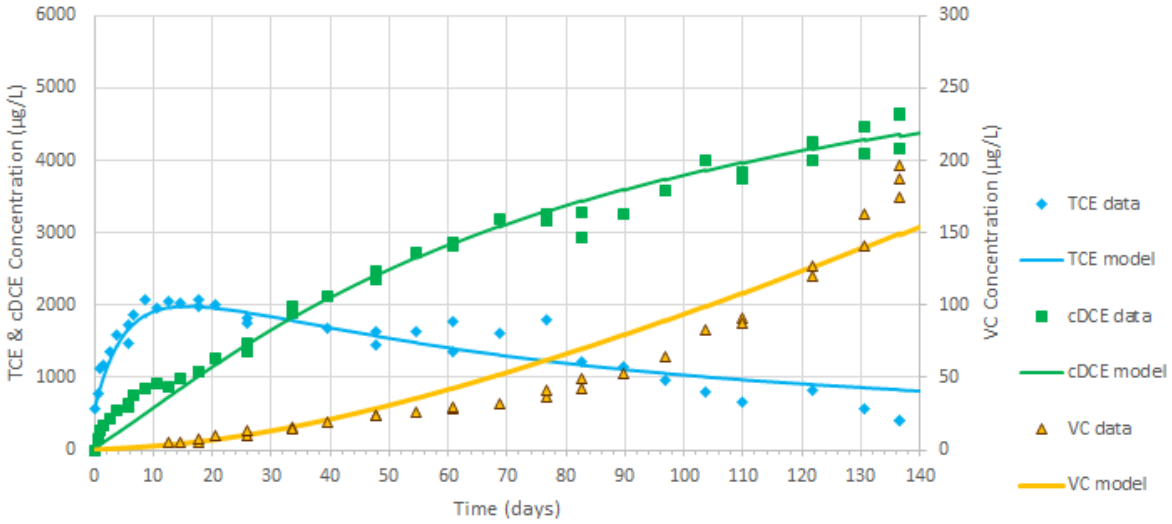

Figure ES- 4. The CVOC concentrations sampled in the middle of the test interval over time during test 71BR-87, (from Allen-King et al. In revision)

The model calibrated to the test data are also shown in Figure ES- 4. Calibration of the numerical model to the test data and borehole concentration history estimates the transport and biodegradation coefficients: these are the tortuosity factor, the TCE sorption coefficient in the matrix, and the rates of TCE and cDCE biodegradation in the borehole. The diffusion coefficients and sorption coefficients for the TCE degradation products are related to the TCE values using physical chemistry data to help constrain the simulations while limiting the number of parameters simulated.

We evaluated the test results in two ways; we compared the calibrated parameters to data from independently measured laboratory data, and we conducted near replicate tests in vertically adjacent sections of the same borehole. Comparisons to independent laboratory experiments show that the estimated parameters are reasonable for similar lithology at the field site. The pre-test TCE concentrations differed by a factor of two which appears to have a significant influence on the TCE biodegradation. The ratio of the maximum TCE biodegradation rates is similar to the pre-test TCE concentration ratio for the two tests; however, we found that the two tests were best fit by different TCE biodegradation kinetic forms (first-order order versus zeroth order).

The similarity between biodegradation rates and sorption coefficients estimated from the laboratory experiments and field tests also indicates that such laboratory tests can be useful methods for estimating these field parameters. The biodegradation microcosm tests used here included water and media that were preconditioned in situ and were thus likely to be populated with the same microbial population as those present in the borehole during the field experiment.

The very fast TCE biodegradation rate in the borehole, up to 1.16 µM/day, has a significant influence on the results in our tests. Although determining the biodegradation rate coefficient and kinetic form in the borehole is not the primary objective of the project because

these are not matrix properties, it was necessary in order to determine the matrix transport properties.

We call the vertically adjacent tests “near replicate” because it is not possible to conduct replicate tests. Importantly, the matrix parameters estimated from the near replicate field tests are similar. The similarity of the tortuosity factors (not different) and TCE sorption coefficients (within a factor of two) support the field test and interpretation method.

We did not observe ADPs in our field tests. Through simulation analysis we show that abiotic degradation of TCE in the dissolved phase at a rate consistent with previous laboratory experiments would be consistent with the field test results, although the ADP concentrations would be below our quantitation limit. Our simulations also show that a much faster abiotic degradation rate would produce unreasonable parameter estimates. Our results suggest the hypothesis that abiotic degradation is of low importance to TCE in the matrix when sorption is high.

ES: Implications and recommendations

The field test method is fully documented in this report and accompanying cited work; these products enable the test to be implemented by experienced technical personnel to a field site similar to the NAWC. The site-specific information gained is equivalent to the results of multiple laboratory studies. The test provides one tool towards filling the gap of limited field methods to collect transport parameters from low permeability zones

We provide model simulations using the site-specific parameters from the field test to illustrate how the test findings can be used to enhance understanding of contaminant distribution and transport at a field site. For one example, the concentration profile simulations indicate that after a decade of exposure from the borehole, most TCE mass was located within 5 cm of the matrix-borehole interface (Figure ES- 5). Additional simulations calculate the masses in the rock matrix, the rate of back diffusion (or mass release) from the rock matrix. We use simulations to conduct a preliminary analysis of the potential significance of abiotic TCE degradation. Hence, this report demonstrates how site-specific information gained from a field test can be used to improve site understanding to inform remediation and/or management.

Additional research is needed to develop the test for application to a broader range of field sites with transport properties that differ from the NAWC. The NAWC has a relatively high mass transfer rate from the matrix to the borehole because of the rock properties and because rapid biodegradation maintains a high gradient. Whether a field test will be successful is site specific and depends on the borehole properties, analysis method, and tool configuration, in addition to the site-specific matrix transport properties and biodegradation rate in the borehole. Application to additional sedimentary rock field site(s) is the next step in broadening the applicability of the test.

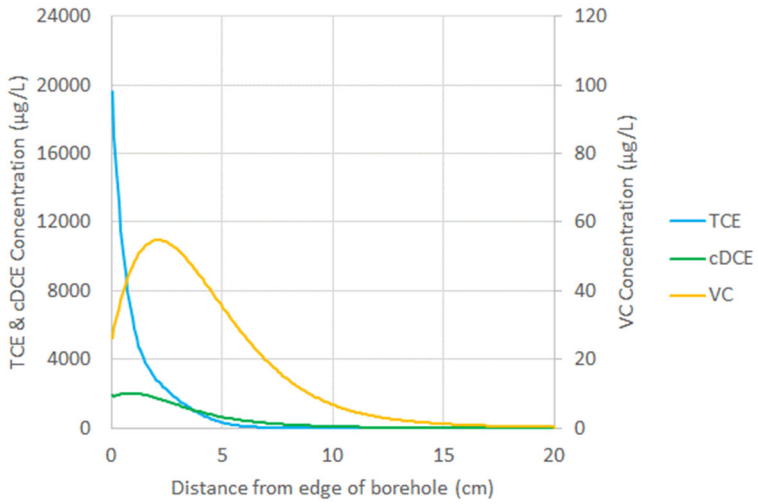

Figure ES- 5. Simulated TCE, cDCE, and VC concentration profiles in the matrix at the start (t=0 days) of test 71BR-85, from (Allen-King et al. In revision)

ES: Contributions to training the next generation of professionals

This SERDP project created a platform for training for 5 graduate and 6 undergraduate students through participating in research at University at Buffalo. Six (of 10 total) students are women who earned degrees in fields where women are underrepresented including Geology, Environmental Engineering and Geological Engineering. Four of the students have completed, or are in the process of completing, an additional degree in a STEM (science, technology, engineering and math) field. This project contributed to the education and advancement of well-trained professionals into environmentally and technically focused STEM professional positions. It also contributed to broadening participation of women in STEM fields in the professions. Although this aspect of productivity is often not underscored in project reports, it is an important product of the SERDP program.

Objective

Contaminants retained in low permeability zones, in either the dissolved or sorbed phases, are released to permeable pathways by desorption and back diffusion and can sustain elevated contaminant concentrations in mobile groundwater. The rates and magnitudes of competing processes – retardation (by sorption), diffusive transport, abiotic and/or biotic degradation reactions – exert a strong control on long term contaminant fate. Knowledge of the rates of both diffusion and biogeochemical transformation are crucial for accurate predictive modeling that leads to effective site management, including the ability to make decisions among remedial options. General scientific knowledge about attenuation processes, and their importance to the long-term behavior of contaminant plumes, is well established. However, field methods that simultaneously quantify these co-occurring processes in low permeability media are limited.

The project objective is to develop and test a field method capable of concurrently quantifying site specific chlorinated volatile organic compound (CVOC) diffusion and degradation rates and sorption coefficients in low permeability zones. The test will evaluate these processes by interrogating low permeability media exposed within an isolated interval of a sedimentary rock borehole that has been exposed to contamination. The project includes evaluation of the field method. Hence, the test method we present here is a field and interpretive package that includes:

- The packer and sampling apparatus - development of a downhole testing system for isolating a borehole or well interval and perturbing and sampling the constituent concentrations in the interval;
- The borehole field test protocol – a test protocol and monitoring strategy;
- The test analysis procedure – an approach for using inverse modeling of the data collected to estimate parameters that characterize the natural attenuation (NA) processes within the low-permeability media;
- Supporting laboratory experiments - to fill knowledge gaps that would otherwise hinder field data interpretation.

The field and interpretive method responds to the ER-15 Statement of Need (SON) in three ways. 1) The field method is capable of determining diffusion coefficients, sorption coefficients, and reaction rate parameters in low-permeability zones for use in long-term simulations and predictions of the fate of contaminants. This addresses a limitation in the current state of practice that focuses on characterization that is biased towards high-permeability zones, while long-term attenuation will be ultimately controlled by release of contaminants from low-mobility zones. These parameters can be used in commonly-used models of NA. 2) Direct measurement at the field scale of back diffusion, desorption, and degradation in low-mobility zones during testing of the field method will improve current understanding of these processes without the confounding effects of mixing induced by monitoring wells open to high-

permeability zones. 3) Numerical simulation tools developed and specifically designed to interpret parameters from the field tests, as well as the estimation methodology, are documented for application.

We selected the former Naval Air Warfare Center (NAWC) site, West Trenton, NJ, for this project because it is a well-characterized field setting for tool development. The existing infrastructure and biogeochemical information facilitate borehole selection for field tests and validation of the test method. Extensive characterization of trichloroethene (TCE) contamination in the fractured-porous sedimentary rocks at NAWC includes measurements of all the subject processes considered by the proposed project, albeit not all at comparable scales or simultaneously under *in situ* conditions

This project is a collaboration between researchers at University at Buffalo (UB) and U.S. Geological Survey (USGS) staff members. The USGS collaborators are: Daniel Goode, Paul Hsieh, Michelle Lorah, Allen Shapiro, Claire Tiedeman, Thomas Imbrigiotta, Pierre Lacombe, and Alex Fiore. In addition to the principle investigator, former graduate students Rebecca Kiekhaefer, Mary Masse, Michele Pugnetti, Jonathan Brotch, and current student Hannah Annunziata made substantial contributions to the project.

Technical Approach

Our conceptual model of the processes occurring prior to and during the field test is illustrated in Figure 1. Prior to borehole drilling, contaminants migrate in permeable connected fractures and diffuse into the rock matrix. Borehole drilling intercepts contaminant flow in fractures allowing contaminants to flow into the borehole and diffuse into the adjacent rock matrix. We use the borehole's contaminant monitoring history to establish the initial condition for the test. We conduct a test by isolating a section of low permeability rock matrix using a dual packer system, and perturbing borehole water quality by removing the contaminant and its degradation products (DPs) and adding tracer(s). The concentrations of the contaminant and tracer(s), and

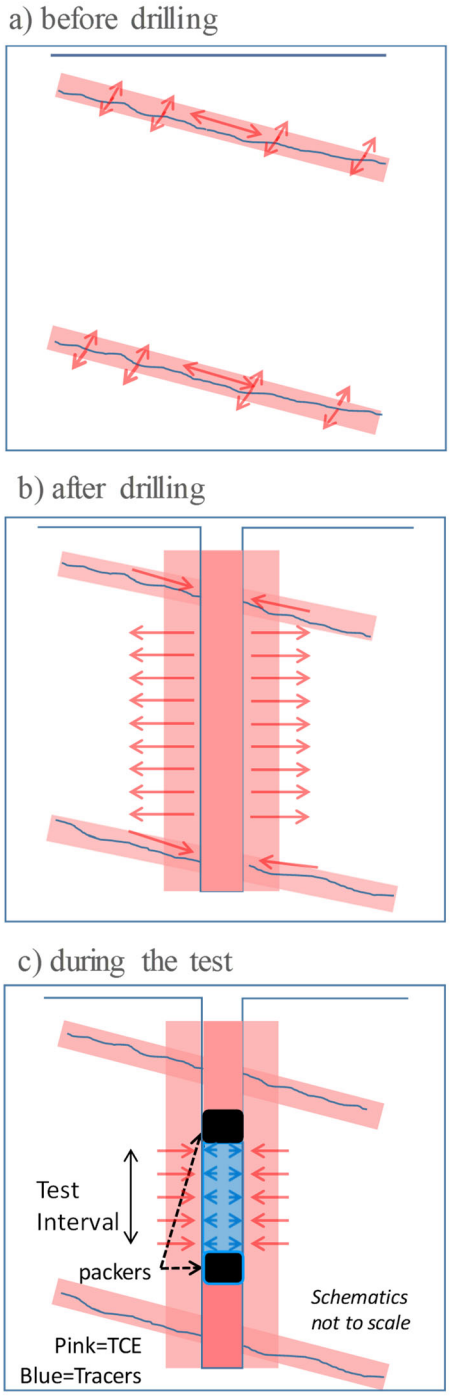

Figure 1. Conceptual diagrams illustrating diffusive mass transfers before (a,b) and during (c) the field test (Allen-King et al. In revision).

their DPs, are monitored over time. The data are analyzed using a numerical model that simulates multi-species transport processes and reactions (e.g. diffusion, sorption, abiotic and biotic reactions) to yield estimates of the rates and coefficients controlling attenuation processes occurring in the low-permeability media.

This report presents results from field tracer tests that demonstrate how the field and interpretive method simultaneously measure *in situ* diffusion and sorption in the matrix, and biodegradation in the borehole. A numerical model is calibrated to the historical borehole concentration data and test results to estimate the unknown transport parameters. Comparison between the calibrated parameters and the results of independent laboratory experiments demonstrate that the extracted parameters are reasonable. Inclusion of abiotic degradation in the numerical model allows exploration of the potential effect of this process. Supporting information on the microbial populations carrying out TCE biodegradation are presented. We use the numerical model and parameters estimated from the field tests to illustrate site-specific insights that can be drawn from these types of measurements.

Background

The retention and release of contaminants in flow-limited regions of aquifers can be viewed as either a "blessing" or a "curse" in managing groundwater at contamination sites. Diffusion of contaminants into the void space of low-permeability zones delays the arrival and reduces peak contaminant concentrations in groundwater advected downgradient. Sorption onto solid surfaces in these zones will retain contaminant mass over long time frames, thus further reducing downgradient contaminant migration. The processes of diffusion and sorption, however, also serve as significant impediments to achieving groundwater remediation objectives. Remediation technologies that rely on groundwater flushing or the introduction of amendments to contact aqueous phase contamination are unlikely to access groundwater in flow-limited regions. Diffusive release of contaminants from low-permeability zones essentially acts as a spatially distributed, long-term contaminant source. The retention of contaminants on solid surfaces in these zones further extends the temporal persistence of the contamination.

Regardless of whether low-permeability aquifer materials are viewed in the context of being a "blessing" or a "curse" in the management of contaminated groundwater, quantifying diffusion and sorption in flow-limited regions is critical in defining remedial objectives and actions. Accurately quantifying contaminant fluxes into and out of low-permeability zones must also account for processes that transform contaminants, such as biotic and abiotic transformations in low-permeability zones and/or at the interface between these zones and permeable groundwater flow paths. The processes of diffusion, sorption, and biotic and abiotic transformations in aquifers have been extensively discussed in the contaminant hydrogeology literature. Laboratory experiments have been widely used to identify the magnitude of these processes and quantify their associated parameters, and some field studies have been conducted. Bradbury and Green (1985), Krom and Berner (1980), Novakowski and van der Kamp (1996), Boving and Grathwohl (2001), and Ibaraki (2001) describe methods of estimating the effective diffusion coefficient of solutes on centimeter-size samples of low-permeability geologic materials. The magnitude of the parameters defining diffusion processes in low-permeability geologic materials at the laboratory-scale, however, may not be consistent with the manifestation of these processes at the field scale (Becker and Shapiro 2000, Shapiro 2001b). For example, Zhou et al. (2007) conducted a survey of field-scale chemical transport experiments showing the disparity between laboratory and field estimates of diffusion in low permeability media. Differences were attributed to the variability in formation properties and mass-transfer processes in heterogeneous materials that behave analogously to diffusion over physical dimensions larger than laboratory-scale specimens.

Retarded diffusion of CVOCs, including TCE, has been well documented for fine-grained, unlithified low permeability sediments in both laboratory (e.g., Barone et al. 1992, Myrand et al. 1992, Young and Ball 1998) and field studies (Ball et al. 1997a, Johnson et al. 1989, Parker et al. 2004). The process of retarded diffusive transport (diffusion and sorption) of CVOCs into the sedimentary rock matrix from high permeability pathways is conceptually similar to that which occurs in unlithified materials. In addition to causing retardation, sorption both increases mass storage capacity of the media and reduces the rate of degradation reactions. It has long been realized that molecules sorbed to nonreactive geologic materials are not available for reactions (Allen-King et al., 2002).

The literature further suggests that the fraction of TCE sorbed is expected to be high. Most low permeability sedimentary units are either fine grained (e.g. silt and clay) aquitards or

lithified sedimentary rock, both of which are associated with relatively high TCE sorption. Because they are deposited in low energy environments, silt and clay units generally accumulate a greater fraction organic carbon content (f_{oc}) compared to sand and gravel. And, it is well known that f_{oc} preservation is enhanced in fine-grained, compared to coarse-grained, units. The burial and heating that cause lithification result in reduced porosity and organic matter diagenesis. thermal alteration of organic matter in sedimentary rocks that occurs during burial and diagenesis increases its affinity to sorb CVOCs (e.g., Allen-King et al. 2002).

Abiotic and biotic TCE degradation reactions follow different pathways that result in differences in intermediate products. The abiotic reaction occurs through beta-elimination that generates chloroacetylene and acetylene as the primary intermediate products (Lee and Batchelor 2002) whereas biodegradation results in primarily *cis*-1,2-dichloroethene (cDCE) and vinyl chloride (VC) intermediates (Bradley 2000).

Similar zero-order TCE and trichlorofluoroethene (TCFE) degradation rates (within a factor of 0.3 to 2.0) were measured in groundwater microcosms when comparable initial TCFE and TCE concentrations were used (Vancheeswaran et al. 1999), although TCFE was transformed 6 to 25 times faster than TCE in push-pull tests when injected TCFE concentrations were 20 times higher than TCE (Hageman et al. 2001). The higher TCFE biodegradation rates may be due to its higher concentration (Hageman et al. 2001). Analogous fluorine-containing DPs were observed for TCFE compared to TCE biodegradation, and the ratio of *cis*-dichlorofluoroethene (or (*Z*)-1,2-choloro-1-fluoroethene) (*z*DCFE) to *trans*-dichlorofluoroethene (or (*E*)-1,2-choloro-1-fluoroethene) (*e*DCFE) was similar to that of cDCE to *trans*-1,2-dichloroethene.

Consistent with expectations based on their very similar physicochemical properties (e.g. solubility, molecular size), field testing has also demonstrated similar TCE and TCFE retardation (Field et al. 2005). However, prior research to determine the abiotic degradation rate and product distribution from TCFE is limited to a single field test that evaluated TCFE in the presence of zero valent iron (emplaced as a remediation treatment). To employ TCFE as a tracer in the proposed project, there is a need for information about its abiotic degradation rate and product distribution as a consequence of reaction with reduced iron minerals, such as pyrite.

Field experiments to quantify these attenuation and transformation processes in low-permeability zones can be confounded by advective groundwater flow and chemical transport in higher-permeability zones. To quantify these processes in low-permeability zones, explicit knowledge or assumptions of the groundwater flow regime is required. Uncertainty in groundwater velocity in permeable regions may mask attenuation processes in the low-permeability regions. To avoid interferences that may arise from chemical advection, Gebrekristos et al. (2008) conducted an in situ chemical diffusion experiment in sections of a borehole that were unaffected by chemical advection and quantified the diffusion coefficient of chloride. The method we developed builds on that of Gebrekristos et al. (2008), and quantifies contaminant sorption and degradation in addition to diffusion. Conducting this type of in situ test to isolate these processes and identify critical parameters controlling their magnitude in low-permeability zones is important for quantifying these processes in the design and implementation of remediation objectives.

To analyze concentration data from in situ experiments and estimate diffusion and transformation rates in low-permeability zones, analytical or numerical models are typically

used. Field experiments that involve advective transport in high-permeability zones as well as diffusive transport in low-permeability zones need to be analyzed with dual-domain types of models that account for the interacting transport processes in the domains with mobile and immobile groundwater (e.g., Shapiro et al. 2008, Mukhopadhyay et al. 2013, Willmann et al. 2013). In contrast, during the borehole test method that we propose to develop, chemical transport will occur only in the low-permeability zone that is isolated within an open borehole. Therefore, much simpler conceptual and simulation models of the subsurface are appropriate, whereby advection is absent and chemical transport is controlled by diffusion.

Materials and Methods

Field site

The NAWC, West Trenton, N.J. field site was chosen for this study because of extensive prior laboratory and field studies of the physical and biogeochemical processes affecting CVOC behavior (Bradley et al. 2009; Brotsch 2017; Chapelle et al. 2012; Lacombe 2011; Révész et al. 2014; Schaefer et al. 2015; Shapiro et al. 2018). Field tests indicate that the permeability of the unfractured mudstone of the Lockatong Formation is low, and often below detection (Goode et al. 2014; Tiedeman et al. 2018), and thus diffusion is the primary contaminant migration mechanism in the unfractured rock.

Field testing was conducted in boreholes at NAWC (Figure 2). Jet-engine testing at NAWC resulted in dense non-aqueous phase liquid TCE, and dissolved TCE, cDCE, and VC, with lower concentrations of other volatile organic compounds, in groundwater (Lacombe 2000). Analysis of bulk concentrations in core show that most CVOC mass in the aquifer is associated with the rock matrix (Goode et al. 2014), and not in flowing water in fractures. A pump and treat (P&T) system operating since the mid-1990's has contained CVOCs in groundwater within the site boundary, but concentrations are only gradually declining (Lacombe 2011), as has been observed at many fractured-rock CVOC-contaminated sites (Steimle 2002; National Academies of Sciences 2015).

The two wells tested, 07BR and 71BR, are 6-inch boreholes with steel casing over the shallow weathered rock and then uncased (open) over the dipping mudstone strata of the Lockatong Formation. The Lockatong Formation is primarily composed of three types of mudstones: light gray or red massive mudstones, medium gray to dark gray laminated mudstones, and carbon-rich dark gray to black fissile mudstones. The massive units are generally the least fractured units, and typically correspond to the low permeability zones, whereas the fissile units are most easily fractured and most transmissive (Lacombe 2000). The two tests are in two different massive units (Figure 3).

Well 07BR was drilled by contractors for the U.S. Navy as a monitoring well during early investigations of site contamination (Lacombe, 2000, 2002). The 6-inch diameter well is 53 ft (11.6 m) deep and has steel casing to a depth of 38 ft (16.2 m). Available geophysical logs include caliper, acoustic televiewer, optical televiewer, flow meter, induction, conductance, resistivity, temperature, deviation, and slug testing (Figure 4, U.S. Geological Survey, 2020; Fiore, 2014).

Borehole 71BR, used for our tests, has a 6 inch diameter in the open portion of the borehole. Geophysical characterization, shown in Figure 5, was completed soon after drilling (Kiekhaefer 2018, p. 160; U.S. Geological Survey, 2020). Figure 6 shows the packer configuration in the borehole prior to our tests. Between our tests, we installed a packer at the depth of the completed tracer test. Figure 7 shows rock core from the strata as our field tests.

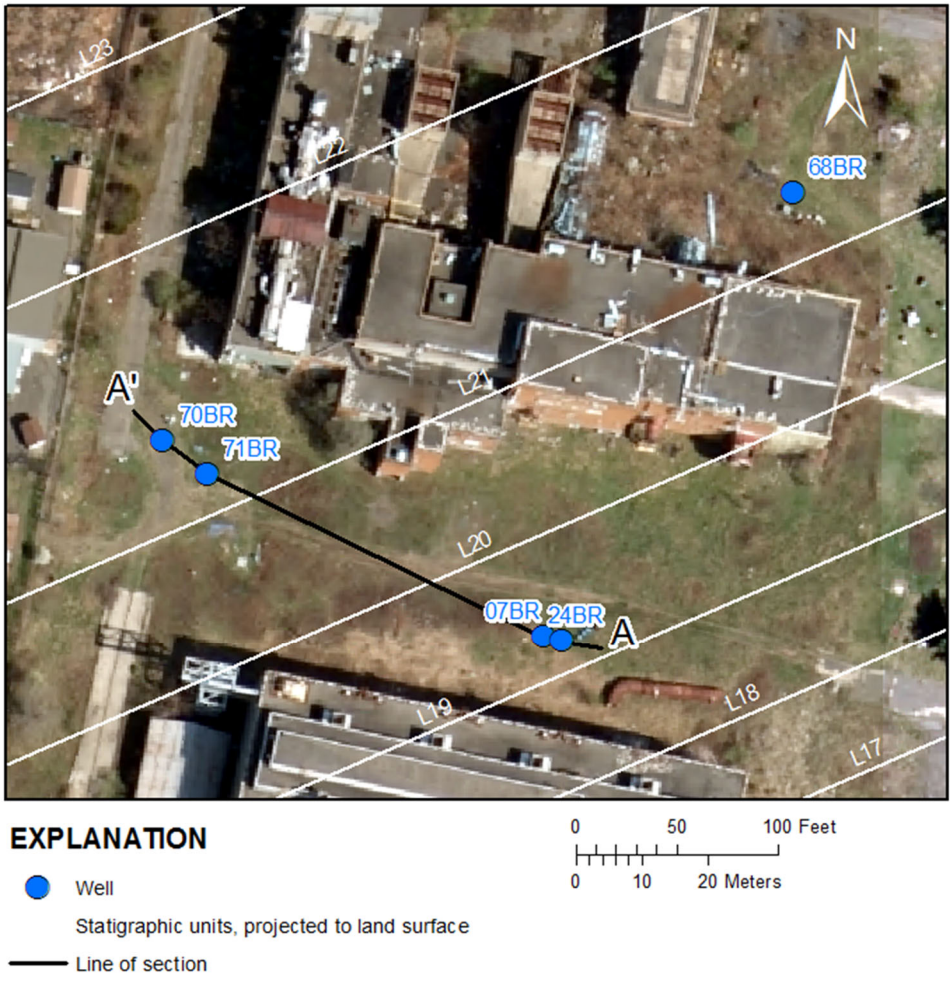

Figure 2.Selected wells and lithologic unit contacts projected to land surface between major stratigraphic units that dip to the northwest, and line of section A-A' at the field site. Map created by A. Fiore for this report.

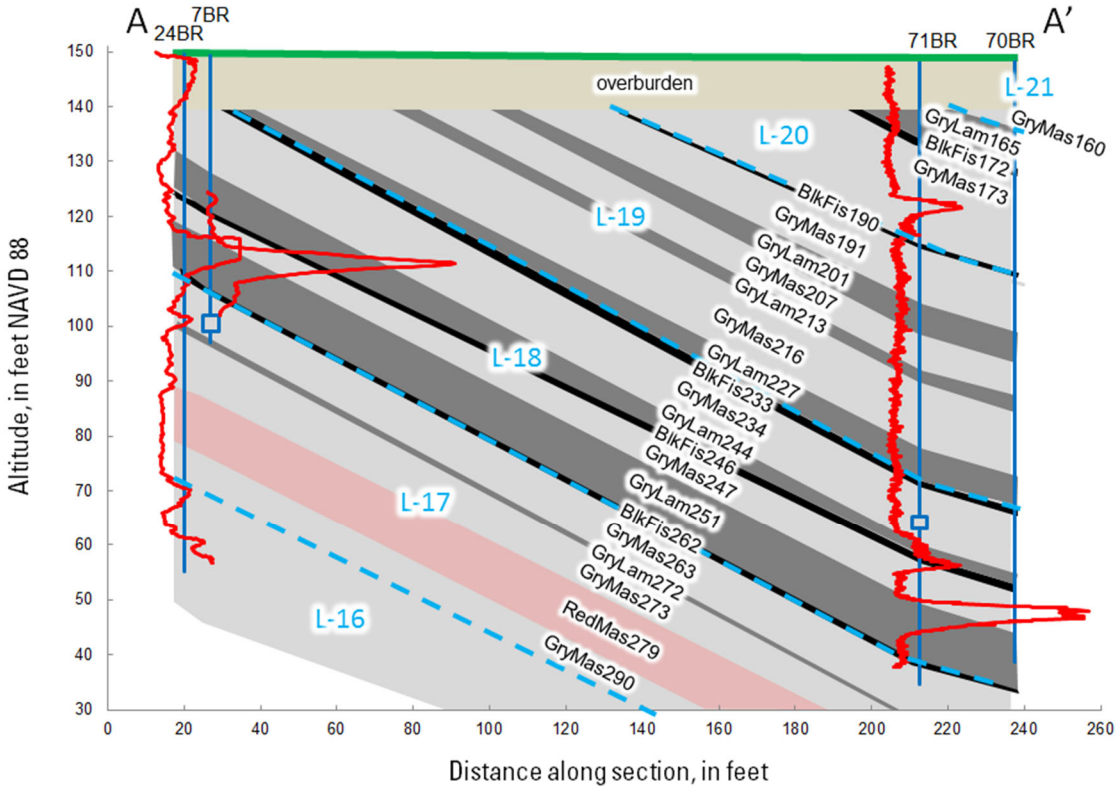

Figure 3. Cross section along A-A' showing dipping mudstone strata, locations of wells (blue lines), and gamma-ray logs (red lines) for wells 24BR, 07BR, and 71BR. Locations of field tests at 07BR-49 and 71BR-85 are indicated by blue squares. Lacombe (2000) presented the initial NAWC stratigraphy (Lithologic units), and the refined stratigraphy was presented by Lacombe and Burton (2010). The individual unit labels (e.g. GryMas-234) are taken from (Tiedeman et al. 2018). Figure created by A. Fiore for this report.

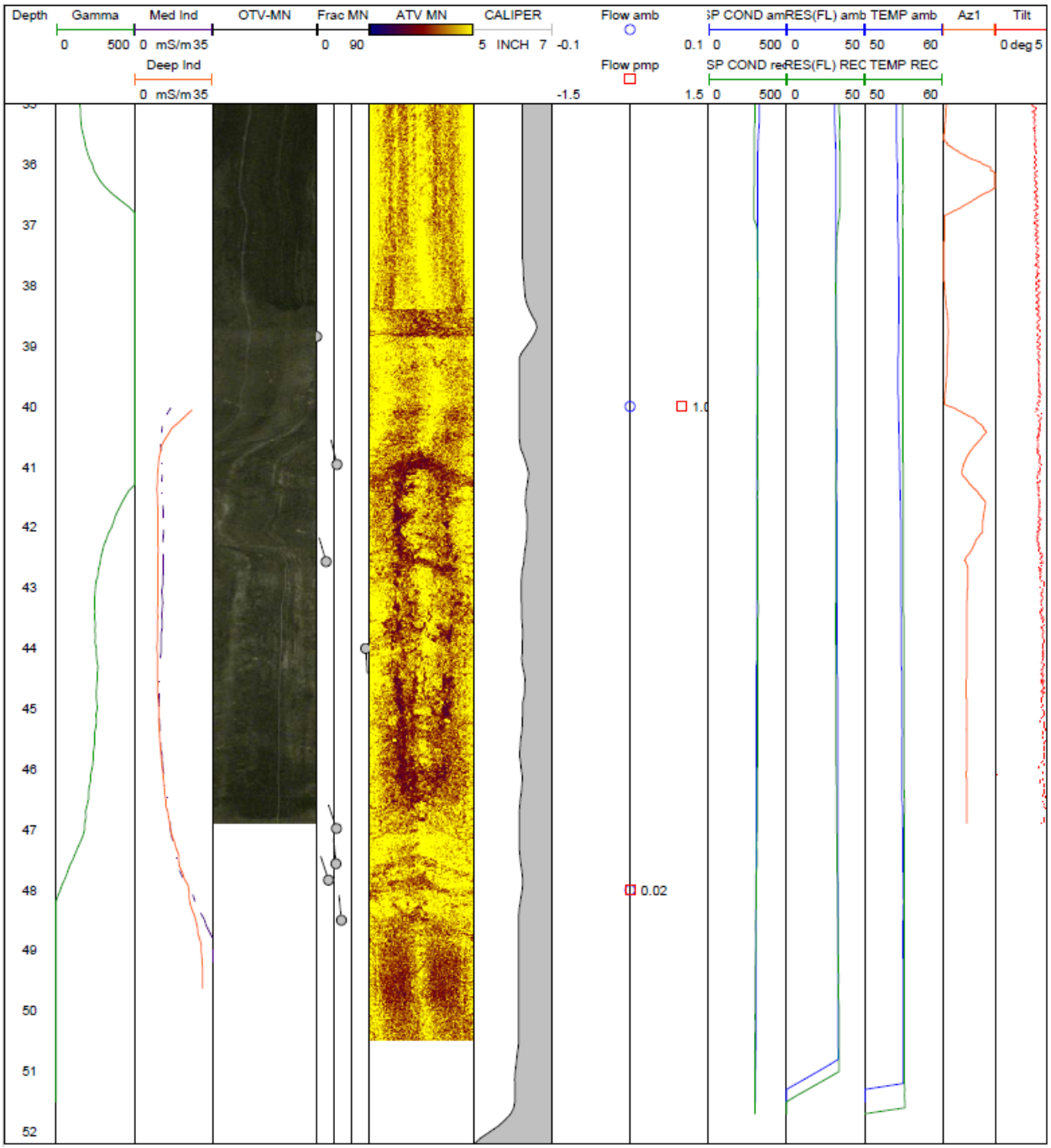

Figure 4. Geophysical Log data for 07BR.

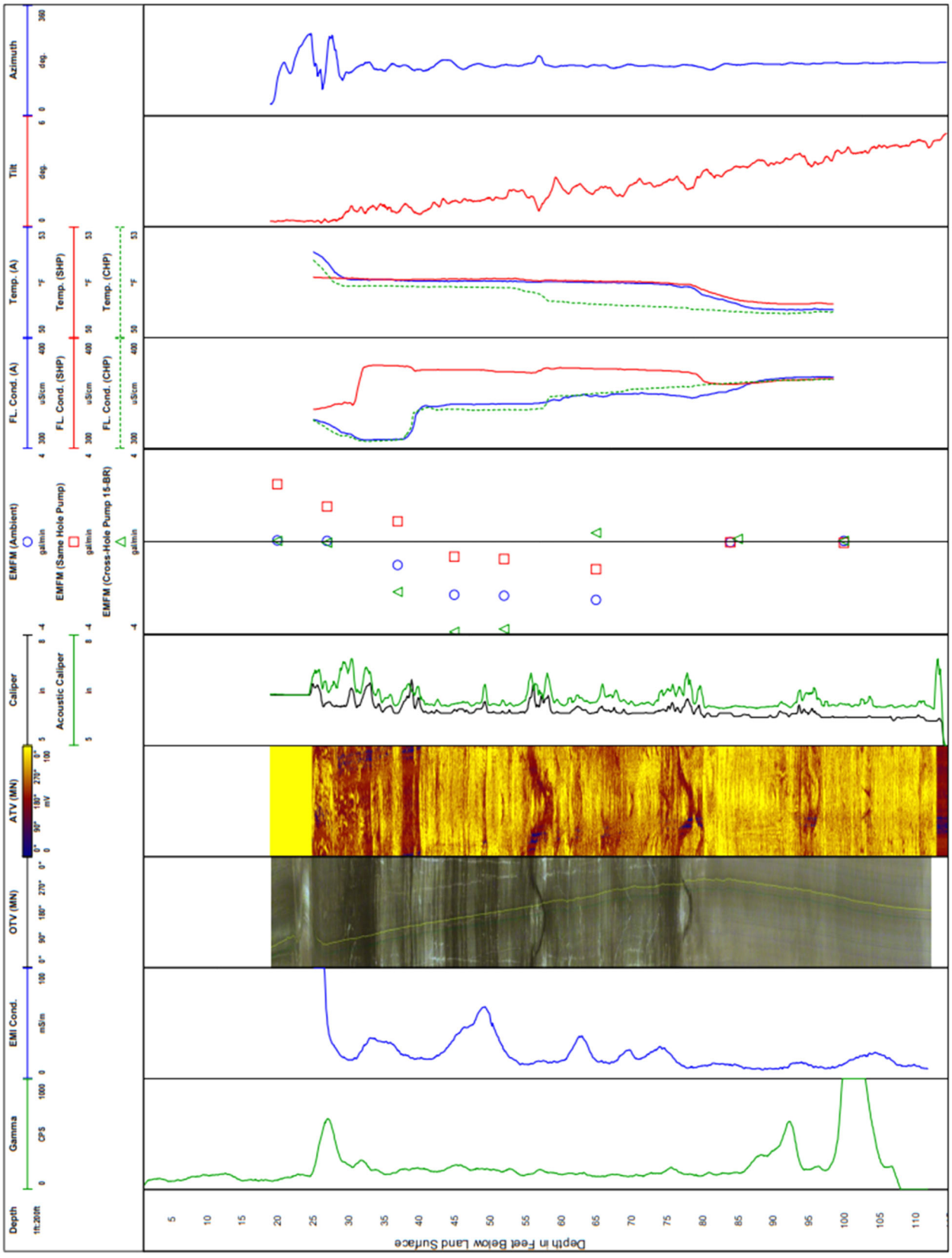

Figure 5. 71BR composite logs.

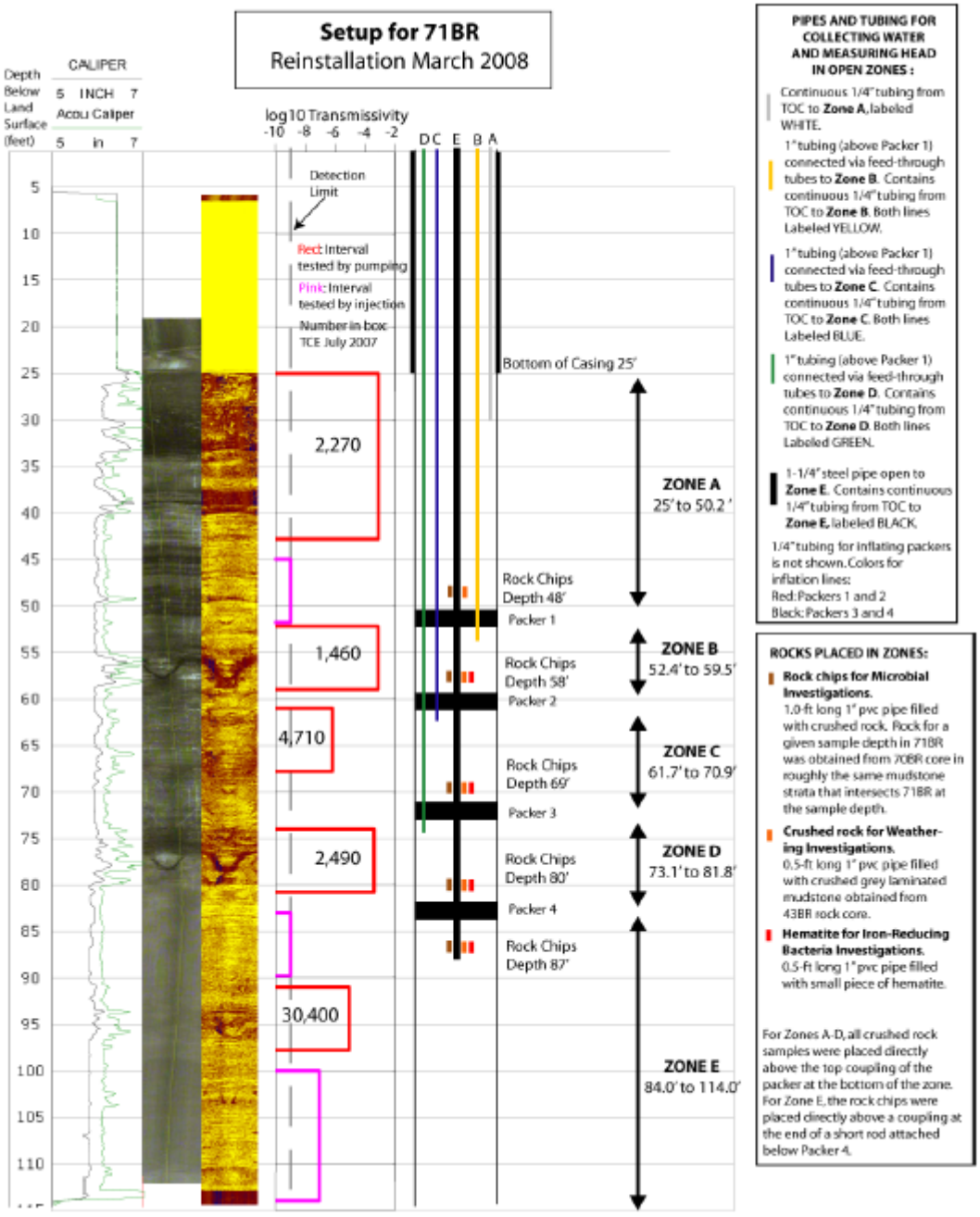

Figure 6. The configuration of packed off intervals in 71BR prior to our tracer tests that were conducted in Zone E, below the deepest packer. Also shown are transmissivity tests for selected borehole intervals.

Figure 7. Photographs of selected rock core from 68BR. Blue box in (a) marks in GryMas-234 strata equivalent to the 71BR-85 test interval and red box in (b) marks rock core that are in GryMas-263 strata equivalent to the 07BR-49 test interval. Numbers represent approximate depths of core in situ, in feet. Image created by A. Fiore for this report.

Downhole straddle packer system

Straddle packers were used to isolate low-hydraulic-conductivity (low-K) sections of aquifer strata in open boreholes. Quinn et al. (2012) provide an overview of packer-testing methods and historical development of field techniques and analysis methods. Straddle packer systems developed at the USGS Mirror Lake field site (Hsieh et al. 1996; Shapiro and Hsieh, 1998), Shapiro's (2007) BAT^3 system, and monitoring systems recently used at NAWC (Tiedeman et al. 2010; Goode et al. 2014) were modified for the prototype system used for this study.

Stainless steel (SS) and Viton were used for all test-interval hardware and the packer gland, respectively. These materials have low permeability to gases, and minimally sorb the chemicals of interest. Custom packers were manufactured by Aardvark Packers (www.aardvarkpackers.com). The upper packer has several SS pass-thru tubes that are open to the test interval (Figure 8). Tubing hardware was standard stainless-steel components from Swagelok (Swagelok.com®). All packers were inflated with nitrogen gas.

Bench-scale testing was performed at the USGS New Jersey Water Science Center. The straddle packers were installed in transparent polyvinyl chloride (PVC) casing and tested for leaks using tap water for overpressure and suction conditions. Tests included re-circulation in the full length of stainless-steel tubing and fittings needed for field installation to identify and repair any leaking fittings prior to field deployment. To develop and evaluate the protocols for tracer addition, mixing, sampling, and fluid replacement, bromide (Br) and blue food-grade dye tracers were used in the transparent PVC casing and in a steel casing in the field. Dye absorbances were analyzed using a Hach DR-890 portable colorimeter set to a wavelength of 610 nanometers. Video and photographs were recorded during mixing tests.

Laboratory testing results were also used to refine the straddle packer system design. One-quarter inch outer diameter (OD) tubing was used to replace the test interval fluid to start a tracer test. Initially this same tubing was also used for sampling, but use of 1/8-inch tubing, which has a smaller volume of fluid isolated from the borehole during the experiment, was tested and subsequently used for sampling. For the tracer test initiation, improved flushing efficiency was achieved by placing the discharge port for the relatively dense Br solution at the bottom of the interval, and the intake port for fluid removal at the top of the interval. The 1/8-inch sample tubing intake was moved to the middle of the test interval to avoid the 'dead' zones very close to the packers on early time test samples that were observed during bench-scale testing.

Field testing was conducted in wells at the NAWC site. Prior to a tracer test, the straddle packer system was installed within the casing of an open borehole, below the water level, and pressure tested. All re-circulating tubing was filled with water from the borehole and closed to atmospheric pressure. Packers were inflated, and peristaltic pumping was used to apply a suction to the test interval, while discharge from the pump was monitored to confirm discharge flow below 1 mL/min. The system was similarly tested at the selected test horizon in the open section of the borehole prior to the tracer test. If discharge was too high, the packer locations were adjusted to identify a borehole section with lower permeability.

During field testing, hydraulic pressures were monitored above and below the test horizon using pressure transducers. The water level above the system was monitored using a standard vented transducer (Druck and Meter transducer module 4-wire transducers, with Campbell Scientific dataloggers) suspended in the annular space of the casing. Manual calibration measurements of water level were also made directly. Likewise, the supporting rod for the straddle packer system was open to the borehole interval below the bottom packer, and a standard vented pressure transducer monitors the water level within the rod. Manual calibration measurements were also made in the rod.

Figure 8. Custom-manufactured packer system being lowered into borehole for field testing. A microbial sampler (stainless-steel mesh bag containing inert sand support) is fixed in the test interval between the packers.

The SS tubing, open only to the test interval, was used to modify the test-interval fluid properties, and to monitor concentration changes during the experiment (Figure 9). Two 1/4-inch OD SS tubes were used to flush water through the test interval at the beginning and end of the tracer test. These lines are isolated from the test interval using pneumatically activated valves, installed just above the top packer, when not in use. Fluid was removed from the test interval by the 1/4-inch SS tube open at the top of the test interval (Top-1/4-Yellow), and fluid was replaced into the test interval by the 1/4-inch SS tube open at the bottom of the test interval (Bot-1/4-Orange). Two 1/8-inch OD SS tubes were used to sample the test interval fluid, pulling fluid up one tube (Mid-1/8-Blue) while pushing fluid down the other (Bot-1/8-Red). Sample fluids were removed via Mid-1/8-Blue open at the mid-point of the test interval, and fluid was replaced by Bot-1/8-Red open at the bottom of the test interval. At the land surface, the tubing for pulling fluid out was connected to viton flexible tubing, through a peristaltic pumping, and to a SS sampling device (described below), and to the tubing used to push fluid into the test interval, for either the 1/4- or 1/8-inch tubes.

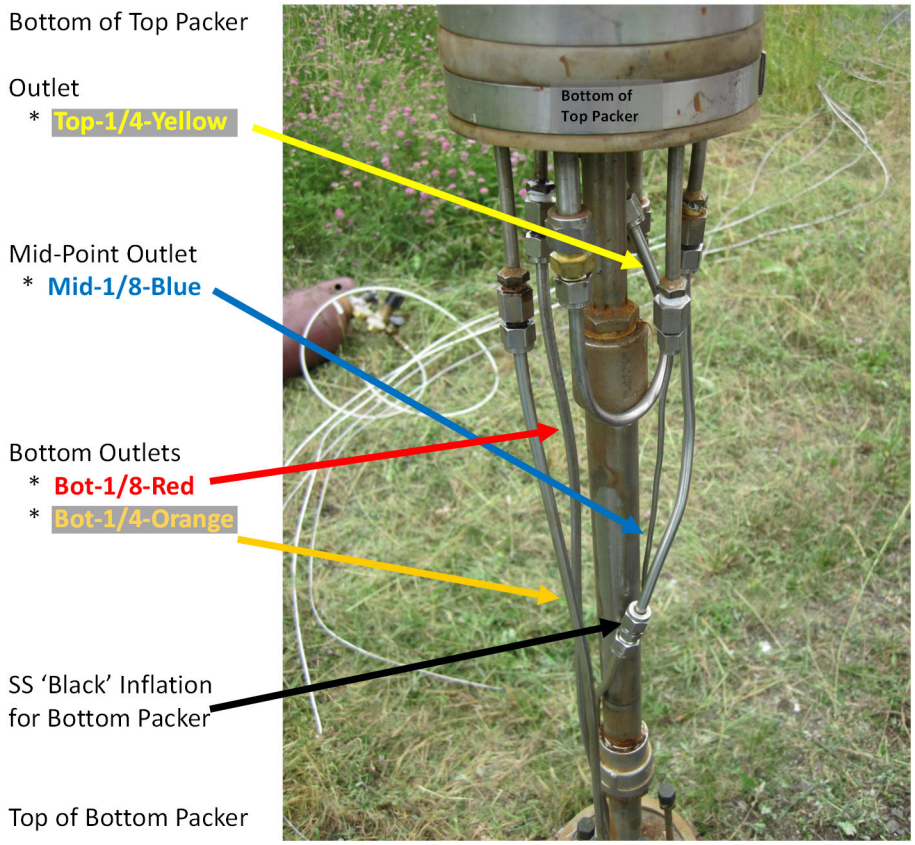

Figure 9. Photograph and identification of components of downhole test-interval equipment prior to installation in 71BR. The yellow and orange indicate ¼-inch tubes used in the injection of water and tracers and the red and blue are 1/8-inch tubes used to sample. Although Bot-1/8-Red is ¼-inch OD in the test interval, it is 1/8-inch OD from above the top packer to ground surface.

Hydraulic test

A hydraulic test was conducted in the selected test intervals to confirm the absence of high-permeability fractures. The straddle packer system was installed at a prospective test interval in an open borehole, and all tubes were filled with water from the borehole. Both packers were inflated, isolating the test interval from the rest of the borehole. Tube Top-1/4-Yellow was connected to a peristaltic pumping using Viton tubing, and valves were closed on the other 3 tubes. The peristaltic pump was used to apply about 15 ft (5 m) of drawdown to the test interval, and stable discharge of below 2 mL/min was considered to represent a diffusion-dominated test interval, having a transmissivity below about 4 x 10^{-9} m^2/sec for the 1.87-ft (0.57-m) thick test interval. Water levels were also monitored above and below the test interval.

Field sampling methods

An innovative method was developed for this project to collect samples and replace water in a closed-loop system. This approach was developed to limit loss of volatile organic compounds (VOCs) and light hydrocarbon gases (LHGs) from samples, to prevent exposure of samples to air, and to maintain a constant water volume in the test interval.

Closed-loop sampling device

The closed-loop sampling device was custom developed for this project and was constructed of 1/8-inch OD SS tubing and valves, glass gas-tight syringes with Teflon-tipped plungers, and Viton tubing (Figure 10). The device was attached to the 1/8-inch SS lines coming up from the test interval at the well head. The Viton tubing could be installed in a peristaltic pump head to allow water from the test interval between the packers to be pumped to the surface. The center valve could be opened to allow circulation of water in the closed loop or closed to collect a sample. The sampling syringe (blue, Figure 10) was used to collect a known volume of sample and the makeup water syringe (red, Figure 10) was used to introduce an equal volume of replacement water back into the system.

Closed-loop device sampling procedure

The closed-loop sampling procedure consisted of circulating water from the test interval up through the 1/8-inch SS tubing to the well head and through the closed-loop sampling apparatus (Figure 10 and Figure 11) for 5-15 minutes prior to sampling. The peristaltic pump was then stopped, and the center valve closed to isolate the water sample collection side (right side, Figure 10) from the makeup water injection side (left side, Figure 10) of the sampling device. The replacement or makeup water was part of the VOC-free water prepared during the pre-test period (discussed below). Makeup water was withdrawn from a gas-tight foil bag using the makeup water syringe and the syringe was then attached to the sampling device. The left side 3-way valve was re-positioned and the makeup water syringe (blue, Figure 10) was used to push 25 ml of VOC-free makeup water into the closed-loop so the system was slightly over-pressured.

To collect a sample during our final test in 71BR-87, the peristaltic pump was turned on at its lowest setting and used to push 4-5 ml of water through the right side 3-way valve which directed the sample into the sample syringe (red, Figure 10). Without removing the syringe, the right side 3-way valve was re-positioned so the 4-5 ml of sample was directed to the sampling port. The syringe plunger was used to push out this initial 4-5 ml sample to waste to rinse the tubing, valves, and sample port needle. This procedure was repeated to fill the sample syringe with 20-21 ml of sample. The sample syringe was then used to push out and collect a 5 ml sample for VOC analysis in a septum-capped vial, a 10 ml sample for LHG analysis in an evacuated nitrogen-filled septum-capped serum bottle, and a 5-6 ml sample for Br in a septum-

capped vial. A second set of duplicate samples were then collected by repeating the above steps. The total volume of water collected and replaced ranged from 35 to 55 mL depending on the number and type of duplicate samples collected. In all cases, the volume of VOC-free makeup water injected using the makeup water syringe was equal to the volume of water removed using the sampling syringe so the total volume of water in the test interval remained unchanged.

Once sampling and replacement were completed, the center valve was opened, and water was circulated for several minutes to force the injected makeup water down into the test interval. All manual valves were closed to seal the 1/8-inch tubes and the sampling device prior to its detachment from the well head lines. The VOC and LHG samples were preserved with hydrochloric acid in the field. Both the samples and the sampling device were transported to and from the laboratory on ice and stored at 4ºC until analysis.

At each designated sampling time during each tracer test, a 'standard suite' of samples were collected for analysis of VOCs, LHGs, and Br using the closed-loop sampling device procedure outlined above. The target VOCs and LHGs quantified were TCE, TCFE and primary known DPs. The main DPs discussed in this report are cDCE, VC, *e*DCFE, *z*DCFE, fluoroethene (FE), ethene, ethane, and acetylene. Chromatographs were also scanned for monochlorofluorothenes and fluoroacetylene for qualitative identification.

Borehole geochemical sampling

During the pre-test and post-test periods, when it was possible to collect larger water volumes without diluting the tracer test, additional samples are collected for characterization of the borehole water chemistry. The characterization included collecting samples for major cations and anions, dissolved organic carbon (DOC), alkalinity, dissolved oxygen (DO), volatile fatty acids, sulfide, and ferrous iron, as well as the standard suite of VOC, LHG, and Br samples. During sparge vessel filling and test interval flushing, a multiparameter sonde in a flow cell was connected to the outlet of one of the ¼-inch SS lines and used to measure field physical and chemical parameters (temperature, pH, specific conductance, and DO). Field ferrous iron and sulfide measurements used filtered samples and a Hach DR-890 portable colorimeter. Ferrous iron determinations used Hach's Method 8008 that is based on the 1,10 phenanthroline method (APHA 2017) and sulfide determinations used Hach's Method 8131 that is based on the methylene blue method (after APHA 2019). Field dissolved oxygen determinations used the Chemets Rhodazine D colorimetric method (after ASTM 2015) on unfiltered samples.

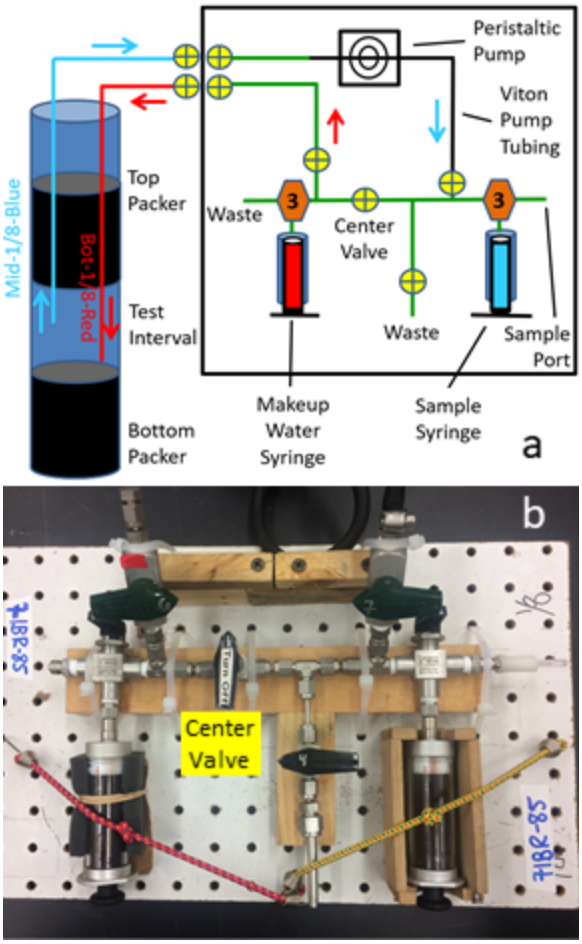

Figure 10. Configuration of the closed-loop sampling manifold attached to packer tool (a) and photograph of the sampling device (b). The peristaltic pump is on and the "Center Valve" is open during circulation. The valve is closed during sampling, and the peristaltic pump is run at low speed to fill the sample syringe. The valve separates the manifold into two distinct flow paths: to the left is the replacement side, where sparged makeup water (red) is injected to the bottom of the test interval via Bot-1/8-Red; to the right is the sampling side, where test interval water (blue) is collected from Mid-1/8-Blue. The sample syringe 3-way valve directs flow either from the pump into the sample syringe or from the sample syringe to the sample port.

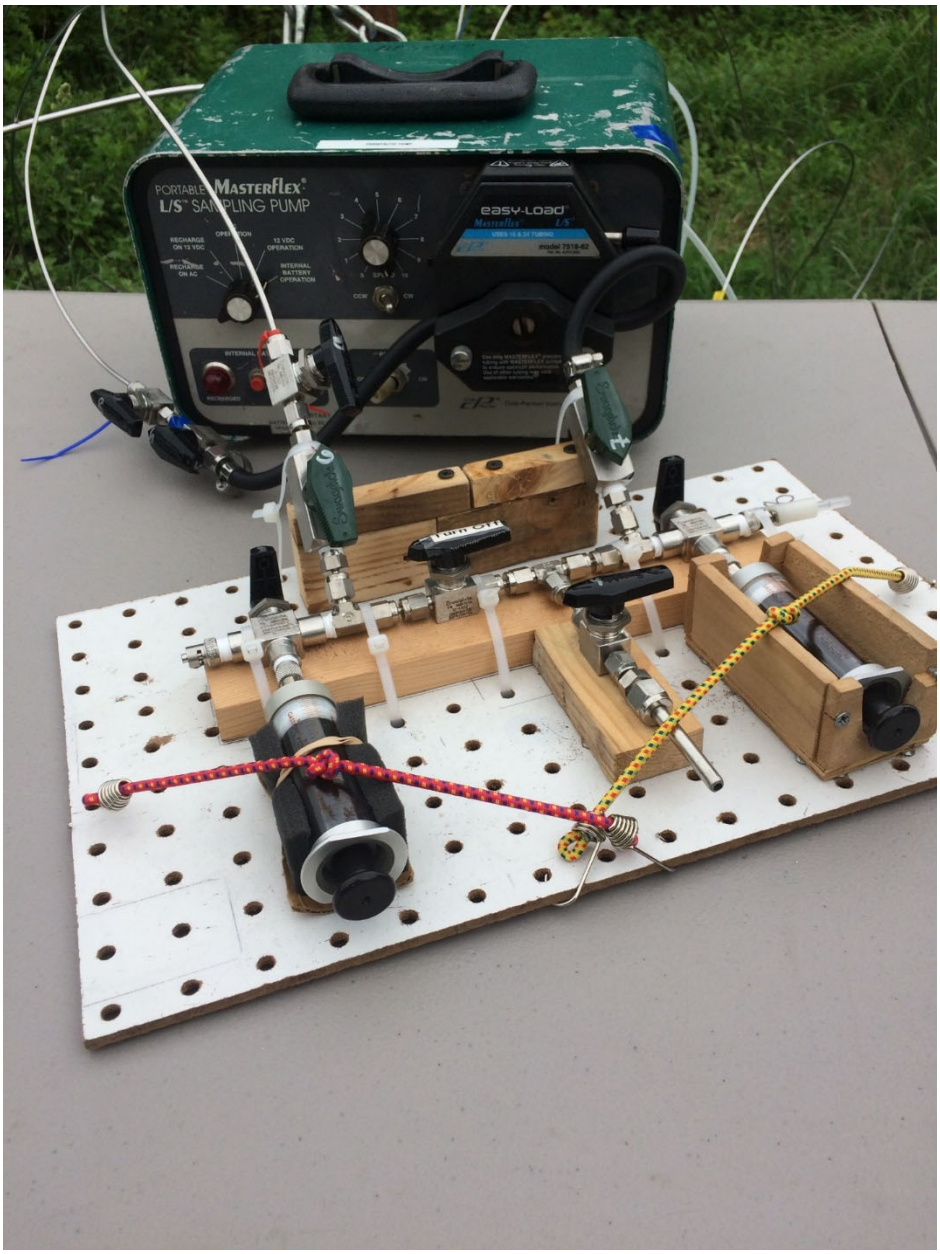

Figure 11. Closed-loop sampling manifold and peristaltic pump during field testing.

Tracer test initiation

Tracer test initiation consisted of four major steps: (1) filling the sparge vessel with groundwater from the test interval, (2) removing VOCs and LHGs from the groundwater by sparging with nitrogen (N_2), (3) flushing the test interval with sparged groundwater, and (4) adding tracers. The methods used to accomplish these tasks are highlighted in this section. Additional technical details are provided by Allen-King et al. (In revision) and Kiekhaefer (2018).

Groundwater pumped from the below the test interval was used in each tracer test to minimize water chemistry perturbation. The 50-liter glass sparge vessel (Figure 12) was filled with groundwater by pumping the two ¼-inch SS lines coming up from the test interval using peristaltic pumps with only the upper packer inflated. In order to maintain the groundwater in its anaerobic state while removing VOCs, the groundwater was pumped into the pre-purged glass sparge vessel while constantly sparging with ultra-high purity grade nitrogen gas (N_2). Positive N_2 pressure was maintained on the sealed sparge vessel until completion of tracer injection. The TCE and cDCE concentrations were reduced to <100 µg/L and this low-VOC groundwater was referred to as "sparged water." Approximately, 40L of groundwater were collected and sparged prior to initiation of each tracer test. Five 1L foil-lined gas-sampling bags were filled with sparged water for subsequent use as makeup water or to create tracer solutions (Figure 13).

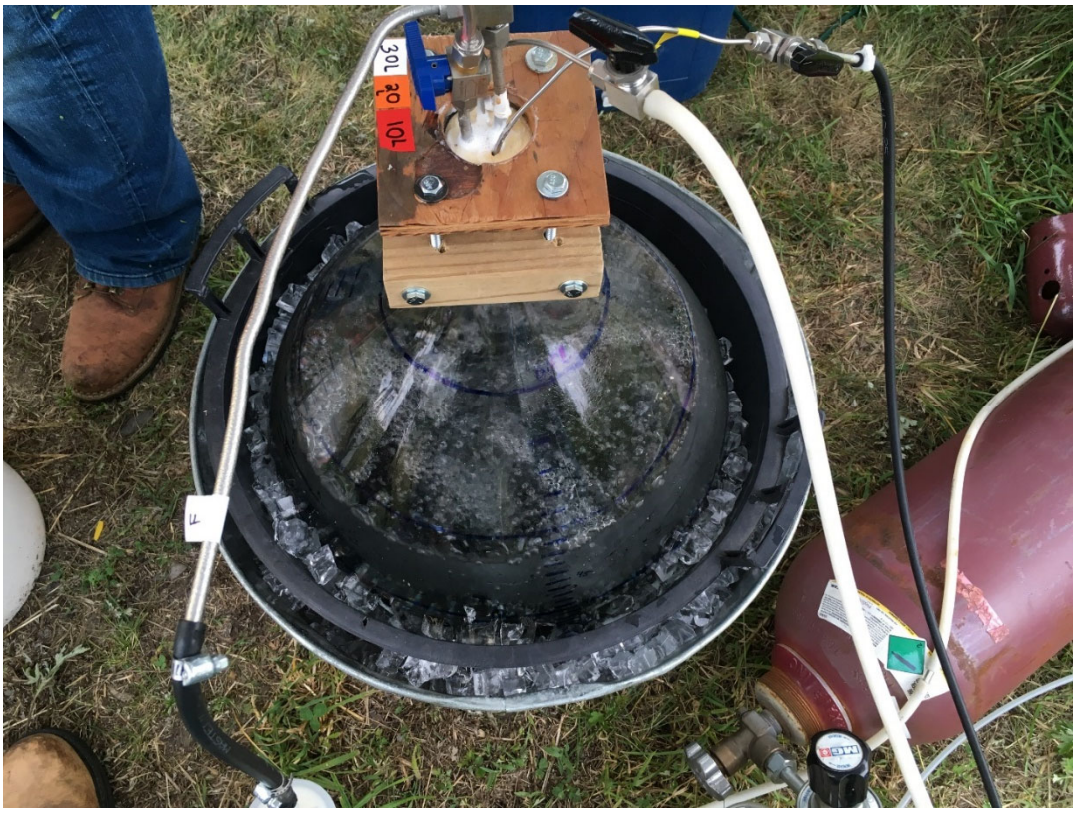

Figure 12. Nitrogen gas was used to remove VOCs from borehole water in a vented glass 'sparge vessel' cooled with an ice jacket. This water was flushed through the test interval to replace the *in situ* water.

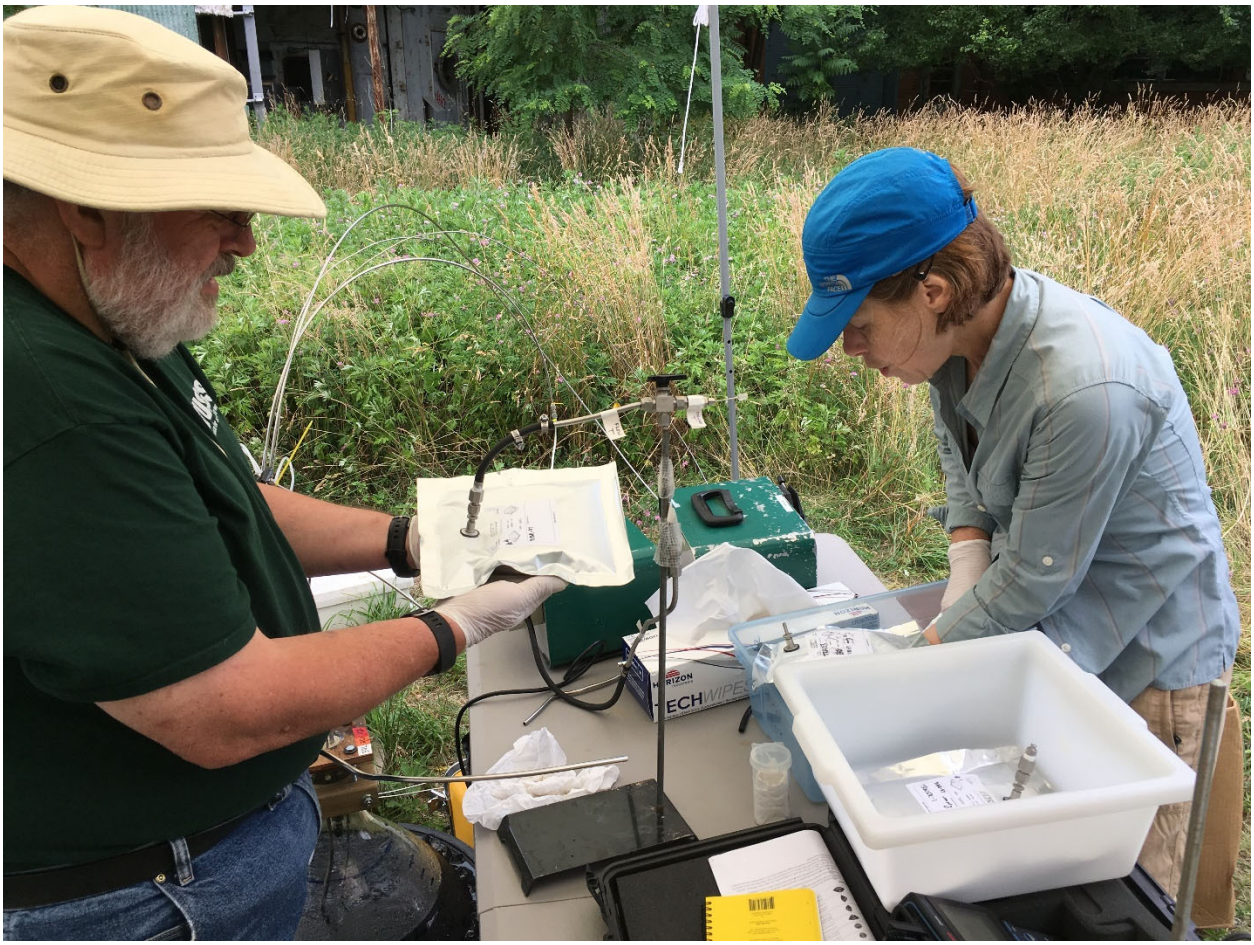

Figure 13. Tracer solution in a foil-lined gas-sampling bag.

Sparging with N_2 did remove dissolved carbon dioxide (CO_2) causing the pH to increase in the sparge vessel. In some tests, CO_2 gas was bubbled through the water in the sparge vessel for a short time prior to tracer test initiation to decrease the pH back to that of the ambient groundwater in the well. This was done to avoid precipitation of calcite and loss of dissolved bicarbonate in the sparge water.

After filling the sparge vessel, the bottom packer was also inflated to isolate the test interval from the rest of the borehole. During the tracer test, water levels were continuously monitored above and below the straddle packer system to characterize fluctuations due to recharge or pump-and-treat system changes, and to confirm the hydraulic separation of the borehole sections above and below the system during the test. Packers were always inflated using N_2. Packer pressures were monitored throughout each test, and N_2 was added as needed to maintain near constant packer pressures.

The test interval was then flushed by pumping approximately 40 L (4 volumes) of low-VOC sparged water down through the interval to replace the high VOC ambient groundwater. prior to the start of the test. This was accomplished using a peristaltic pump pumping at the rate of ~500 ml/min through the ¼-inch lines. The 1/8-inch sample tubes were also flushed near the end of the test interval flushing.

Approximately 60 ml of each tracer (Br and TCFE) were prepared as a concentrated solution in N_2-purged reagent water (ASTM Type I deionized water, (ASTM 2018) filtered through an activated carbon cartridge to remove organics). The concentrated solutions were transferred to a known volume (~500 ml) of sparged water in a foil-lined gas-sampling bag to make up the final tracer solution at approximately 20 times greater than the target test interval concentration. The tracer solution was injected into flow circulating from/to the test interval by attaching a dosing device in a closed loop with the ¼ inch SS tubes and the peristaltic pump (Figure 14). Following injection, water was circulated through the closed-loop system to mix the tracers with the water in the test interval. Both ¼-inch tubes were sealed for the duration of the tracer test by closing the downhole pneumatic valves and the dosing apparatus was removed.

Figure 14. Dosing test interval without volume change by simultaneous injection of concentrated tracer solution into continuous flow (circulation from the test interval) and withdrawal of return flow.

Tracer test completion

At the completion of the tracer test, the test interval water was flushed out to remove any remaining tracers. A peristaltic pump was used to pump water from above the top packer down one of the ¼-inch SS lines (Bot-1/4-Orange), through the test interval, and up the other ¼-inch SS line (Top-1/4-Yellow) to the land surface. The displaced test interval water was collected and

discharged to the onsite treatment plant. Periodic samples of the pumped water verified the reduction of tracer concentrations during the cleanout of the test interval.

Contaminant and tracer analysis

The CVOC and LHG samples were analyzed using an SRI 8610C field portable gas chromatograph (GC). A dry electric conductivity detector (DELCD) and flame ionization detector (FID) were used in parallel, adapted from the methods used by Louie (1999). Each detector was preceded by a GSQ-PLOT column. Results for LHGs and high concentrations of TCE, cDCE, and VC were determined from the FID and results for low concentrations of TCFE, TCE, cDCE, and VC were determined from the DELCD. A total sample volume of 1050 µL was injected into the sample loop for each analysis, with 1000 µL directed to the FID and 50 µL directed to the DELCD.

After the diffusion tests in 2017 began, the DELCD malfunctioned and could not be used to determine TCFE concentrations and low concentrations of TCE, cDCE, and VC. Additional samples were collected at each sampling event for analysis by gas chromatograph with mass spectrometer (GC/MS) using EPA method 524.2 (Majcher et al. 2007). Subsamples were taken from those samples that were collected prior to the detector malfunction that had not been analyzed. Samples with a known concentration of CVOCs were sent for GC/MS analysis alongside the samples for comparison purposes. Samples collected for GC/MS analysis, either directly in the field or from a previously collected sample, were subject to volatilization losses during collection or transfer. An experiment was conducted to compare concentration results between the different types of collection, storage, and analysis. Typical serum vial gas-water partitioned samples were analyzed on the SRI 8610C gas chromatograph and all other samples were analyzed using an HP 5890 gas chromatograph. As detailed in Kiekhaefer (2018) correction factors were determined and applied to the CVOC results.

Alkalinity samples collected during the test initiation and conclusion sampling events were analyzed using EPA method 310.1 (Godfrey 1988). DOC samples were analyzed on a Shimadzu TOC-V analyzer using the standard high temperature method (5310B, APHA 2005). Anions, including Br, were analyzed by ion chromatography on a Dionex ICS-1000 (EPA method 300.0, Pfaff 1993).

Simulation method

The numerical model for simulating the field test is similar to the model described in Allen-King et al. (In revision) that considers the following processes that are also illustrated in Figure 15:

- Molecular diffusion of dissolved phase TCE, its biodegradation products (cDCE and VC), and the added tracers, bromide and TCFE,
- Equilibrium-controlled sorption (modeled by linear isotherms) of dissolved phase TCE, cDCE, VC, and TCFE onto solid grains in the rock matrix, and
- Biodegradation of dissolved phase TCE, cDCE, VC, and TCFE in the borehole.

The model described herein also includes

- Abiotic degradation of TCE and TCFE (both dissolved and sorbed phases) in the rock matrix, and

- Describes either first or zeroth order TCE and TCFE biodegradation in the borehole.

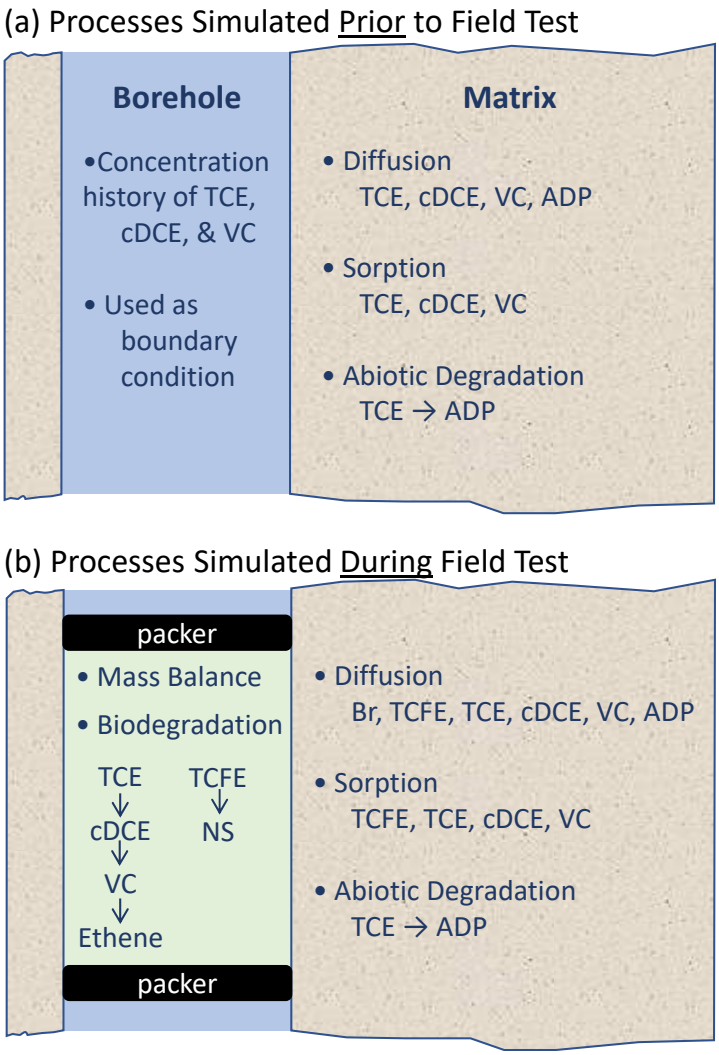

Figure 15. Schematic of processes simulated to interpret the field test (a) before and (b) during the field test. Created by Paul Hsieh.

The following equations are solved numerically using the finite-difference method. The numerical calculations are implemented using a finite difference method in a Fortran program (Hsieh and Goode 2021).

In the rock matrix, the governing equation for chemical species i (where i may represent TCE, cDCE, VC, TCFE, ADP or Br) is of the form:

$$R_i\theta\frac{\partial C_i}{\partial t}=\frac{1}{r}\frac{\partial}{\partial r}\left(r\theta D_i\frac{\partial C_i}{\partial r}\right)-\Lambda_i C_i-\bar{\Lambda}_i\rho_b K_{d,i}C_i \quad \text{for} \quad r_w<r<\infty\,, \tag{1}$$

where

θ = matrix porosity,

C_i = molar concentration of species i,

D_i = effective diffusion coefficient of species *i*,

Λ_i = first-order abiotic degradation rate constant for the dissolved phase of species *i*,

$\overline{\Lambda}_i$ = first-order abiotic degradation rate constant for the sorbed phase of species *i*,

ρ_b = bulk density of the rock matrix,

$K_{d,i}$ = distribution coefficient characterizing sorption of species *i*,

t = time,

r = radial distance from the center of the borehole,

r_w = borehole radius.

The effective diffusion coefficient characterizes molecular diffusion in the rock matrix. It is equaled to the free water diffusion coefficient multiplied by the tortuosity factor (τ) of the rock matrix ($D_i = D_i^o \tau$). The free water diffusion coefficients used in the simulations are 15, 6.0, 6.3, 7.0, 7.4, and 17.0 each x10^{-10} $m^2 \cdot s^{-1}$, for Br, TCFE, TCE, cDCE, VC, and ADP, respectively. The retardation factor, R_i, is given by

$$R_i = 1 + \frac{\rho_b}{\theta} K_{d,i} \tag{2}$$

In the simulation method, abiotic degradation is permitted only for TCE and TCFE. Therefore $\Lambda_i = \overline{\Lambda}_i = 0$ when *i* represents cDCE, VC, or Br. Additionally, as Br is non-sorbing, R_{Br} = 1. Production rate of the ADP is equivalent to abiotic TCE degradation rate.

The simulation begins at the time when the borehole is drilled. The initial condition is $C_i = 0$ at $t = 0$, $r_w < r < \infty$. From the start of the simulation to the beginning of the test, the boundary condition at the borehole wall sets the concentration of TCE, cDCE, and VC to the corresponding historically measured values, linearly interpolated in time from one measurement to the next. In effect, the model simulates the diffusion of these CVOC's from the borehole into the rock matrix, as well as sorption and abiotic degradation in the matrix. During this pretest period, the boundary concentrations for TCFE and Br are zero.

At the start of the test, the TCE, cDCE and VC concentrations at the borehole wall are set to their corresponding values measured after purging, while the TCFE and Br concentrations set to their corresponding measured values after these tracers are added to and mixed in the borehole test interval. The boundary conditions are specified as

$$V \frac{dC_i^*}{dt} = -VA_i + VB_i + 2\pi r_w \ell \theta \left(\frac{\partial C_i}{\partial r} \right)_{r=r_w} \tag{3}$$

where

C_i^* = molar concentration of species *i* in the borehole test interval,

V = volume of water available for mixing in borehole test interval,

ℓ = length of borehole test interval.

The term VA_i represents the loss of species i by biodegradation in the borehole test interval.

We generally assume biodegradation is first-order in concentration, but include a choice of first-order or zeroth-order forms for TCE and TCFE. The first-order biodegradation in the borehole test interval is governed by:

$$A_i = \lambda_i C_i^* \tag{4}$$

where λ_i is the first-order biodegradation rate constant for TCE, TCFE, cDCE, or VC. Alternatively, for zeroth-order biodegradation of TCE and TCFE, we assume that their combined molar concentration biodegrades at a zeroth-order rate ψ, which is apportioned to TCE and TCFE according to their concentrations as a percentage of the combined concentration.

$$A_{TCE} = \frac{C_{TCE}^*}{C_{TCE}^* + C_{TCFE}^*}\psi \tag{5}$$

$$A_{TCFE} = \frac{C_{TCFE}^*}{C_{TCE}^* + C_{TCFE}^*}\psi \tag{6}$$

As Br is non-reactive, $A_{Br} = \lambda_{Br} = 0$.

The term VB_i in equation (3) represents the creation of species i from degradation of its parent species. For cDCE or VC that are produced by biodegradation, the B_i is equal to the rate of parent biodegradation,

$$B_{cDCE} = A_{TCE} \tag{7}$$

$$B_{VC} = A_{cDCE} \tag{8}$$

For all other species i, $B_i = 0$. The poor mass balance of the TCFE DPs in the field test experiment rendered it not useful to model their production and degradation.

After a field test is completed, the simulation model is used to estimate model parameter values. The computer program PEST version 14 (Doherty 2016) is used to solve for model parameters so that the simulated concentrations optimally match the observed concentrations. PEST uses the Gauss-Marquardt-Levenberg method to implement nonlinear least squares regression to estimate model parameters by minimizing the sum of squares of the differences between measured and simulated concentrations (Doherty 2015).

Hsieh and Goode (2021) provide input and output files for simulations presented by (Allen-King et al. In revision). Additional details are also provided to allow the model input text files to be modified for other field tests. The source code for the numerical model is also provided.

Supporting Laboratory Experiments

Sorption

We measured equilibrium sorption isotherms for samples representative of the major Lockatong lithologies at NAWC using standard batch procedures designed to eliminate contaminant loss by volatilization. A complete description of the method is in Brotsch (2017). We measured TCFE sorption isotherm with and without TCE for one sample (#131) to compare to the TCE isotherm (Pugnetti 2018). Samples were selected from the 68BR archived core and the sample numbers are the sample depths (in feet). Samples with low to no TCE in them prior to sorption measurements were selected to simplify experiment mass balances. Mass balances were completed for selected batch systems to confirm that no significant degradation occurred during the experiments. The f_{oc} contents of the samples span approximately an order of magnitude (0.2%-3.7%).

Aerobic abiotic TCE:TCFE degradation rate comparison

We completed batch experiments to evaluate the relative rates of aerobic abiotic degradation of TCFE and TCE. Because we are most interested in evaluating the utility of TCFE as a tracer of TCE behavior, we completed the experiments using pyrite rather than NAWC rocks. The experiment set up replicated the proportions of headspace:water:pyrite surface area (estimated) used by (Pham et al. 2008) but used smaller experiment vials. Experiments were conducted with TCE and TCFE individually and together.

Biodegradation rate measurements

Microcosm experiments were conducted with site microbes and groundwater from different boreholes investigated for conducting field trials of packer-based tools (Dugan et al. 2021). Initial experiments focused on verifying TCE:TCFE biodegradation ratios with a range of initial TCE and TCFE concentrations and testing a suitable matrix for collection of microbial samples within the test zone during the packer tests. Later tests focused on defining biodegradation rates, process, and DPs within field test intervals for comparison to model simulations. Because many subsurface microorganisms prefer to be attached to a solid matrix, using only groundwater for biodegradation experiments and evaluation of microbial communities may not be representative of site conditions (Holm et al. 1992). Thus, passive “microbial samplers” containing a solid matrix for colonization by microbes were incubated downhole to obtain material with attached microorganisms for biodegradation testing, in conjunction with groundwater samples to obtain planktonic microorganisms. Fresh crushed rock from soil cores available for the site were initially used as the solid matrix but were then compared to medium Ottawa sand as a microbial attachment matrix that would have minimal sorption or other abiotic interactions with the VOCs. Microbial samplers used for the current study were constructed of a stainless-steel mesh filled with washed drillers sand and were attached, using stainless-steel wire, to the center rod supporting the packers (Figure 8).

For some microcosms that were used to evaluate biodegradation, microbial samplers were placed above the packed interval. However, microbial samplers also were placed between the packers to obtain biodegradation rates and microbial communities within the test interval during the field packer tests at borehole 71BR. Only sand samplers were used for microbial community collection within the packed interval during testing to minimize sorption of injected tracers. Microbial samplers (in duplicate or triplicate) were incubated downhole for a minimum of 8 weeks or for the duration of the field test. Upon retrieval, the intact microbial samplers were placed in autoclaved mason jars that were pre-filled and flushed with groundwater from the same

depth interval; jars were sealed with minimal headspace. In the laboratory, the samplers were placed in an anaerobic glove box, where at least one sampler was opened to remove a subsample for microbial community analysis. Microbial community samples were frozen at -80ºC until analysis. The remaining sand or crushed rock was stored in the groundwater at -4ºC until construction of sediment microcosms to determine rates of biodegradation.

The first set of experiments evaluated degradation rates with site microbes collected from 2 wells (07BR and 68BR) on crushed rock samplers, using initial TCE and TCFE concentrations of about 70 to 20 mg/L that were similar to site conditions. For the second experiment, sand and crushed rock microbial samplers were incubated together at the same depth in 07BR to allow evaluation of the sand as a representative attachment matrix. The experiments for well 71BR were conducted with crushed rock that were incubated at the 87 ft depth interval prior to the first field test at 71BR, and then with sand that was incubated in or near the packed test intervals at a depths of 85 ft and 87 ft during the field tests of the packer tool.

All microcosms were constructed in an anaerobic chamber in sets of duplicate or triplicate vials. Background VOC concentrations in the groundwater were removed by nitrogen degassing before use in the microcosms. TCE and TCFE were amended together at the same planned initial concentrations for most microcosms, although TCE alone was added in some treatments for comparison to the TCE+TCFE treatments. The effect of lactate as an added donor and of addition of a known dechlorinating culture, WBC-2, was also tested. In most tests, added lactate concentrations (1 mM) were relatively low, but the set of experiments conducted with sand that was incubated in or near the packed test interval in 71BR at a depth of 87 ft included reamendments with lactate and TCE.

Bioaugmentation with WBC-2 was used as positive control to assist in evaluating reasons for incomplete degradation of TCE in batch experiments. Microcosms prepared with groundwater only were used as controls to evaluate the effect of suspended versus attached microbial populations on degradation. In one set of experiments, different sterilizing agents to establish "killed controls" were evaluated. All microcosms were prepared without headspace and 2:1 ratio (by volume) of groundwater to sand or crushed rock. Except for the last microcosm experiment, microcosms were sacrificed at each sampling interval and analyzed by USGS. For the last experiment, microcosm bottles were subsampled repeatedly and analyzed by UB; filtered groundwater that was purged of VOCs was added periodically to replace the small volumes of water removed for sampling.

Except for the last microcosm experiment, VOCs in the water were analyzed at each time step by GC/MS at the USGS Maryland-Delaware-DC Water Science Center Research Laboratory, Baltimore, MD, using a modification of USEPA Method 524.2 (Majcher et al. 2007). Water samples from each time step also were transferred to serum vials that had been pre-purged with nitrogen, and the headspace was analyzed for gases (FE, ethene, ethane, methane) by GC FID in the USGS laboratory. After removal of the water for analysis in microcosms, selected samples of the rock chips or sand in the vials also were analyzed for VOCs by methanol extraction and analysis. For the last microcosm experiment that was conducted in conjunction with UB, samples were analyzed using an SRI 8610C GC with a DELCD and FID, with a method slightly modified from Kiekhaefer (2018). Headspace analysis was used with the FID to analyze ethylene, FE, VC, and (*Z*)-1-chloro-2-fluoroethene (*z*CFE); solid phase microfiber extraction (SPME) was used with the DELCD and a heated injector to analyze TCE, TCFE, cDCE, *z*DCFE, and *e*DCFE. Standards for TCE, cDCE, and VC in methanol were purchased from Supelco or

Restek; fluorinated compounds (TCFE, *z*DCFE, *e*DCFE, *z*CFE, and FE) were purchased from Synquest Laboratories. The 1,1-chlorofluoroethene (1,1-CFE) was not available as a standard or pure compound.

Microbial community analyses

A portion of the incubated sand or crushed rock from the microbial samplers was frozen (-80ºC) immediately for microbial community analysis by 16S ribosomal ribonucleic acid (rRNA) Illumina iTag sequensscing. In addition, sand/crushed rock was collected and immediately frozen at different sampling intervals during microcosm experiments to obtain changes in microbial communities during biodegradation. The Illumina next-generation sequencing method allows for total community fingerprinting, as well as identifying to the level of individual species. Deoxyribonucleic acid (DNA) was extracted with a Power Soil DNA Isolation Kit (Mo Bio Laboratories, Carlsbad, CA), and sequencing of the V4 region of the 16S rRNA gene was performed. Microbial sequence data were analyzed using mothur (Schloss 2015; Schloss et al. 2009) and the vegan package in R (Team 2015; Oksanen et al. 2015; Kozich et al. 2013).

Results

Supporting Laboratory Experiments

The primary purpose of our laboratory experiments is to provide independent constraints on the parameter estimation of the field test results, as needed. We measured the relative TCE:TCFE coefficients of sorption, biodegradation rate and anaerobic abiotic degradation rate. The TCE biodegradation rate coefficients and sorption coefficients from the field test are also compared to the laboratory results. We present the results of our laboratory experiments below.

TCE and TCFE sorption

Equilibrium sorption isotherms for TCE are nonlinear for all of the NAWC lithologies for isotherms that span about four orders of magnitude dissolved TCE concentration. The isotherm slopes (n) are similar for all of the samples (0.52-0.57). The range of the Freundlich sorption coefficients (K_f) is greater than two orders of magnitude (Table 1). Normalizing the sorbed concentrations (C_s) by the sample f_{oc} reduces the sorbed concentration range between samples to approximately an order of magnitude (Figure 16).

Table 1. TCE sorption isotherm coefficients for NAWC mudstone samples from the Lockatong. The units on K_f are $((\mu g/kg)/(\mu g/L)^n)$

Sample #	Lithologic Unit	f_{oc} (%)	log K_f	n
95	black fissile	3.74	4.1	0.51
131	black fissile	1.6, 1.2	3.4	0.57
122	gray laminated	0.74, 0.79	3.0	0.53
152	reddish gray massive	0.14, 0.21	2.1	0.52
72	gray massive	0.46	1.9	0.52

Over nearly the entire dissolved concentration range studied, the TCE K_{oc} (K_d/f_{oc} corresponding to a specific dissolved concentration) are much greater than would be predicted by the empirical approach., i.e. $K_d=K_{oc}\,f_{oc}$. The K_{oc} reference line shown on Figure 16 was calculated by the empirical approach using the EPA value of K_{oc} = 100 L/kg (U.S. Environmental Protection Agency 2013) and an f_{oc} of 1.0%, a mid-range value for the samples tested (Table 1). In other words, the empirical approach substantially underpredicts sorption in this sedimentary aquifer, despite the aquifer having f_{oc}>0.1% (the rule of thumb minimum value for using this approach). The reason for high TCE sorption is because of the organic matter structure that results from geologic processes associated with burial, as described by (Brotsch 2017). The extreme conditions to which the NAWC rocks were exposed cause them to be described as “over mature”. Our finding underscores the need for site specific testing to accurately determine the sorption coefficient and retardation factor.

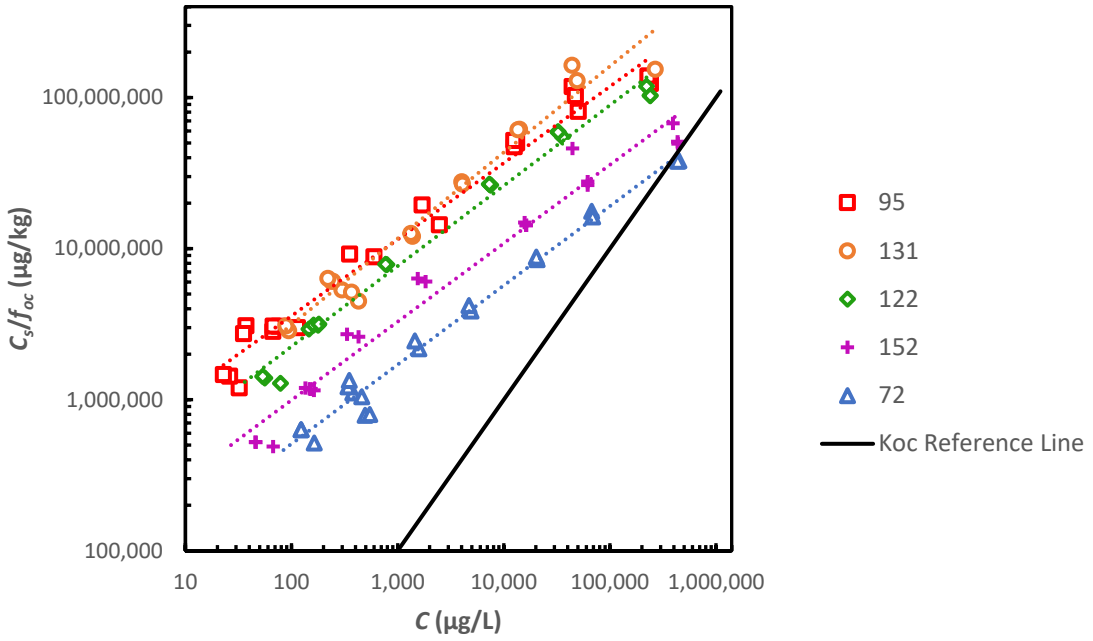

Figure 16. Sorption isotherms for TCE for representative samples of NAWC lithologies from 68BR. The sample numbers are the depth, in ft. The sorbed concentrations are normalized by f_{oc}.. The reference line is as described in the text. From Brotsch (2017).

Sorption isotherms for TCFE were measured independently and with TCE for sample 68BR-131. The isotherms for the two compounds have similar Freundlich exponents (Figure 17) and a consistent sorbed concentration ratio over the range of solution concentrations analyzed. (Pugnetti 2018). Over the concentration range 300-35,000 µg/L, the TCFE sorption coefficient is 1.6 times greater than the TCE sorption coefficient.

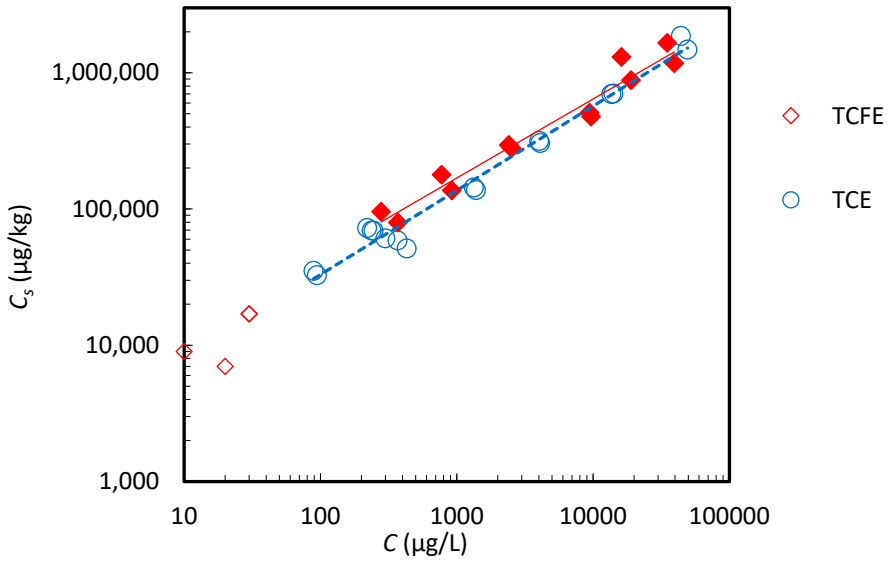

Figure 17. The TCE and TCFE sorption isotherms for 68BR-131 are shown. Data are not f_{oc} normalized. Data for TCE from Brotsch (2017) and TCFE from Pugnetti (2018). Solid symbols are used for the TCFE isotherm fit for comparison as described in the text.

Aerobic abiotic TCE:TCFE degradation rate comparison

Our TCE results are qualitatively similar to those reported by Pham et al. (2008). Relatively rapid TCE degradation occurred during the initial week (160 hours) of the experiments with approximately 55% of the TCE degraded in the systems with only TCE. The reaction slowed markedly after 7 days, presumably because the oxygen was exhausted. The chloride mass balance at the end of the experiments was good. The average chloride mass in solution at the end of the approximately two-week long experiments was 89% of the TCE mass removed from the vial, assuming that all TCE mass not recovered was completely dechlorinated. The primary products of this reaction are formic acid that is further degraded to CO_2 (Pham et al. 2009). The control vials (without pyrite) showed loss from the solution over time, most likely due to partitioning to the viton septa seal. This sorption apparently had a little effect on TCE degradation.

The chloride concentrations indicate that the moles of solvent degraded were consistent for the two compounds. The average chloride concentrations in vials with TCE only, TCFE only, or both TCE and TCFE were not significantly different (0.39-0.45 µmol with 0.07 µmol=average of 1 standard deviation within the replicate sets). However, the TCFE measurements showed greater concentration reductions than we observed for TCE. Sorption to the septum would be consistent with the observations.

From these experiments, we conclude that both compounds are degraded by the aerobic abiotic pathway at similar rates under the experiment conditions. However, significant sorption to the batch systems prevents determination of the rate coefficients from these experiments.

Although we take all precautions to maintain the anaerobic groundwater chemistry at the beginning of each field test, the above results show that the TCFE and TCE are likely to degrade at consistent rates if a trace of oxygen was introduced at the start of a field test. The results also show that degradation would cease when the oxygen was consumed. Additional work to develop TCFE as a tracer of this reaction pathway for more widespread application would require additional experimental work. However, because conditions favoring this pathway are not characteristic of the boreholes in our field tests, additional effort on this reaction pathway was not pursued further in the current project.

Biodegradation rate measurements

Initial batch tests conducted with groundwater and crushed rock incubated in wells 07BR, 68BR, and 15BR showed that anaerobic degradation rates of TCE and TCFE were best estimated as first-order kinetics (Figure 18;

Table 2). Figure 18 shows experimental results with crushed rock for 07BR as an example; similar degradation patterns were observed for other crushed rock experiments with first-order rate constants shown in

Table 2. Relative rates of degradation of TCE and TCFE generally were nearly equal in these microcosms where both the attached and planktonic *in situ* microbial communities were used in microcosm construction (Figure 19). The similar TCE and TCFE degradation rates indicate that TCFE is good reactive tracer of biodegradation rate for the field tests. The use of sand or crushed rock for 07BR microcosms did not cause a substantial difference in the TCE and TCFE degradation rates (

Table 2; Figure 19), although a delay was evident before the onset of degradation of both compounds in the microcosms constructed with incubated sand in well 07BR. A period of microbial growth probably was needed before biodegradation occurred in these sand microcosms. The low potential for sorption effects, however, made the sand microbial samplers desirable for collection of microbes within the packed interval during field testing with the packer-based tool.

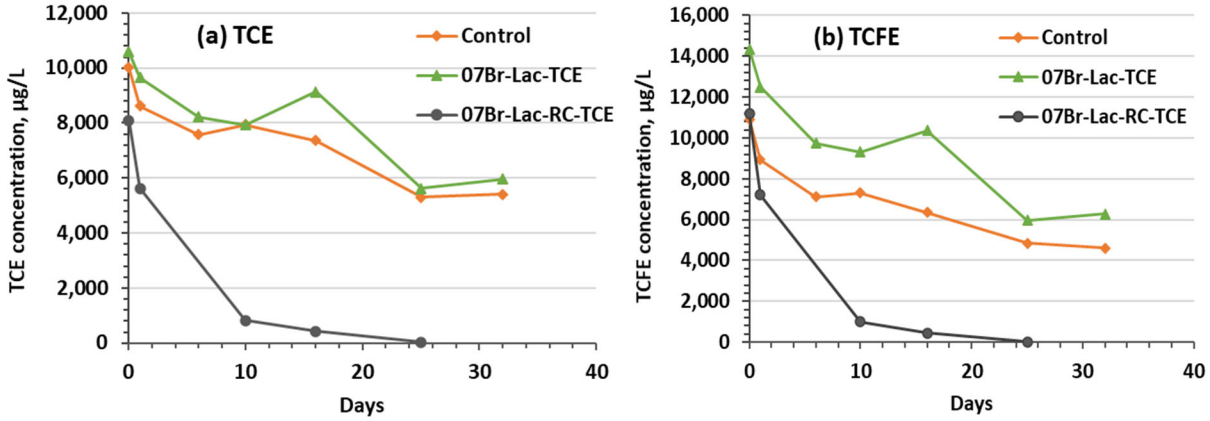

Figure 18. Concentrations of (a) TCE and (b) TCFE in microcosms constructed with groundwater and the in situ microbial community obtained from passive samplers containing crushed rock incubated in well site 07BR.

Table 2. Estimated first-order rate constants and half-lives ($t_{1/2}$) for degradation of TCE and TCFE in microcosms constructed for well sites (a) 07BR and (b) 68BR with groundwater only or groundwater plus the microbial community passively collected by incubation on crushed rock or sand, and with or without the addition of lactate. TCE and TCFE were added together in these microcosms to give combined initial concentrations of 10 to 20 mg/L.

	λ_{TCE} day^{-1}	$t_{1/2}$ TCE days	λ_{TCFE} day^{-1}	$t_{1/2}$ TCFE days	TCE:TCFE ratio
(a) 07BR					
Groundwater, lactate	0.017	40.8	0.025	27.7	0.68
Rock, lactate	0.20	3.47	0.21	3.33	0.96
Sand, lactate	0.26	2.69	0.20	3.47	1.29
Sand, no lactate	0.20	3.55	0.16	4.44	1.25
(b) 68BR					
Groundwater, no lactate	0.011	63.0	0.017	40.8	0.65
Rock, no lactate	0.11	6.5	0.12	5.6	0.86

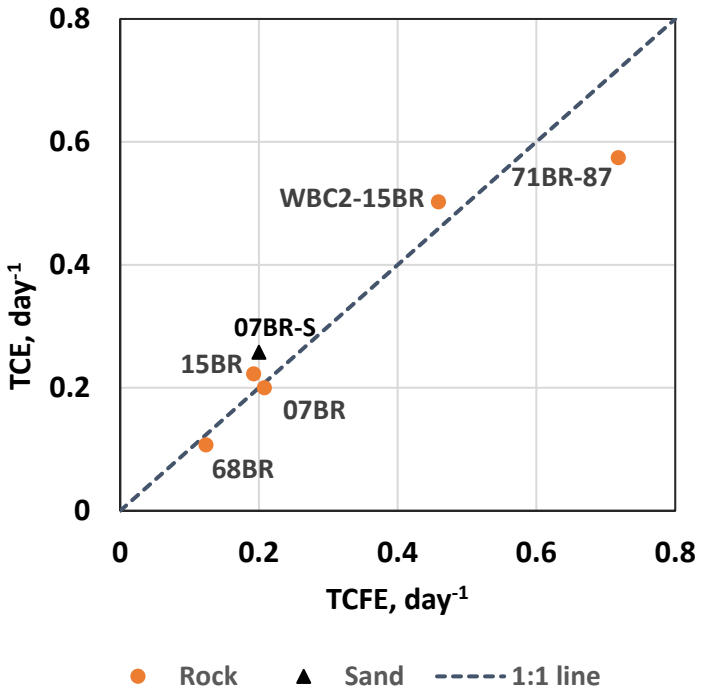

Figure 19. Estimated first-order rate constants for degradation of TCE compared to those for degradation of TCFE in microcosms constructed with the in situ microbial community and groundwater from the indicated well sites. Attached in situ microbial communities were obtained from passive samplers containing crushed rock, except for a second microcosm for well site 07BR constructed with incubated sand.

Degradation rates of TCE and TCFE were about a factor of 10 lower in the 07BR and 68BR microcosms constructed only with groundwater (planktonic microorganisms) compared to microcosms constructed with both the planktonic and attached microbial communities (

Table 2). These results support other studies that have shown dechlorinating bacteria favor being attached on surfaces rather than suspended in water (*Schaefer et al.*, 2010). The TCE degradation was slower than the TCFE degradation in the groundwater only microcosms, giving TCE:TCFE rate constant ratios of 0.65 to 0.68 (

Table 2). The addition of lactate to the groundwater microcosms did not appear to affect degradation rates of the TCE or TCFE, indicating that donor limitations were not a factor in the low degradation rates (

Table 2).

In contrast, batch tests conducted with sand incubated at depths of 85 or 87 ft in 71BR showed that anaerobic degradation rates of TCE and TCFE were best estimated as zero-order kinetics for the individual treatments (Table 3; Figure 20). For 71BR-85 at initial concentrations of about 30 μM, the TCE degradation rate was 1.9 and 2.1 μM/day, with and without the presence of TCFE (Figure 20; Table 3). Thus, TCFE did not appear to inhibit TCE degradation at these concentrations, which were representative of the field site concentrations of TCE. A microcosm treatment constructed with similar TCE and TCFE concentrations added to the groundwater only from a depth of 85 ft showed an 18-day delay in the onset of degradation (Figure 20). TCE and TCFE then degraded at a rate that was about 50 percent lower than observed in microcosms with the incubated sand and groundwater; degradation rates in these groundwater microcosms for 71BR85 were higher than observed in earlier experiments with 07BR and 68BR (

Table 2 and Table 3). The delay in degradation indicates that microbes capable of degrading the TCE and TCFE were present in the groundwater but in lower population density than in the attached community. In a treatment with nearly a factor of 10 higher initial concentrations, TCE and TCFE degradation also were delayed (until day 14); however, degradation of both compounds then occurred at a higher rate (8 to 11 μM/day) than those observed at lower initial concentrations (Table 3).

Table 3. Estimated zero-order rate constants (ψ) for degradation of TCE and TCFE and first-order rate constants (λ) for production of cDCE in microcosms constructed for well site 71BR with groundwater only or groundwater plus the microbial community passively collected by incubation of sand at a packed interval depth of either 85 ft (71BR-85) or 87 ft (71BR-87) depth.

			TCE Degradation		TCFE Degradation		cDCE Production
		ψ_{TCE}:ψ_{TCFE}	C	ψ	C	ψ	λ
Treatment description	Treatment name	ratio	μM	μM·day^{-1}	μM	μM·day^{-1}	day^{-1}
sand, TCE+TCFE	71BR85-SA-TCFE	1.38	33.3	1.9	28.7	1.4	0.21
sand, TCE only	71BR85-SA-TCE	--	28.2	2.1	--	--	0.31
sand, TCE+TCFE, WBC-2	71BR85-WBC2-TCFE	1.32	25.3	4.4	19.6	3.3	0.45
groundwater, TCE+TCFE	71BR85-LAC-TCFE	1.31	32.3	1.0[a]	24.5	0.99	0.12
sand, high TCE+TCFE	71BR85-SA-highTCFE	1.38	237	11[b]	158	8[b]	38
sand (90 ft), TCE+TCFE, lactate respiked	71BR87 sand		23	6.7 to 7.9		not calculated	not calculated

[a]Onset of significant degradation delayed until day 18; rate shown is maximum rate after the delay.

[b]Onset of significant degradation delayed until day 14; rate shown is maximum rate after the delay.

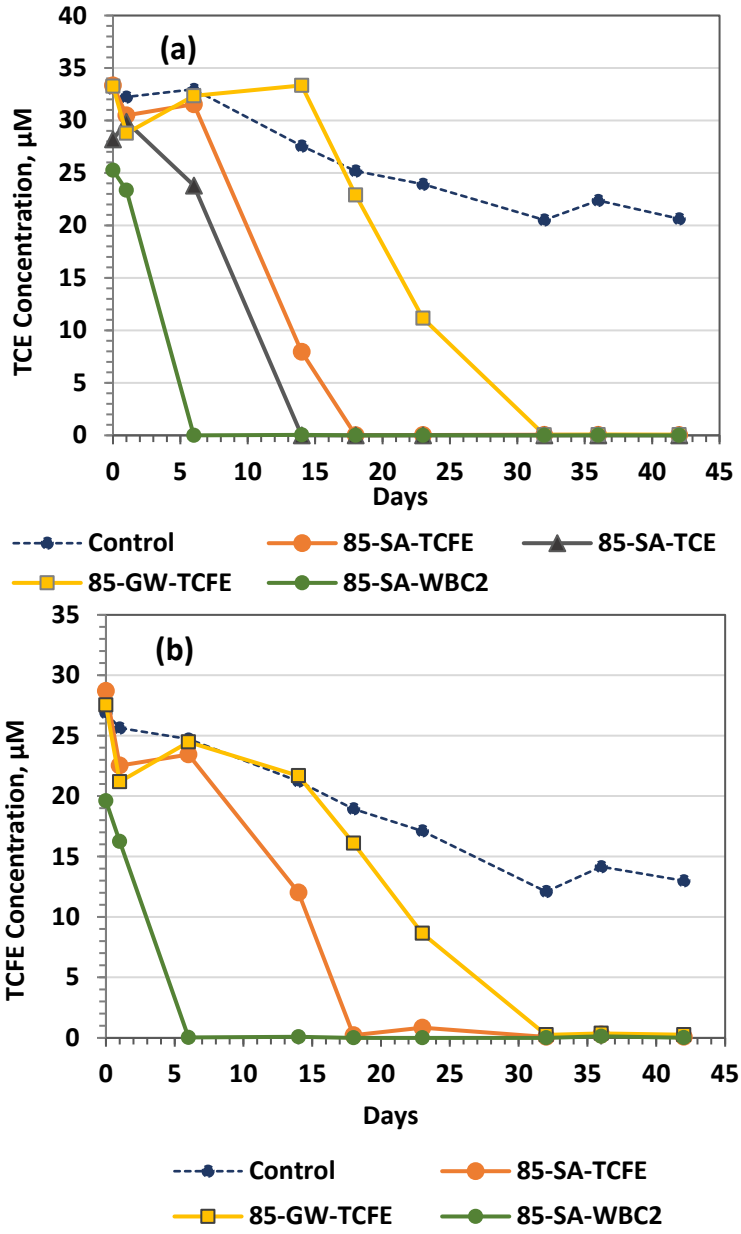

Figure 20. Concentrations of (a) TCE and (b) TCFE in microcosms constructed for well site 71BR with groundwater only or groundwater plus the microbial community passively collected by incubation of sand at a packed interval depth of 85 ft (71BR-85).

The only degradation product compounds observed in all the TCE and TCFE amended microcosms from 07BR, 68BR, and 71BR-85 were cDCE and DCFE, except that FE was also detected at later time points in the WBC-2 amended microcosms for 71BR-85 (Dugan et al. 2021). Figure 21 gives the cDCE and DCFE distributions in the 71BR-85 microcosms as examples. Except in the control treatment, approximately equimolar production of was observed as TCE concentrations declined (Figure 21). The cDCE production was best estimated by first-

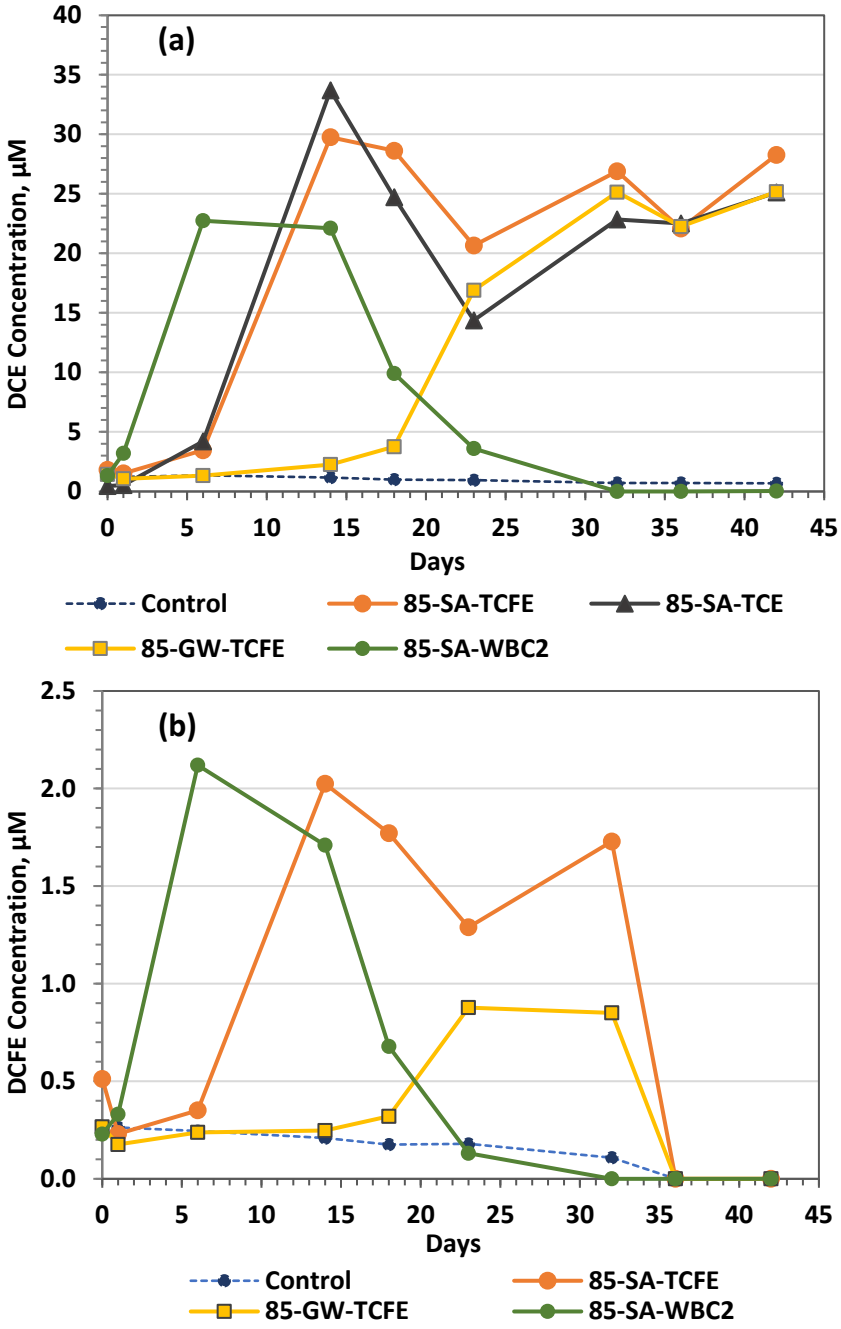

Figure 21. Concentrations of (a) DCE and (b) DCFE in microcosms constructed for well site 71BR with groundwater only or groundwater plus the microbial community passively collected by incubation of sand at a packed interval depth of 85 ft (71BR8571BR-8571BR85).

order kinetics (Table 3). Degradation of cDCE (and subsequent production of VC and ethene; see Dugan et al. 2021) was observed only in the treatment bioaugmented with the dechlorinating culture WBC-2, indicating an absence or insubstantial populations of bacteria capable of complete dechlorination of TCE at 71BR-85. Earlier microcosms for 07BR and 68BR also showed cDCE production without further degradation to VC, ethene, or ethane (Dugan et al.

2021). Thus, although anaerobic TCE degradation was relatively rapid, reductive dechlorination was not complete. In contrast to cDCE production, peak DCFE concentrations were much lower (by approximately a factor of 10) than the initial concentration of TCFE, and a subsequent decline in DCFE concentrations indicated further degradation (Figure 21). Standards were not available for other possible fluorinated daughter compounds for these experiments, however, besides fluoroethene. Other standards were obtained for the 71BR-87 microcosms that are discussed below.

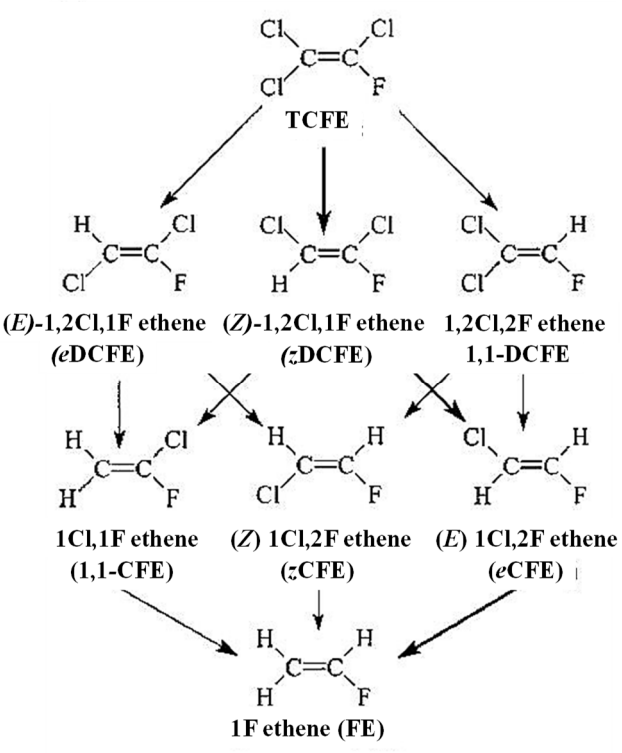

Figure 22. Possible anaerobic biodegradation products of TCFE (after Hageman et al. 2001)

Microcosms with sand incubated at a depth of 87 ft in 71BR during the field test were conducted largely to obtain a better mass balance for TCFE and identify DPs. Figure 22 shows the possible anaerobic biodegradation pathways for TCFE with acronyms used in this report. After addition of initial low concentrations of TCE, TCFE, and lactate, these microcosms were re-amended with TCE, TCFE and lactate and sampled over a 10-day period (TCFE and its DPs shown in Figure 22). Calculated zero-order degradation rates for TCE in these microcosms ranged from 6.7 to 7.9 µM/day and were higher than those observed for the 71BR-85 microcosms. Whereas others have reported TCFE degradation to primarily *z*DCFE (Hageman et al. 2001), degradation to *e*DCFE was primarily observed here. In addition, *z*CFE and/or 1,1-CFE production was observed after 72 hours (Figure 23). (The *z*CFE and putative 1,1-CFE were not resolved by the analytical method used here.) With cDCE degradation to VC and ethylene was observed within 10 days in the 71BR-87 microcosms with the native microbial community, indicating that re-spiking allowed enrichment of bacteria capable of complete dechlorination. After the 10-day sampling point, the microcosms were left undisturbed before sampling again at 55 days to analyze for specific possible terminal products (Table 4). The average initial TCFE concentration measured in the killed control microcosms was 22.4 $\pm$ 0.9 µM and in the active systems we measured 0.8 $\pm$ 1.5 µM total DCFEs from the first amendment. (There was no detectable TCFE remaining from the first amendment.) The sum of CFE and FE measured at day 55 ranged from 25 to 34 µM (Table 4). Thus, CFE and FE appear to be the major end products of TCFE degradation, and the high mass recovery of DPs at day 55 likely includes degradation of TCFE that was initially sorbed to the batch system. TCE degradation resulted in similar concentrations of VC at day 55 as the CFE produced from TCFE degradation, but ethylene concentrations were relatively low compared to the FE produced from TCFE degradation (Table 4). The 71BR-87 microcosm results confirm that the DCFEs are a

relatively minor DP of TCFE, degrading more rapidly to other daughter compounds than occurred for cDCE at this site.

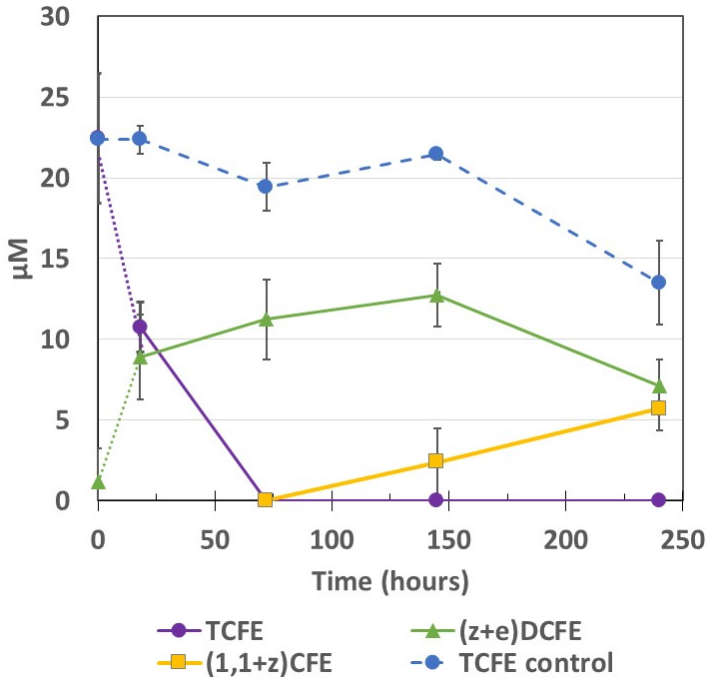

Figure 23. TCFE degradation in microcosms amended with the groundwater and microbial community passively collected by incubation on sand at a depth of 87 ft in 71BR. TCFE concentrations (in triplicate bottles) decreased (purple) as degradation product compounds concentrations increased (combined *z*DCFE and *e*DCFE concentration shown, green). Yellow line shows production of 1,1CFE and *z*CFE combined. TCFE in killed controls is shown in blue. The error bars are 1σ. Initial concentrations of TCFE and (*z*+*e*)DCFE are estimated. The initial (*z*+*e*)DCFE is the concentration measured 24 hr before the second addition of TCFE. The initial TCFE concentration is estimated as the sum of the observed concentrations of TCFE, *z*DCFE and *e*DCFE at 18 hour, the first measurement following the second TCFE addition. Measurement of the CFEs began at 72 hr.

Table 4. Concentrations (in µM) for daughter compounds analyzed at 55 days in triplicate 71BR-87 microcosms amended with TCE and TCFE. Analyses were conducted to assess production of terminal biodegradation products; TCE, TCFE, cDCE, and the DCFEs were not analyzed in these samples.

	VC	ethylene	CFE	FE	Total TCE DPs	Total TCFE DPs
A-1*	11.5	5.80	13.7	20.0	17.3	33.6
A-2*	0.000	9.60	1.93	23.2	9.60	25.1
A-3*	25.7	4.57	24.4	4.82	30.2	29.2

Microbial communities

To evaluate the microbial samplers as matrices for microbial attachment, microbial communities were obtained from crushed rock and sand microbial samplers that were placed above the packed interval in borehole 07BR, adjacent to each other, and allowed to incubate over the same time period (Figure 24). Another microbial sampler containing sand was placed within the packed interval at 07BR. Overall, the microbial community analyses showed similar composition among the three samplers, with the crushed rock and sand microbial samplers placed above the packed interval appearing the most similar (Figure 24). Total microbial abundance, compared as the total reads, was about 80,000 in the crushed rock sampler and 110,000 in the sand sampler placed above the packers, indicating that the sand and crushed rock were equally favorable as attachment substrates for microbes (Figure 24). The microbial abundance recovered from the sand sampler within the packed interval was lower (about 60,000 total reads) but sampled a narrower depth within the packed interval.

The microbial community composition was also monitored over time in microcosms that were constructed with sand that had been incubated in the packed test interval 71BR-85 for the duration of the field test and compared to the *in situ* microbial community (Figure 25). Community compositions were compared in two sets of microcosms that were amended with moderate and high concentrations of TCE and TCFE, 71BR-85-SA-TCFE and 71BR-85-SA-high TCFE (Table 3), to try to discern the major microbial group involved in TCE and TCFE degradation. The moderate TCE and TCFE concentrations amended to microcosm 71BR-85-SA-TCFE corresponded well to the observed concentrations in 71BR-85 and 71BR-87. A family called MA-28-198C in the Desulfuromonadia class was the major group that showed a large change in relative population abundance with time in the microcosms that corresponded to when the greatest degradation of TCE and TCFE occurred. In the microcosms that contained high concentrations of TCE and TCFE, the onset of degradation was delayed until after day 14; an increase in the population of MA-28-198C was also delayed in this microcosm compared to the microcosm with moderate TCE and TCFE concentrations. MA-28-198C are closely related to *Geobacter* species, known partial dechlorinators that have been reported by others to be dominant near DNAPL source areas.

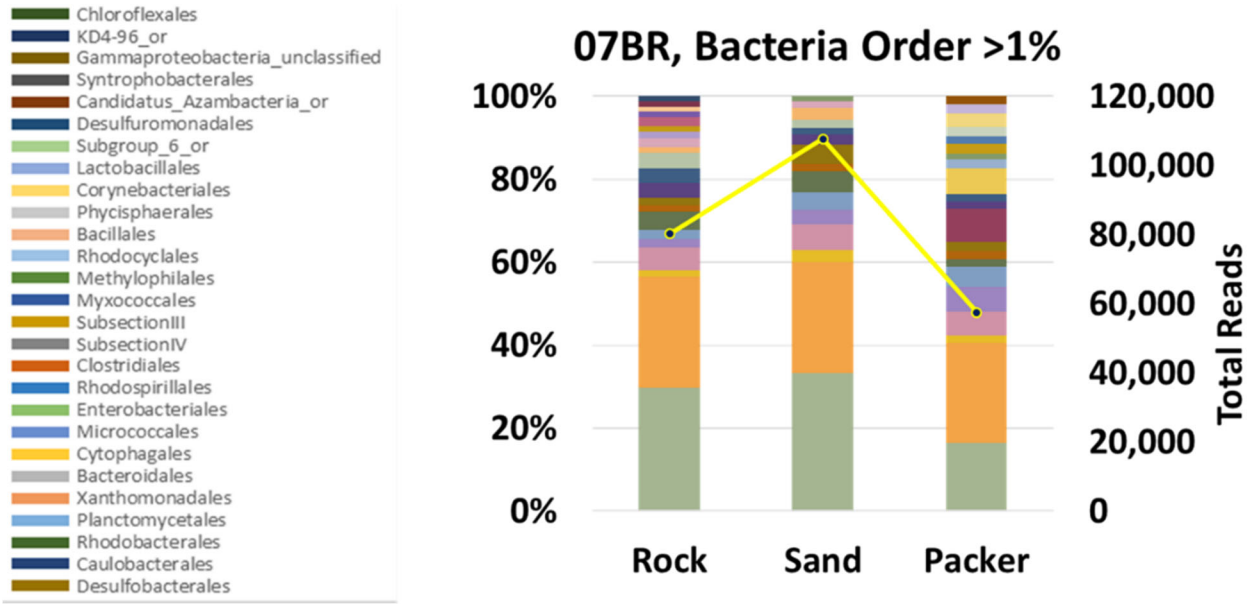

Figure 24. Microbial community composition at the order level in passive microbial samplers incubated in borehole 07BR, including samplers containing crushed rock and sand samplers that were placed adjacent to one another above the packed interval and a third sampler containing sand that was incubated within the packed interval.

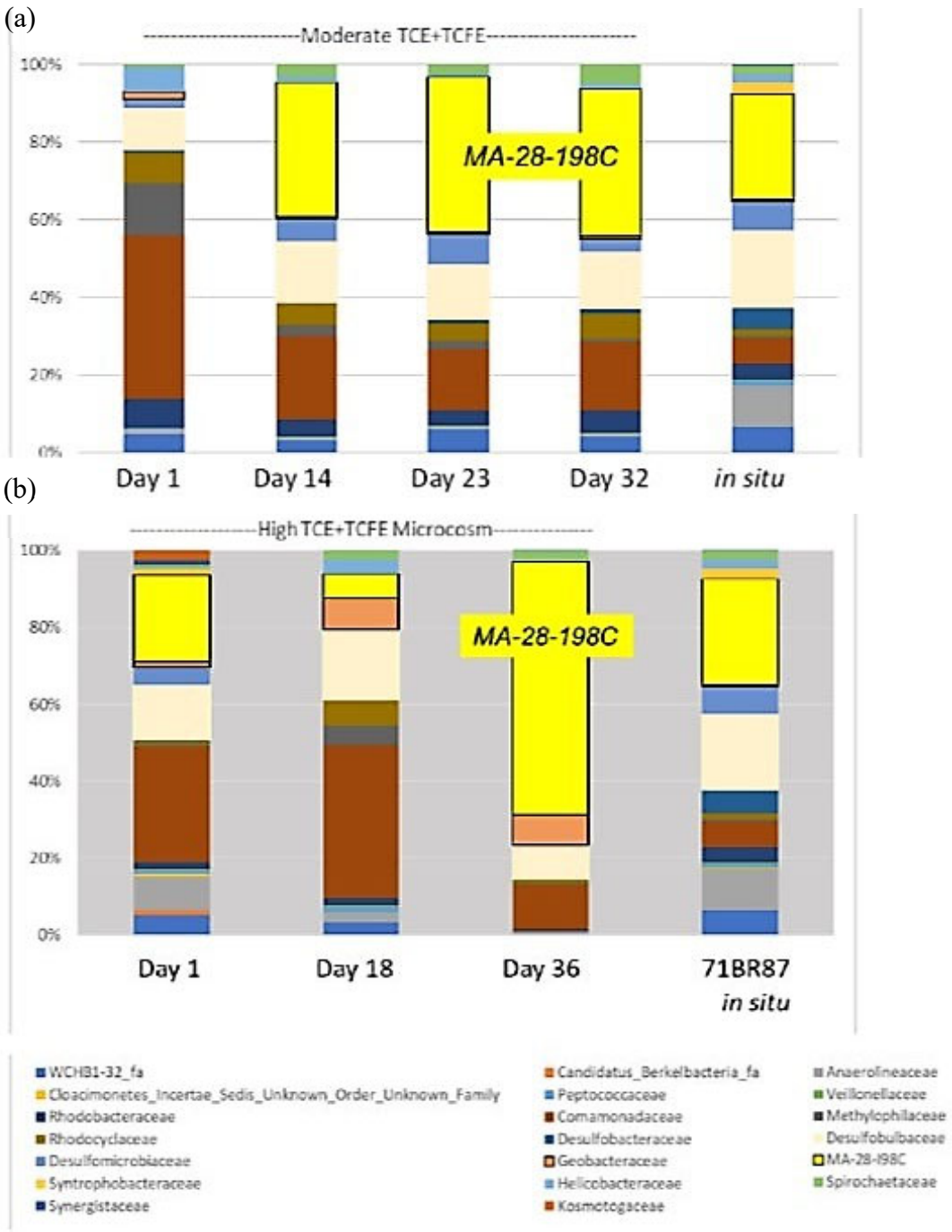

Figure 25. Microbial community composition at the family level in a sand microbial sampler incubated in the packed interval during the field test in 71BR-87 (in situ) compared to compositions over time in microcosms constructed with sand from the 85 ft depth in 71BR-87 and amended with (a) moderate concentrations of TCE and TCFE and (b) high concentrations of TCE and TCFE at day 0. The microcosm treatments correspond to 71BR-85-SA-TCFE and 71BR-85-SA-highTCFE in Table 3.

Field Test Results

Field Tests in 71BR at 85 and 87 ft depths

The two title tests were conducted in the same borehole over adjacent intervals and in successive summer seasons. We chose this approach to evaluate test reproducibility to the extent possible. Because the tested interval is affected by the test, it is not possible to evaluate test reproducibility by replicating the test in the same interval. We view that these two tests are as near to duplicates as possible for a field test. The test intervals are in the same lithologic unit and have the same concentration history. (Both test intervals were in Zone E during the monitoring period that preceded the tests.) A packer was maintained at approximately the depth of the lower packer of the 71BR-85 test until we began the 71BR-87 test in order to maintain the typical borehole geochemical and contaminant conditions between the tests.

A test was also conducted in 07BR at the 49 foot depth (07BR-49). The Br tracer in this test indicated poor mixing in the test interval at the start of the test. For this reason, this tracer test was not modelled. The Br and VOC results and historical data for the 07BR-49 test are provided in Appendix A and additional details about it are in Kiekhaefer (2018).

The VOCs diffused into the matrix from the borehole during the decade from well drilling to the beginning of our tests. The monitoring data is therefore critical to loading the matrix and controlling the back diffusion. The historical VOC data for zone E that includes the test intervals from drilling to the start of each of the two field tests is shown in Figure 26. The historical average concentrations for VOCs and other analytes were calculated from the relatively stable period of late 2008-2012 (

Table 5).

After 2011, sampling frequency decreased to annual or biennial and sampling dates coincided with times that Well 15BR of the P&T system was off, which was not a usual occurrence. Pumping tests at the site previously showed that the permeable strata within 71BR-E had a strong hydraulic connection to Well 15BR Tiedeman et al. (2010). The historical data suggests that the pumping rate in Well 15BR also affects the VOC concentrations in 71BR-E. The sampling in 2013 occurred after one week shut down and the TCE and cDCE concentrations were below the historical averages while the VC concentration was similar to the historical average concentration. Prior to collection of the 2015 sample, the pump was off for a year. The cDCE and VC concentrations were approximately two and ten times greater than the historical average concentrations, respectively, while the TCE concentration was less than half of the historical average concentration (Kiekhaefer. There was a significant change in the LHG concentrations that mark active anaerobic dichlorination reactions as well; the methane and ethene concentrations increased to nearly 60 µg/L and nearly 20 µg/L, respectively, compared to historical averages of 10 µg/L and 2 µg/L, respectively. No samples were collected between 2015 and our 2017 pre-test samples. We use the approach of connecting the concentrations on sampled dates (model lines in Figure 26) for the base case of our model calibrations (described in a later section).

At >20,000 µg TCE/L, the pre-test concentration for the 71BR-85 test was approximately 80% greater than the historical average concentration. In contrast, the pre-test concentration for the 71-BR-87 test was similar to the historical average concentration. The pretest concentrations of the measured analytes are listed in

Table 5.

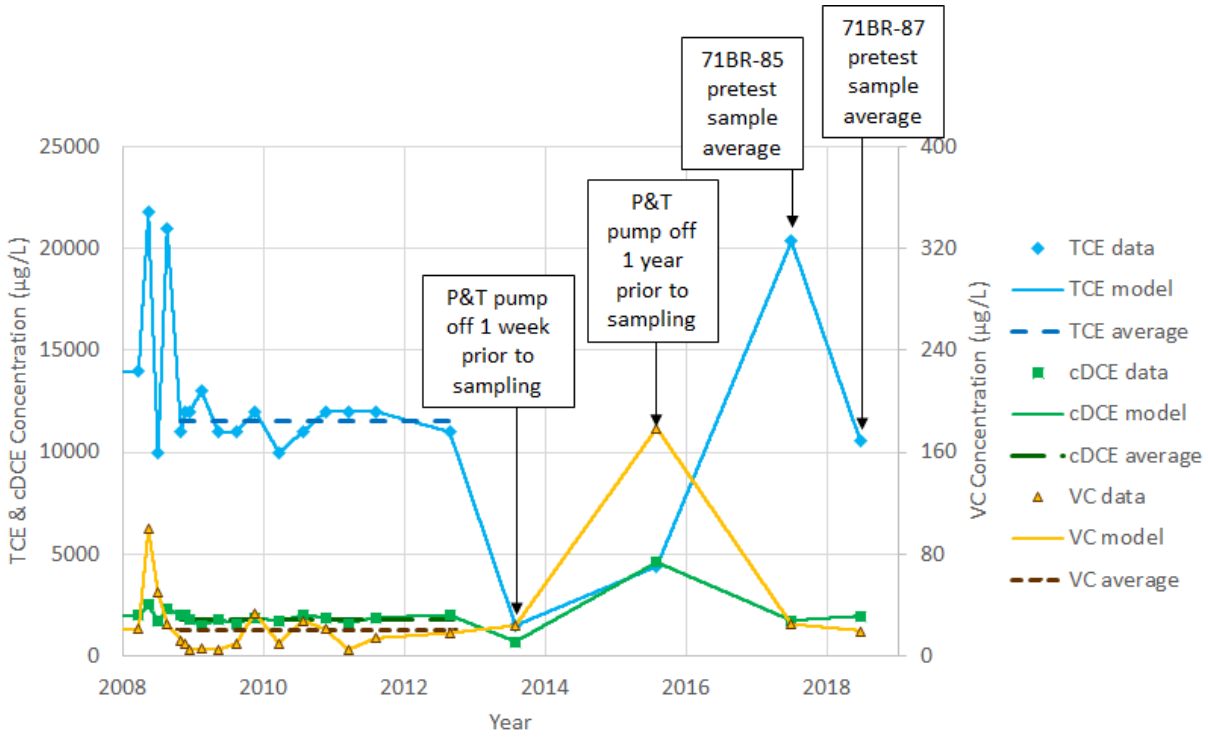

Figure 26. The TCE and DPs concentrations for borehole 71BR-E (zone E) from drilling to the start of the test at 87 feet. Note that the pre-test concentration for the 71BR-85 test is nearly double that of the 71BR-87 test. The periods used for the reported average concentrations and periods when the P&T pump in 15BR was off are also noted. After (Allen-King et al. In revision)

During both field tests the nonreactive tracer concentrations declined throughout (Figure 27). The modestly different initial Br concentrations (~20%) are because we diluted the initial, highly concentrated tracer solution by different groundwater volumes in the field. The reactive tracer, TCFE, concentration declined more rapidly than the Br to <30 µg/L by 97 days in the 71BR-85 test (Figure 28). The more pronounced TCFE decline is a consequence of sorption and biodegradation that will be discussed in later sections. All samples analyzed by the GC/MS (28 days and $\geq$ 50 days) identified low concentrations of dichlorofluoroethenes (DCFEs) that are TCFE biodegradation products.

Table 5. Historical and pre-test average concentrations for the 71BR-85 and 71BR-87 tests.

Parameter	Units	Historical Average	71BR-85 Pre-Test Average	71BR-87 Pre-Test Average
VOCs				
TCE	µg/L	11500	21000	10600
cDCE	µg/L	1800	1800	1960
VC	µg/L	20	<25[1]	20
TCFE	µg/L	NS[2]	<25	NA[3]
Hydrocarbons & DOC				
Methane	µg/L	10	<35	<10
Ethylene	µg/L	2	<35	<10
Acetylene	µg/L	NS	<35	<15
Ethane	µg/L	0.6	<35	<25
DOC	mg/L	0.6	0.5	0.5
Field parameters				
pH	-	7.48	7.37	7.25
Specific Conductance	µS/cm	500	525	512
Dissolved Oxygen	mg/L	0.1	<0.05	<0.05
Fe(II)	mg/L	0.5	0.25	0.65
Major ions & Bromide				
Calcium	mg/L	50	NS	56
Magnesium	mg/L	20	NS	22
Sodium	mg/L	15	NS	16
Potassium	mg/L	2	NS	2.4
Chloride	mg/L	55	60	59
Sulfate	mg/L	30	30	30
Bicarbonate	mg/L	175	180	170
Bromide	mg/L	0.05	0.25	NS

[1]Below quantification limit (limit listed)

[2]Not sampled

[3]Not applicable

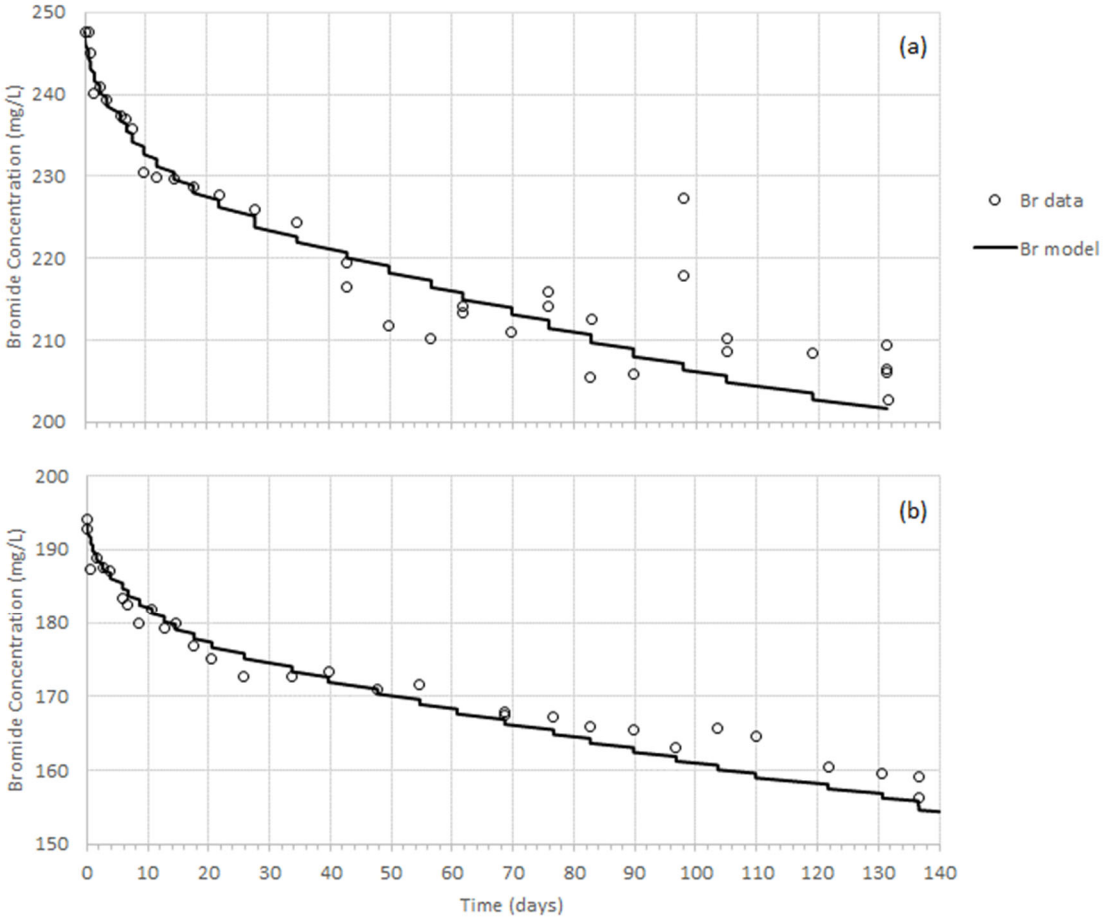

Figure 27. Nonreactive Br tracer concentrations with time during the a) 71BR-85 and b) 71BR-87 tests, respectively.

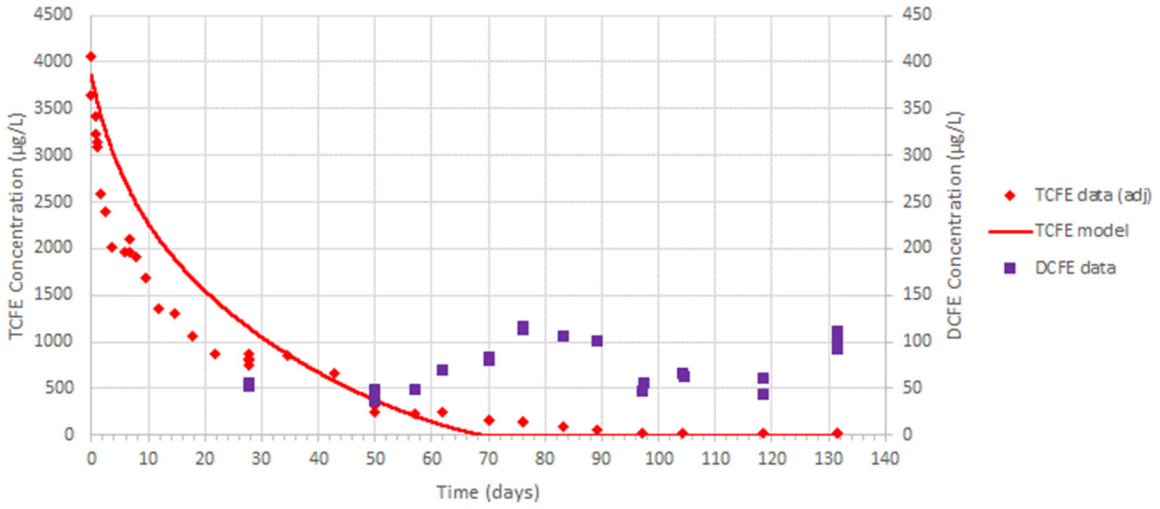

Figure 28. Sorbing and biodegradable tracer TCFE concentrations during test 71BR-85. Discussion about the degradation product is later in the text.

The TCE concentration patterns during the tests show many similarities. The TCE concentration rose rapidly during the first 10 days then plateaued at a maximum at <20% of the pretest concentration (Figure 29) and then declined. The cDCE concentrations increased throughout the duration of both tests, surpassing the pretest concentrations by 30-40 days. The final cDCE concentrations approached 50% of the pretest TCE concentration by the end of the tests (48% and 44% of the pretest TCE concentration for the 71BR-85 and 71BR-87 tests, respectively). The VC concentrations were initially low, similar to the pretest concentration; following the TCE concentration decline, the VC concentration increased relatively rapidly, although the concentration was low throughout the test (<200 µg/L). TCE biodegradation during the test is evidenced by the cDCE concentration surpassing the pretest concentration. The cDCE build up indicates that biodegradation to VC was much slower.

The most obvious differences between the two tests are the pre-test TCE concentrations and the rate of TCE decline 20 days into each test. Inclusion of TCFE in the 71BR-85 test is another difference. These differences are further discussed following presentation of the simulation results.

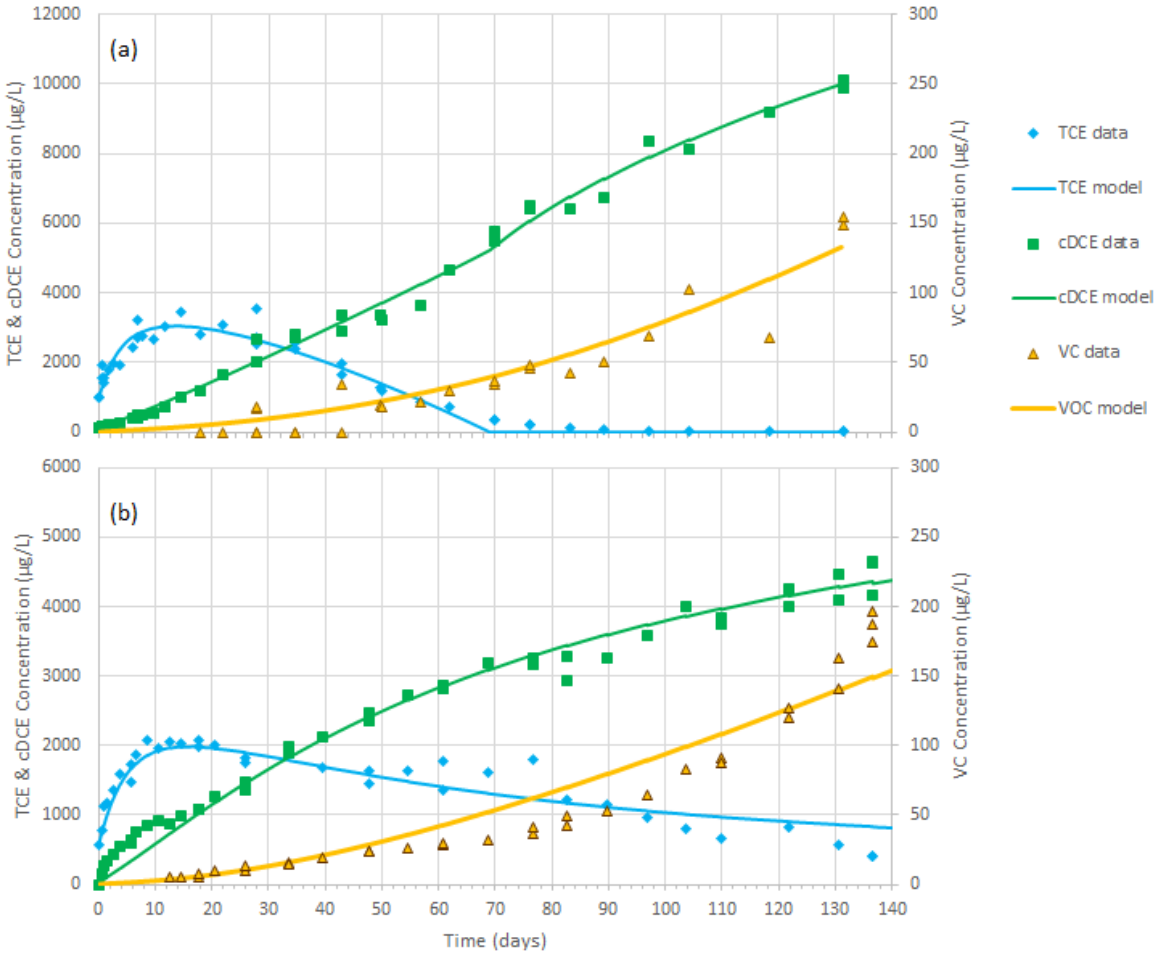

Figure 29. The TCE, cDCE and VC concentrations during the a) 71BR-85 and b) 71BR-87 test. Note the difference in TCE concentration scale between panels.

Parameters estimated

We estimate the diffusion and sorption coefficients, and biodegradation rate coefficients for each of the tests, as listed in Table 6. The corresponding models are shown as lines in Figure 27-Figure 29. For each test, the model was calibrated simultaneously to the concentrations of Br, TCFE (for the 71BR-85 test), TCE and the biodegradation products cDCE and VC. We assumed a reasonable porosity for the mudstone at the field site of 0.05 (Shapiro et al. 2017) and estimated the tortuosity factor.

The estimated tortuosity factors are the same for the two tests. Thus, the effective diffusion coefficients, the product of each compound's free water diffusion coefficient and the estimated tortuosity factor, used in the simulations are the same for the two tests. The TCE K_d estimated from the 71BR-85 test (2.7 L/kg) is within a factor of two of the K_d estimated for the 71BR-87 test (4.0 L/kg). The effective diffusion coefficients used in the simulations are the product of each compound's free water diffusion coefficient and the estimated tortuosity factor.

Table 6. Simulation and estimated parameters (bold) of the 71BR-85 and 71BR-87 tests are listed. Sorption coefficients for VOCs are estimated by a fixed ratio to the estimated TCE K_d.

Compound	τ^a [/]	K_d ($L \cdot kg^{-1}$)	Biodegradation rate coefficient
71BR-85 test [b]			
Br	**0.20**	0[c]	0[c]
TCFE		4.4	**1.16 μM·day^{-1}**
TCE		**2.7**	
cDCE		0.55	**3.78 x 10^{-9} s^{-1}**
VC		0.22	Assumed 0
71BR-87 test			
Br	**0.20**	0[c]	0[c]
TCE		**4.0**	**4.4 x 10^{-7} s^{-1}**
cDCE		0.80	**7.9 x 10^{-9} s^{-1}**
VC		0.32	Assumed 0

[a] Assumed porosity=0.05.

[b] For this test, we show the calibration results for the adjusted [TCFE], simultaneous [Br] and [CVOC] case, which is Case I in Allen-King et al. (in review). The different cases all gave similar results, as discussed in the cited manuscript.

[c] Known.

The different TCE concentration decline patterns are best fit by different biodegradation kinetic formulations. The rapid TCE concentration decline to 210 μg/L by 76 days during the 71BR-85 test indicated zeroth order kinetics (Figure 29a). The slower rate of TCE concentration decline during the 71BR-87 test was better fit by first-order kinetics (Figure 29b).

Concentration and mass profiles

The model generates the concentration profiles of TCE and its DPs in the matrix that illustrate the effects of diffusion, sorption and biodegradation (in the borehole). The concentration distributions at the initiation of each of the two tests are shown in Figure 30.

In both tests, the TCE concentrations are very high near the interface and decline sharply with distance; TCE is mostly <5 centimeters (cm) from the borehole interface. The cDCE is mostly <7 cm from the interface, and the VC extends about 15 cm into the matrix. The variable compound extents into the matrix reflect both differences in retardation factors and borehole concentrations that drive diffusion.

The most dramatic differences between the profiles of the two tests reflect relatively recent pre-test borehole concentration history, such as the two-fold difference in maximum TCE

concentration that reflects pre-test conditions (Figure 26 and Figure 30). The reduced maximum VC concentration in the 71BR-87 compared to the 71BR-85 test reflects the passage of an additional year since the high concentration perturbation that occurred in 2015 (Figure 26).

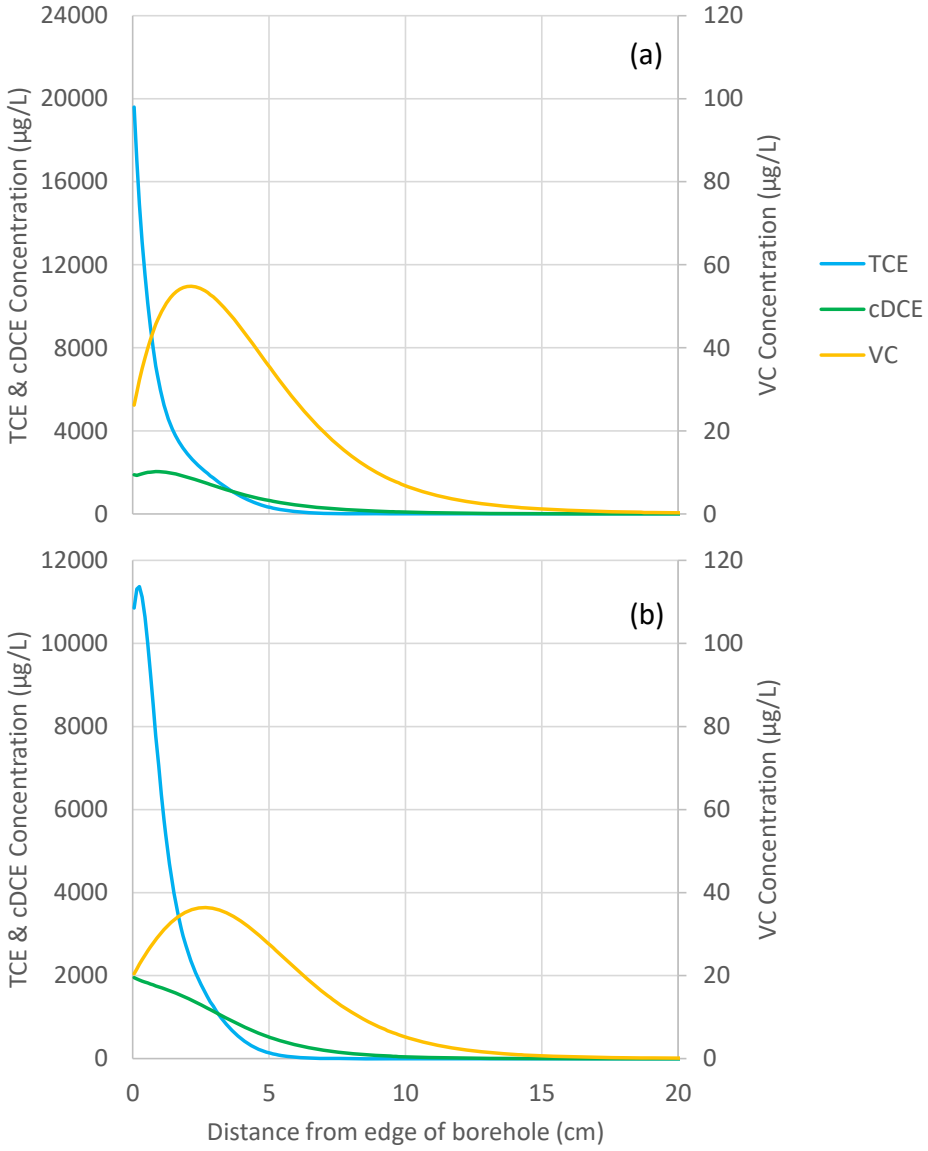

Figure 30. Simulated TCE and DP concentration profiles in the matrix at the start (t=0 days) of each of the two tests: (a) 71BR-85, (b) 71BR-87. Note the difference in vertical axis scale. Panel (a) from (Allen-King et al. In revision)

Anaerobic abiotic degradation in matrix

The products of abiotic degradation (ethene, ethane, and acetylene) were not detected in the test interval during our tests. We ask the question: could abiotic degradation occur at a rate previously determined in laboratory experiments with NAWC samples and be undetected in our field test? We use the numerical simulation of the 71BR-85 test as the base case with abiotic degradation rate parameters determined in laboratory experiments with NAWC rocks by Schaefer et al. (2013).

Schaefer et al. (2013) assume that the abiotic degradation of TCE sorbed to the matrix occurred. The sorption in Schaefer et al.'s (2013) experiments were much lower than what we found in our field tests. This entirely consistent with the nonlinear sorption that we observed because the laboratory experiments were conducted at much greater TCE concentrations (0.0023M or approximately 300 mg/L) than the field tests. However, contaminants sorbed to nonreactive sites are generally considered sequestered or protected from degradation. The abiotic degradation is caused by ferrous iron containing minerals while TCE sorbs primarily to organic matter. Hence, while the compound is sorbed and retarded, it is not available for abiotic reaction and only the dissolved phase is available to interact with a reactive site. Here, we consider both possibilities. To avoid confusion, we begin with the basic governing equation in one dimension, as applied by Schaefer et al. (2013) and then consider its application to two cases, degradation of either dissolved or sorbed TCE.

The governing transport equation for diffusion with sorption and first-order reaction of dissolved and sorbed phases in the matrix for one-dimensional transport is:

$$R\frac{\partial C}{\partial t} = D\frac{\partial^2 C}{\partial x^2} - \Lambda C - \frac{\rho_b \overline{\Lambda}}{\theta} C_s \qquad (9)$$

where C_s is the sorbed concentration, and the other variables are as defined in the *Simulation method* section. Additionally, here we eliminate the *i* subscripts for simplicity. Assuming linear sorption and substituting the retardation factor expression (eq.(2)) yields

$$R\frac{\partial C}{\partial t} = D\frac{\partial^2 C}{\partial x^2} - \left(\Lambda + \frac{\rho_b \overline{\Lambda} K_d}{\theta}\right) C \qquad (10)$$

Abiotic degradation of sorbed phase

For degradation of sorbed phase only, eq. (10) becomes

$$R\frac{\partial C}{\partial t} = D\frac{\partial^2 C}{\partial x^2} - \frac{\rho_b \overline{\Lambda} K_d}{\theta} C \qquad (11)$$

They introduce $k' = \rho_b \overline{\Lambda} K_d$ so that eq. (11) becomes:

$$R\frac{\partial C}{\partial t} = D\frac{\partial^2 C}{\partial x^2} - \frac{k'}{\theta} C \qquad (12)$$

They reported laboratory measured values of k' for mudstones from NAWC and they suggested that $k'=5 \times 10^{-9}$ s^{-1} was a reasonable value to expect for the long-term rate (Schaefer et al. 2013).

We use data from Schaefer et al. (2013) to compute the $\overline{\Lambda}$ needed for our simulations from the k', K_d, and ρ_b observed in their experiments. Schaefer et al. (2013). reported ρ_b =2.6

kg/L and TCE K_d values ranging from 0.10 to 0.17 L/kg for light gray mudstone and from 0.081 to 0.086 L/kg for dark gray mudstone (Schaefer, pers. comm.). We assume 0.1 L/kg as a reasonable K_d for their laboratory experiments and compute the value of $\overline{\Lambda}$ as 2×10^{-8} s^{-1}.

Abiotic degradation of dissolved phase

If abiotic degradation occurs from the dissolved phase only, then eq. (12) becomes

$$R\frac{\partial C}{\partial t} = D\frac{\partial^2 C}{\partial x^2} - \Lambda C \qquad (13)$$

Comparing the dissolved phase degradation eq. (13) with the sorbed phase degradation eq.(12), we see that if Λ in eq. (13) has the same value as k'/θ in eq.(12), the two equations are identical. Therefore, eq. (13) could fit the Schaefer et al. (2013) laboratory data equally well as eq. (12). If we want to explain Schaefer et al. (2013) laboratory result under the assumption that abiotic degradation occurs only in the dissolved phase, we would use $\Lambda = 6.6\times 10^{-8}$ s^{-1}. Here, we use the average θ=0.076 determined from their (Schaefer et al. 2013) reported values of 0.064 for light gray mudstone and 0.089 for dark gray mudstone.

Schaefer et al. (2013) also assumed that the ADP sorbed to the matrix with a K_d that was the same as the relatively low TCE K_d, in their experiments that used very high TCE concentrations. Here, we assume that ADP sorption is negligible.

Calibrations with abiotic degradation

We calibrated the results of the 71BR-85 test with abiotic degradation in either the sorbed or dissolved phase and with no ADP sorption to yield the following two Cases:

Case D – abiotic degradation of dissolved phase TCE
Case S– abiotic degradation of sorbed phase TCE

The results are compared to the calibration that had no abiotic degradation (termed Case I). No VC biodegradation is assumed in all cases.

Overall, the fit between simulated and observed VOC concentrations are good. Case D gives virtually the same fit as Case I and Case S give a slightly poorer fit to the data (judged by the sum of squares of weighted residuals), but nonetheless can be considered good (Table 7). Table 7 summarizes the parameters for these calibrations.

Table 7. Calibrated results (parameters estimated) for cases with abiotic degradation of TCE in the matrix.

	Case I	Case D	Case S
Assumed			
TCE phase degrading	no abiotic degradation	dissolved	Sorbed
Rate constant (s-1)	NA	$\Lambda = 6.6 \times 10^{-8}$	$\overline{\Lambda} = 2.0 \times 10^{-8}$
Estimated			
Tortuosity factor	0.197	0.195	1.4
TCE K_d (L/kg)	2.73	2.81	6.85
(TCE+TCFE) 0^{th}-order biodegradation rate constant (µM/day)	1.16	1.16	1.19
cDCE 1^{st}-order biodegradation rate constant (s^{-1})	3.78×10^{-9}	3.77×10^{-9}	3.65×10^{-9}
Sum of squares of weighted residuals	9.84×10^{6}	9.82×10^{6}	1.07×10^{7}

If only dissolved phase TCE is abiotically degraded (Case D), the simulated ADP concentration rises from 0 µmol/L to 1.0 µmol/L on day 130 (Figure 31). Assuming that the ADP is composed of equal parts (one-third each) of ethane, ethene, and acetylene as Schaefer et al. (2013) found, then the simulated ADP concentrations would be 0.33 µmol/L each or 8.7-10.0 µg/L of each ADP. These concentrations are less than MDL of the analytical method used during the field test. Hence, abiotic degradation at this rate could have occurred during the test without detection of ADP. The results of the simulation and field test are consistent.

If only sorbed TCE is degraded (Case S), the simulated ADP concentration rises to 22.7 µmol/L on day 130 (Figure 31). The simulated ADP concentration for Case S is 23 times greater than for Case D. In Case S, the term k' is 4×10^{-7} s^{-1} and is much greater than the long-term estimate suggested by (Schaefer et al. 2013). This is due to the significantly higher value of K_d in our field test compared to the K_d determined by Schaefer et al. (2013).

The term k'/θ in eq. (13) for Case S is 7×10^{-6} s^{-1}. By contrast, the term Λ in eq. (14) for Case D (that corresponds to k'/θ for Case S) is much lower at 6.6×10^{-8} s^{-1}.

If we assume an equal distribution between the three ADP, the simulated ethene and ethane concentrations for Case S at the end of the test would be 200-228 µg/L of each compound. These concentrations are well above the detection limits. However, these compounds were not detected during our experiment. Furthermore, these concentrations are more than two orders of magnitude greater than the observed historical average concentrations of ethene and ethane (

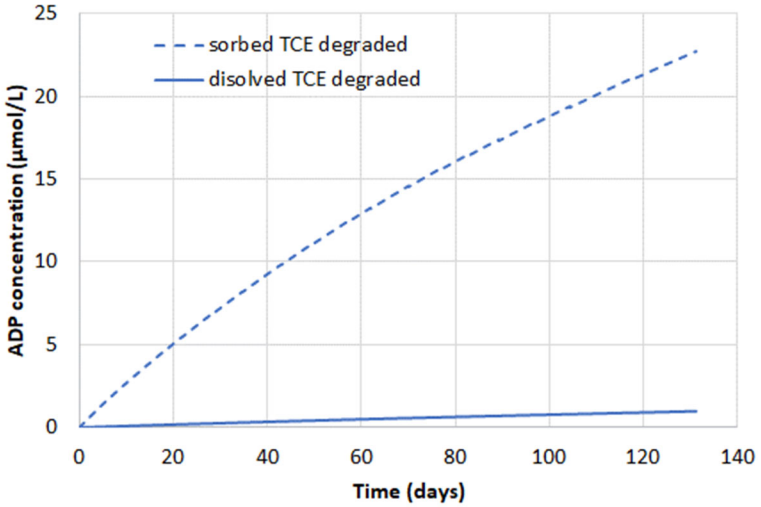

Figure 31. Simulated abiotic degradation product accumulation during test 71BR-85. In the D or S case, abiotic degradation of only the dissolved or sorbed phases occurs, respectively. The maximum concentration of ADP for dissolved degradation is 1.0µg/L.

Table 5). In order for this rate of abiotic degradation to have occurred during our experiment without ADP detection, further transformation of all ADPs would need to have occurred at a rate sufficient to cause them to remain less than detectable. In other words, the ADP transformation rate in the borehole would have to equal or exceed the ADP production rate in the matrix. Ethene and acetylene are known to transform under anaerobic conditions. Ethene can be transformed to either ethane, another ADP, or carbon dioxide. Aerobic ethane metabolism in groundwater is well known, but less so for anaerobic transformation. In order to remain below the detection limits in our tests, it appears that the primary abiotic degradation pathways would need to favor acetylene and ethene, and both would need to further degrade via pathways that do not produce significant ethane.

The calibration for degradation of sorbed TCE also gives an unreasonably large tortuosity factor (Table 1Table 7), or $\tau\theta$=0.07. This is an order of magnitude larger than the highest value from independent laboratory measurements that also used NAWC rocks (Schaefer et al., 2013).

Our simulations show that abiotic degradation of dissolved TCE at a rate consistent with the prior laboratory studies is entirely consistent with our field test. However, based on all of the above reasoning, we conclude that abiotic degradation of sorbed phase TCE at a rate consistent with prior laboratory study is unlikely. This same conclusion applies to degradation of dissolved TCE at a greater rate (comparable to the rate of sorbed TCE degradation).

Discussion

Comparison between field and independently determined parameters

Allen-King et al. (In revision) compared parameters estimated from the 71BR-85 test to parameters measured in independent laboratory studies that were conducted either as part of this project or published. These comparisons are a means to evaluate the reasonableness of the results. We summarize the comparisons briefly here. Because there was not core sample from the 71BR borehole on which to measure matrix properties, we compare the matrix measurements to published measurements for the NAWC gray mudstones.

The physical and chemical properties of the gray mudstones are characterized by variability over approximately an order of magnitude over relatively small scales, including within units (Table 8) (Shapiro et al. 2017; Shapiro and Brenneis 2018). The porosity that we used to model the field test is near the middle of the range characterizing the gray mudstones (majority of samples between 0.01-0.1, Shapiro et al. 2017).

Table 8. Comparison between parameters for the matrix estimated from the 71BR-85 test and values in published studies for gray mudstones from the NAWC

Parameter	Field Test Result	Laboratory Measurements	Reference(s)
θ	0.05[a]	80% of samples within 0.01-0.1	Shapiro et al. (2017)
τθ	0.01	0.0001-0.007[b]	Schaefer et al. (2013), Rossi et al. (2015)
TCE log K_{oc}	3.0±0.5[c]	2.9-3.4[d]	Shapiro et al. (2018); Brotsch (2017)

[a]Value assumed for field test calibrations. [c] Calculated from Schaefer et al. diffusion experiments using TCE free solution diffusion coefficient for 20C estimated from the Wilke-Chang relationship with coefficients from Rossi et al. [c]The field test TCE K_d was normalized by the geometric mean (± 1σ) of 144 f_{oc} measurements (Shapiro and Brenneis 2018).[d]Range calculated from TCE sorption isotherm corresponding to TCE concentration range of 500-4000 µg/L.

The porosity and tortuosity factor cannot be estimated independently from our field test. Therefore, we compare the $\tau\theta$ from our test to the results from the laboratory diffusion study completed by Schaefer et al. (2013) that used samples from the NAWC. We normalized the effective diffusion coefficients for TCE determined by Schaefer et al. (2013) in laboratory experiments by the free solution diffusion coefficient extrapolated from Rossi et al. (2015) to obtain the tortuosity factors that describe their laboratory experiments. The range of $\tau\theta$ that we calculate from their experiments (Schaefer et al. 2013) is 0.0001 to 0.007, spanning nearly two orders of magnitude. The $\tau\theta$ value from both of our tests is 0.01, which is approximately 50% greater than the greatest value of the laboratory-generated range.

We compare the TCE K_{oc} from the field test to the K_{oc} observed in the laboratory batch experiments. We use sample 68BR-72, that represents the gray massive sediments, of the laboratory experiments for the comparison. We compute the geometric mean f_{oc} for the laminated gray mudstone ($\log f_{oc}$ = -2.6±0.5, ±1σ) as characterized by Shapiro and Brenneis (2018) to normalize the TCE K_d from the field test to yield $\log K_{oc}$ =3.0±0.5. This is within the range of $\log K_{oc}$ computed from our sorption isotherm (2.9-3.4) at concentrations characterizing the field test (500-4000 μg/L).

The TCE and TCFE biodegradation rate coefficient for the 71BR-85 field test (1.16 μM/day; Table 6) is similar (within a factor of 2) to the rates determine in batch microcosm experiments constructed with sand from the microbial sampler from within the test interval (Table 3). The initial TCE and TCFE concentrations in the microcosm were approximately 4,000 μg/L, comparable to the maximum concentrations observed in the field test.

Comparisons between parameters estimated from the *in situ* test to independent laboratory measurements support the validity of the test method. The above comparisons indicate that the field test produced a TCE $\log K_{oc}$, θ and ψ within the ranges characterized independently in laboratory experiments and are considered reasonable. The τ (or τθ) is moderately greater than the range reported for laboratory measurements. It is possible that the larger scale of the field measurements compared to the laboratory measurements contributes to this result. Additionally, there are fewer experiments that characterize the τ (or τθ).

Comparisons between tests: reproducibility

The primary purpose of conducting the two tests in 71BR as near to one another in elevation as possible is to evaluate the test result reproducibility. The similarity of the tortuosity factors (not different) and TCE sorption coefficients (within a factor of two; Table 6) support the reproducibility of the field test and interpretation method.

Biodegradation of TCE to cDCE in the borehole is rapid in field tests at the NAWC. Direct comparison of the rate coefficients is not useful because of the difference in kinetic formulations. The TCE biodegradation rate during the 71BR-87 test is shown in Figure 32. The ratio between the maximum biodegradation rate during the 71BR-87 test (0.60 μM/day) and the zeroth order rate of 1.16 μM/day estimated for the 71BR-85 test is 0.52. This ratio is similar to the pre-test TCE concentration ratio of 0.50 for the 71BR-87:71BR-85 tests (

Table 5). After reaching a maximum, the TCE biodegradation rate in the 71BR-87 test declined to 0.25 µM/day by the end of the test as the TCE concentration declined (Figure 32).

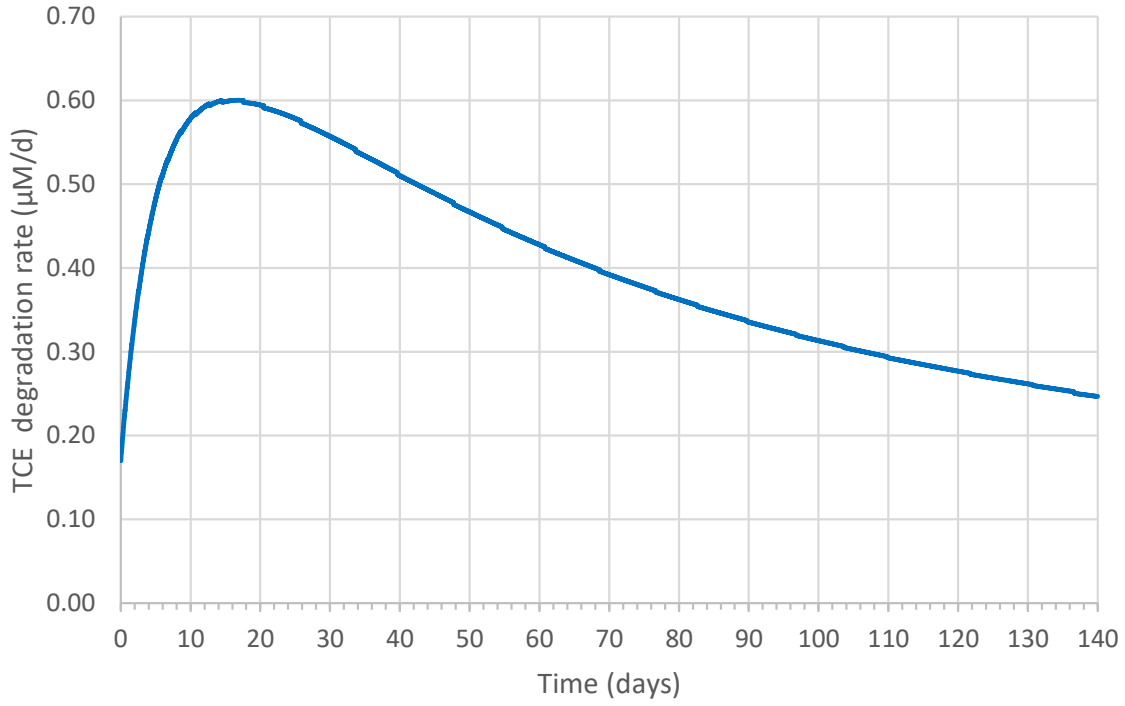

Figure 32. The TCE degradation rate during the 71BR-87 test.

The observed zeroth order kinetic formulation that fit the 71BR-85 test indicates that TCE was not rate limiting during the test. Zeroth-order degradation can occur when the microbial population has adapted to a greater contaminant concentration than the concentration of interest. In the case of the 71BR-85 test, the microbial community was exposed to, and apparently adapted to, the pre-test TCE concentration of 21,000 µg/L. The test response suggests that other reactants, e.g. electron donors, also were present in sufficient quantity to support rapid degradation and that the supply of another reactant limited the reaction rate.

Electron donor (i.e. DOC) supported the rapid biodegradation observed during the tests. However, our efforts to measure the dissolved organic compounds that could support biodegradation yielded no insights. Non-volatile DOC (NVDOC) was low before and after the tests (

Table 5, Table A.2. 3 in Appendix A.2 for 71BR-87) (Kiekhaefer 2018 for 71BR-85 test)). Only very low concentrations Only very low concentrations of volatile fatty acids that are known to support anaerobic TCE biodegradation were detected before the 71BR-87 test and these compounds were not detectable at the end of the test (Table A.2. 4). Because of high volatility, hydrocarbon contaminants would not be quantified by the standard DOC measurement that acidifies and purges the sample to remove interference from carbonates prior to DOC measurement. Regulated hydrocarbon contaminants, such as benzene, toluene, ethylbenzene or xylenes, would have been detected by the GC/MS analysis if present at a sufficient concentration to detect. It is not known whether natural electron donors or hydrocarbon contaminants, also known to be present at the NAWC site, supported the rapid TCE biodegradation observed.

Anecdotal comparison to 2015 field observation

The 2015 historical sample from 71BR-E (collected after the P&T system pump in 15BR had been off for a year) provides insight into the consequences of increased residence time at the NAWC. We compare the field concentrations from 2015 to the historical average concentrations and to the behavior observed in our field test that stopped flow through the borehole altogether.

In 2015, the DP concentrations were greater than the historical average concentrations while the TCE concentration was lower than the average. The June 2015 sample indicates greater TCE biodegradation compared to the historical average period, as indicated by cDCE, VC, ethene and ethane that were >2.5 fold, 9 fold, 9 fold and >3 fold the historical average concentrations, respectively (Kiekhaefer 2018). The TCE concentration was approximately 1/3 of the historical concentration. More reducing conditions were indicated by marked increases in methane and dissolved iron. Some of these patterns were mimicked by our field test. We documented rapid TCE biodegradation and cDCE transformation to VC. The similar overall responses to increased residence time in the unperturbed borehole and the field test provided confidence in the test result.

TCFE tracer

The TCFE is supported as a good tracer of TCE sorption, diffusion and biodegradation rate based on our laboratory experiments, as well as that of prior workers. Additionally, because it is an added tracer, its diffusion direction is counter to the primary TCE diffusion direction.

The TCFE was not a suitable tracer of TCE DP distribution or degradation rate. The DCFEs did not accumulate in the test interval as did the cDCE. Our laboratory experiments showed that the DCFEs were more rapidly biodegraded to CFEs compared to the rate of cDCE degradation to VC. For this reason and because biodegradation so rapidly converted the TCFE to products *in situ*, TCFE was not very useful to interpreting the 71BR-85 field test. It could be useful in field settings where biodegradation in the borehole occurs at much slower rate.

Comparing TCE masses and mass transfer rates to potential abiotic degradation rates

In order to provide perspective on the processes affecting, or potentially affecting, TCE in the matrix, we simulated the TCE masses in the matrix, mass transfer rates from the matrix to the borehole, and abiotic degradation rates. We use the 71BR-85 Case I and Case D for this comparison. In particular, we give a perspective on how the rate of abiotic degradation compares overall.

The TCE mass in the matrix at the start of the test is 0.45 g, equivalent to 3400 μmole, for a cylinder of the matrix with sufficient radius to encompass all of the TCE over the full

length of the test interval (Figure 33a). The TCE diffuses out of the matrix initially (at t=0) at rate of 8.2 x 10^{-2} µg/s (Figure 33b) or 56 µmole/day. For comparison, in the Case D calibration, the TCE degrades abiotically in the matrix at the start of the test at 1.5 x 10^{-6} µmol/s, equivalent to 0.13 µmol/day. At the start of the test, the rate of TCE diffusion out of the matrix is 1.6% of the total mass per day and abiotic degradation rate is much lower, comprising 0.004% per day. The rate of diffusion declines steeply for about a month, after which the decline in diffusion rate slows. At the end of the test, the mass of TCE remaining in the matrix is 0.35 g and the diffusion rate is 3.6 x 10^{-3} µg/s (311 µg/day). In other words, at the end of the test, <0.1% of the TCE matrix mass diffuses out per day. The abiotic degradation rate is proportional to the dissolved concentration and therefore remains over two orders of magnitude slower than the diffusion rate. Because TCE is biodegraded rapidly to cDCE in the borehole during the test, a strong diffusion gradient towards the borehole is maintained. Abiotic degradation at this rate has an effect on TCE concentration that is not significant compared to the diffusion rate. High retardation from sorption limits the matrix volume involved in abiotic degradation. As the TCE concentration declines, the rates of diffusion and abiotic degradation will decline proportionally, assuming pseudo first order kinetics.

The above example is a scenario in which abiotic degradation does not contribute significantly to TCE mass reduction in sedimentary rocks with significant sorption. High sorption retains the TCE near matrix interfaces and limits the availability of TCE to abiotic degradation. An important point is that the TCE K_{oc} at the NAWC is very high compared to some other sediments because the organic matter in the rocks is overmature (Brotsch 2017). However, this case is an illustration of how sorption and retardation can affect abiotic degradation by limiting the extent of the matrix rock exposed to the contaminant.

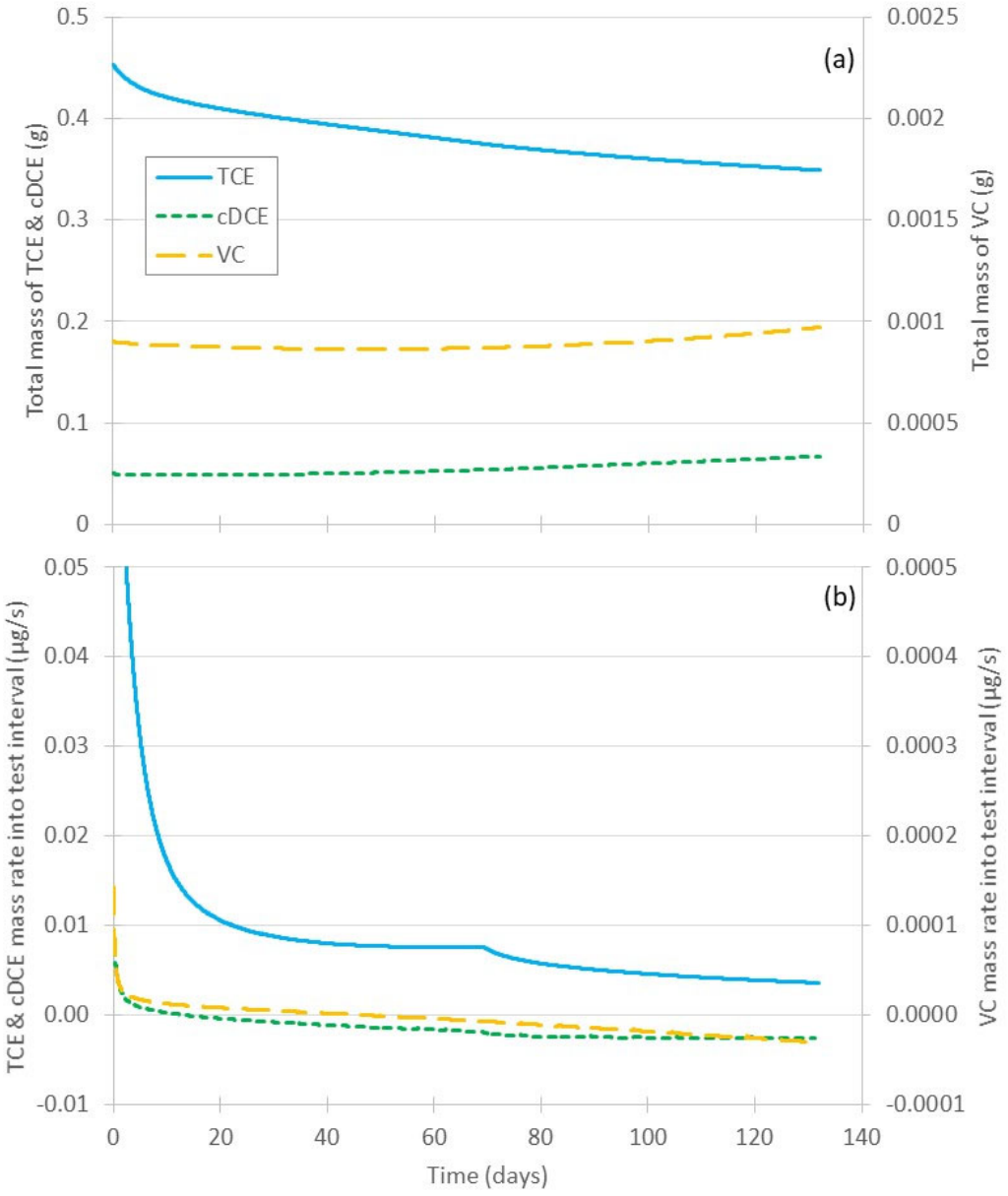

Figure 33. The simulated VOC matrix mass (a) and rate of mass diffusion from the matrix (into the borehole) (b) during the 71BR-85 test. All quantities are calculated for the entire borehole interval and surrounding matrix. In panel (b), negative numbers indicate diffusion into the matrix from the borehole.

Conclusions

This report presents our development of a field test and analysis method ("test") that simultaneously determines site-specific transport coefficients for the matrix in the low permeability matrix of sedimentary rock. Calibration of the radial diffusion model, with retardation, to the test data and borehole concentration history estimates the transport coefficients; these are the tortuosity factor (or the product of the tortuosity factor and porosity), the TCE sorption coefficient in the matrix, and the rates of TCE and cDCE biodegradation in the borehole. We document the test method and model, as well as independent laboratory tests used to validate the method here and in associated publications (Allen-King et al. In revision; Kiekhaefer 2018; Hsieh and Goode 2021; Dugan et al. 2021; Pugnetti 2018; Brotsch 2017), successfully accomplishing the main objective of the project.

Successful test execution relied on development of specific hardware and protocols for each significant step. In addition to the configuration of the dual packer hardware system, the procedures for closed-loop water sampling (near simultaneous sampling and replacement of water), preparation of low VOC groundwater with limited introduction of oxygen, tracer introduction, and flushing the test interval are all examples of steps that required prototype testing in the laboratory and/or field, followed by modification and retesting, to insure reliable field results.

The test results are reasonably reproducible for units of similar lithology and TCE concentration, as demonstrated by two tests conducted in adjacent intervals within the same lithologic unit and concentration history. The conceptual model of retarded TCE diffusion from the matrix to the borehole provides a good fit to the data. The coefficients estimated are within the range, or similar to, those produced from independent laboratory measurements.

The sorption coefficient estimated for TCE from the 71BR-85 experiment is within the range of expected values determined independently in laboratory experiments with field site samples. Good agreement between the field and lab results supports both findings. The field TCE K_d (2.7 L/kg) is approximately 50 times greater than would be predicted by the empirical approach, i.e. $K_d = K_{oc} f_{oc}$, using the EPA value of K_{oc} = 100 L/kg and an f_{oc} of 0.5%, a reasonable value for the lithologic unit tested. In other words, the empirical approach substantially underpredicts sorption in this sedimentary aquifer. Our finding underscores the need for site specific testing to accurately determine the sorption coefficient and retardation factor.

The very fast rate of biodegradation in the borehole significantly influences the results of our tests. Although determining the biodegradation rate coefficient and kinetic form in the borehole is not the primary objective of the project because it is not a matrix property, it is necessary in order to determine the matrix transport properties. The similarity between biodegradation rate coefficients determined in laboratory microcosms and those identified by calibration of the model of the field test indicates that such laboratory tests can be useful methods for estimating these field parameters. The laboratory tests used here included water and media that were preconditioned in situ and were thus likely to be populated with the same microbial population as those present in the borehole during the field experiment.

The reactive tracer TCFE is not useful to constrain the biodegradation rate of lesser chlorinated TCE degradation products in our field experiment. Prior workers demonstrated that TCFE biodegraded to produce fluorinated surrogates of TCE biodegradation. In our experiments, the biodegradation rate of TCFE is similar to that of TCE in both the laboratory experiments and

the field test. However, laboratory experiments with native groundwater microorganisms show that the TCFE product distribution is not a good surrogate of the TCE degradation product distribution. The DCFEs biodegrade more rapidly to CFEs than the cDCE degrades to VC. The DCFEs did not accumulate in the test interval as did cDCE. Therefore, the DCFE conversion rate could not be used as an independent constraint for cDCE biodegradation rate parameter estimation. Thus, we show that the behavior of TCFE with respect to utility as a tracer of TCE biodegradation is variable between field sites. We show that TCFE is a good tracer of TCE sorption and diffusion behavior.

We selected boreholes with contrasting pre-test cDCE:TCE concentration ratios with the goal to evaluate the effect of different initial conditions on the test results. Unfortunately, the shallower borehole 07BR had only one low permeability zone sufficient for testing. The general patterns of CVOC response are similar to the patterns observed in the 71BR tests. However, the test had two important problems: the Br tracer showed that the test interval was not well mixed initially and could not be interpreted, and the packers leaked between 2-3 months into the test. The results are included in Appendix A for completeness.

We did not observe ADPs in our field tests. Through simulation analysis we show that abiotic degradation of TCE in the dissolved phase at a rate consistent with previous laboratory experiments would be consistent with the field test results, although the ADP concentrations would be below our detection limit. Our simulations also show that a much faster abiotic degradation rate would produce unreasonable parameter estimates. Our results suggest the hypothesis that abiotic degradation is of low importance to TCE in the matrix when sorption is high.

Implications for Implementation/Future Research

The field test method is fully documented in this report and accompanying cited work; these products enable the test to be implemented.by experienced technical personnel to a field site similar to the NAWC. The site-specific information gained is equivalent to the results of multiple laboratory studies. The test provides one tool towards filling the gap of limited field methods to collect transport parameters from low permeability zones.

We provide model simulations using the site-specific parameters estimated from the field test to illustrate how the findings can be used to enhance understanding of contaminant distribution and transport at a field site. For one example, the concentration profile simulations indicate that after a decade of exposure from the borehole, most TCE mass was located within 5 cm of the matrix-borehole interface. Additional simulations calculate the masses in the rock matrix and the rate of back diffusion (or mass release) from the rock matrix. We use simulations to conduct a preliminary analysis of the potential significance of abiotic TCE degradation. The model could be used to conduct a sensitivity analysis that explores how variations in transport properties or concentration history affect mass distribution in the matrix or mass release from the matrix. Hence, this report demonstrates how the site-specific information gained from a field test can be used to improve site understanding to inform remediation and/or management.

Additional research is needed to develop the test for application to a broader range of field sites with transport properties that differ from the NAWC. The NAWC has a relatively high mass transfer rate from the matrix to the borehole because of the rock properties and because rapid biodegradation maintains a high gradient. Whether a field test will be successful is site

specific and depends on the borehole properties, analysis method, and tool configuration, in addition to the site-specific matrix transport properties and biodegradation rate in the borehole.

Application to additional sedimentary rock field site(s) is the next step in broadening the applicability of the test; field site application would direct test adaptations in the most useful ways. We envision that applications would use forward modeling, using the simulation tool developed for this project (Hsieh and Goode 2021), to identify whether a need for modification of the test apparatus or procedures is required for success. Forward simulations would use the best available matrix property information to produce back diffusion simulations comparable to those shown for our tests. These would guide considerations of the need for lower analytical detection limits, an alternative nonreactive tracer, or to reduce the borehole dead volume by including a solid spacer. Such modifications were not necessary to attain a successful test at the NAWC. However, we anticipate that such modifications will be needed to create a tool adaptable to field sites with a broad range of properties.

Contributions to Training the Next Generation of Professionals

This SERDP project created a platform for training for 5 graduate and 6 undergraduate students to participate in research at UB (Table 9). Six (of 10 total) students are women who earned degrees in fields where women are underrepresented including Geology, Environmental Engineering and Geological Engineering. Four of the students have completed, or are in the process of completing, an additional degree in a STEM (science, technology, engineering and math) field. Additionally, seven students participated in the project as student interns at the USGS and at least two of them (Carol Morel, Jessica Teunis) are since have gained employment as USGS professionals at the National Climate Adaptation Science Center and in California. This project contributed to the education and advancement of well-trained professionals into STEM professional positions (Table 9). It also contributed to broadening participation of women in STEM professions. Although this aspect of productivity may not often be underscored in project reports, it is an important product of the SERDP program.

Table 9. Students that participated in project related research at UB.

Student name	Degree Program During Participation[a]	Subsequent Degree	Current Employer
Rebecca Kiekhaefer	M.S. Geology		GIS Analyst, SynTerra
Jonathan Brotsch	M.S. Geology		Chemical Technician, Goodyear Chemical
Michele Pugnetti	M.S. Geology	Ph.D. Geology, ETH, Switzerland (current)	
Mary Masse	M.S. Geology		
Hannah Annunziata	B.S Env. Geosci.	M.S. Geology (expected 2021)	
Matthew Buzzeo	B.S Env. Geosci.		Parsons
Rory Dishman	B.S. Geology & Chemistry		Process Development Technician, Honeywell
Kassandra Kimmey	B.S. Env. Eng	M.S., Environmental and Water Resources Engineering	Staff Professional, Geosyntec Consultants
Virginia (Cistaro) Halloran[b]	B.S. Geol. Eng., Michigan Tech		Gas Operation Engineer, MI Dept of Licensing and Regulatory Affairs
Katie Tresino[b]	B.S. Chemistry, SUNY Fredonia	M.S. Chemical Engineering, NC State University, (current)	Lab Analyst, Town of Holly Springs, NC

[a]Env. Geosci. Is Environmental Geosciences, Env. Eng. Is Environmental Engineering, Geol. Eng. Is Geological Engineering

[b]These students were part of a National Science Foundation Research Experiences for Undergraduates program that brings students from other institutions to UB for a summer of research.

Literature Cited

Allen-King, R. M., P. Grathwohl, and W. P. Ball (2002), New modeling paradigms for the sorption of hydrophobic organic chemicals to heterogeneous carbonaceous matter in soils, sediments, and rocks, *Adv. in Water Resour.*, 25, 985-1016.

Allen-King, R.M., R.L. Kiekhaefer, D.J. Goode, P.A. Hsieh, M.M. Lorah, and T.E. Imbrigiotta. In revision. A borehole test for chlorinated solvent diffusion and degradation rates in sedimentary rock. *Ground Water Monit. Rem.*

APHA. 2005. Standard Methods for the Examination of Water and Wastewater. American Public Health Association.

Ball, W. P., C. X. Liu, G. S. Xia, and D. F. Young (1997a), A diffusion-based interpretation of tetrachloroethene and trichloroethene concentration profiles in a groundwater aquitard, *Water Resour. Res.*, 33(12), 2741-2757.

Barone, F. S., R. K. Rowe, and R. M. Quigley (1992), A Laboratory Estimation of Diffusion and Adsorption Coefficients for Several Volatile Organics in a Natural Clayey Soil, *J. Contamin. Hydrol.,* 10(3), 225-250.

Becker, M.W., and Shapiro, A.M., 2000, Tracer transport in fractured crystalline rock—Evidence of nondiffusive breakthrough tailing: *Water Resour. Res.*, v. 36, no. 7, p. 1677-1686.

Boving, T. B., and Grathwohl, P., 2001, Tracer diffusion coefficients in sedimentary rocks: Correlation to porosity and hydraulic conductivity, *J. Contamin. Hydrol.*, 53, 85-100.

Bradbury, M. H., and Green, A., 1985, Measurement of important parameters determining aqueous phase diffusion rates through crystalline rocks matrices, *J. Hydrol.*, 82(1-2), 39-55

Bradley, P., 2000, Microbial degradation of chloroethenes in groundwater systems: *Hydrogeol. J.*, 8(1): 104–111.

Bradley, P.M., P.J. Lacombe, T.E. Imbrigiotta, F.H. Chapelle, and D.J. Goode. 2009. Flowpath Independent Monitoring of Reductive Dechlorination Potential in a Fractured Rock Aquifer. *Ground Water Monit. Rem.* 29 no. 4: 46-55 10.1111/j.1745-6592.2009.01255.x

Brotsch, J. 2017. Trichloroethylene (TCE) Sorption to Organic Matter in Sedimentary Rocks of the Newark Basin, Geological Sciences, Thesis (M.S.)--University at Buffalo, State University of New York, Buffalo, NY, pp.

Chapelle, F.H., P.J. Lacombe, and P.M. Bradley. 2012. Estimated trichloroethene transformation rates due to naturally occurring biodegradation in a fractured-rock aquifer. *Rem. J.* 22 no. 2: 7-20 10.1002/rem.21307.

Doherty, J. 2015. Calibration and Uncertainty Analysis for Complex Environmental Models. Brisbane, Australia: Watermark Numerical Computing.

Doherty, J. 2016. *PEST Model-Independent Parameter Estimation User Manual Part I: PEST, SENSAN, and Global Optimisers*. Brisbane, Australia: Watermark Numerical Computing.

———. 2016. PEST Model-Independent Parameter Estimation User Manual Part I: PEST, SENSAN, and Global Optimisers. Brisbane, Australia: Watermark Numerical Computing.

Dugan, C.M., M.M. Lorah, E.H. Majcher, and T.P. Needham. 2021. Volatile Organic Compound and Other Analyses Associated with Laboratory Microcosm Experiments to Determine Biodegradation Rates in Fractured Sedimentary Rock at the Former Naval Air Warfare Center in West Trenton, New Jersey, 2016–18. U.S. Geological Survey data release https://doi.org/10.5066/P9M010JV.

Field, J.A., R.L. Reed, J.D. Istok, L. Semprini, P. Bennett, and T.E. Buscheck. 2005. Trichlorofluoroethene: A reactive tracer for evaluating reductive dechlorination in large-diameter permeable columns. *Ground Water Monit. Rem.* 25 no. 2: 68-77 10.1111/j.1745-6592.2005.0016.x.

Fiore, A.R., and T.E. Imbrigiotta. 2021. Concentrations of chlorinated volatile organic compounds and per- and polyfluroalkyl substances in groundwater and surface water, former Naval Air Warfare Center, West Trenton, New Jersey, 1989-2018. U.S. Geological Survey In prep.

Gebrekristos, R.A., A.M. Shapiro, and B.H. Usher. 2008. In situ estimation of the effective chemical diffusion coefficient of a rock matrix in a fractured aquifer. *Hydrogeol. J.* 16 no. 4: 629-639 10.1007/s10040-007-0255-0.

Godfrey, P.J. 1988. Acid rain in Massachusetts – The Massachusetts Acid Rain Research Program in Action. Water Resources Research Center, University of Massachusetts, Amherst, 54 p.

Goode, D.J., T.E. Imbrigiotta, and P.J. Lacombe. 2014. High-resolution delineation of chlorinated volatile organic compounds in a dipping, fractured mudstone: Depth- and strata-dependent spatial variability from rock-core sampling. *J. Contamin. Hydrol.* 171: 1-11 10.1016/j.jconhyd.2014.10.005.

Goode, D.J., Tiedeman, C.R., Lacombe, P.J., Imbrigiotta, T.E., Shapiro, A.M., and Chapelle, F.H., 2007, Contamination in fractured-rock aquifers – Research at the former Naval Air Warfare Center, West Trenton, New Jersey: USGS Fact Sheet 2007-3074, 2 p.

Hageman, K.J., J.D. Istok, J.A. Field, T.E. Buscheck, and L. Semprini. 2001. In situ anaerobic transformation of trichlorofluoroethene in trichloroethene-contaminated groundwater. *Environ. Sci. Technol.* 35 no. 9: 1729-1735 10.1021/es001577j.

Holm, P.E., P.H. Nielsen, H.J. Albrechtsen, and T.H. Christensen. 1992. Importance of unattached bacteria and bacteria attached to sediment in determining potentials for degradation of xenobiotic organic contaminants in an aerobic aquifer. *Appl. Environ. Microbiol.* 58 no. 9: 3020-3026 10.1128/AEM.58.9.3020-3026.1992.

Hsieh, P.A., and D.J. Goode. 2021. A finite-difference algorithm used to simulate radial diffusion, sorption, and reactions of chlorinated ethenes in porous media. U.S. Geological Survey data release https://doi.org/10.5066/P99I50JE.

Hsieh, P.A., R.L. Perkins, and D.O. Rosenberry. 1996. Field instrumentation for multi-level monitoring of hydraulic head in fractured bedrock at the Mirror Lake site, Grafton County, New Hampshire. In U.S. Geological Survey Toxic Substances Hydrology

Program--Proceedings of the technical meeting, Colorado Springs, Colo., September 20-24, 1993, ed. D. W. Morganwalp and D. A. Aronson. U.S. Geological Survey Water-Resources Investigations Report 94-4015.

Ibaraki, M., 2001, A simplified technique for measuring diffusion coefficients in rock blocks, *Water Resour. Res.*, 37(5), 1519-1523.

Jeong, S., M. M. Wander, S. Kleineidam, P. Grathwohl, B. Ligouis, and C. J. Werth (2008), The role of condensed carbonaceous materials on the sorption of hydrophobic organic contaminants in subsurface sediments, *Water Resour. Res.*, 42(5), 1458-1464.

Johnson, R. L., J. A. Cherry, and J. F. Pankow (1989), Diffusive Contaminant Transport in Natural Clay: A Field Example and Implications for Clay-Lined Waste Disposal Sites, *Environ. Sci. Technol.*, 23(No. 3), 340-349.

Kiekhaefer, R. 2018. Evaluation of a Field Method for Monitoring the Diffusion of Trichloroethene (TCE) and its Degradation Products in Fractured Sedimentary Rock. M.S. Thesis, Department of Geosciences, Thesis (M.S.)--University at Buffalo, State University of New York, 232 pp., https://ubir.buffalo.edu/xmlui/handle/10477/78634.

Kozich, J.J., S.L. Westcott, N.T. Baxter, S.K. Highlander, and P.D. Schloss. 2013. Development of a Dual-Index Sequencing Strategy and Curation Pipeline for Analyzing Amplicon Sequence Data on the MiSeq Illumina Sequencing Platform. *Appl. Environ. Microbiol.* 79 no. 17: 5112-5120 10.1128/AEM.01043-13.

Krom, M. D., and Berner, R. A., 1980, The diffusion coefficients of sulfate, ammonium, and phosphate ions in anoxic marine sediments, *Limnol. Oceanogr.*, 25(2), 327-337.

Lacombe, P.J. 2000. Hydrogeologic framework, water levels, and trichloroethylene contamination, Naval Air Warfare Center, West Trenton, New Jersey, 1993-97. U. S. G. Survey Water-Resources Investigations Report 98-4167, 139 pp., 10.3133/wri984167.

———. 2011. Mass of chlorinated volatile organic compounds removed by Pump-and-Treat, Naval Air Warfare Center, West Trenton, New Jersey, 1996-2010. U. S. G. Survey Scientific Investigations Report 2011-5003, 32 pp., 10.3133/sir20115003.

Lacombe, P.J., and W.C. Burton. 2010. Hydrogeologic framework of fractured sedimentary rock, Newark Basin, New Jersey. *Ground Water Monit. Rem.* 30 no. 2: 35-45 10.1111/j.1745-6592.2010.01275.x.

Lee, W.; Batchelor, B., 2002, Abiotic reductive dechlorination of chlorinated ethylenes by iron-bearing soil minerals. 1. Pyrite and magnetite. *Environ. Sci. Technol.* 36 (23), 5147-5154.

Louie, E.N. 1999. Effect of electron donors on the reductive dechlorination of trichlorofluoroethylene in anaerobic microcosms and in situ push-pull tests, Oregon State University, https://ir.library.oregonstate.edu/concern/graduate_thesis_or_dissertations/jq085p623.

Majcher, E.H., M.M. Phelan, M.M. Lorah, and A.L. McGinty. 2007. Characterization of preferential ground-water seepage from a chlorinated hydrocarbon-contaminated aquifer to West Branch Canal Creek, Aberdeen Proving Ground, Maryland, 2002-04: U.S. Geological Survey Scientific Investigations Report 2006-5233, https://doi.org/10.3133/sir20065233.

Mukhopadhyay, Sumit, Liu, H. H., Spycher, N., Kennedy, B. M. (2013). Impact of fluid–rock chemical interactions on tracer transport in fractured rocks. *J. Contamin. Hydrol.* 154(0): 42-52.

Myrand, D., R.W. Gillham, E.A. Sudicky, S.F. Ohannesin, and R.L. Johnson, 1992, Diffusion of volatile organiccompounds in natural clay deposits – Laboratory tests: *J. Contam. Hydrol.*, v. 10, no. 2, p. 159-177.

National Academies of Sciences, Engineering, Medicine,. 2015. Characterization, Modeling, Monitoring, and Remediation of Fractured Rock. Washington, DC: The National Academies Press.

Novakowski, K.S., and G. van der Kamp. 1996. The Radial Diffusion Method: 2. A semianalytical model for the determination of effective diffusion coefficients, porosity, and adsorption. *Water Resour. Res.* 32 no. 6: 1823-1830 10.1029/95wr03720.

Oksanen, J., F.G. Blanchet, R. Kindt, P. Legendre, P.R. Minchin, R.B. O'Hara, G.L. Simpson, P. Solymos, M.H.H. Stevens, and H. Wagner. 2015. vegan: Community Ecology Package.

Parker, B.L., J.A. Cherry, and S.W. Chapman, 2004, Field study of TCE diffusion profiles below DNAPL to assess aquitard integrity: *J. Contam. Hydrol.*, v. 74, no. 1-4, p. 197-230.

Pfaff, J.D. 1993. Method 300.0 Determination of inorganic anions by ion chromatography. US Environmental Protection Agency, Office of Research and Development, Environmental Monitoring Systems Laboratory, https://www.epa.gov/sites/production/files/2015-08/documents/method_300-0_rev_2-1_1993.pdf.

Pham, H.T., K. Suto, and C. Inoue. 2009. Trichloroethylene Transformation in Aerobic Pyrite Suspension: Pathways and Kinetic Modeling. *Environ. Sci. Technol.* 43 no. 17: 6744-6749 10.1021/es900623u.

Pham, H.T., M. Kitsuneduka, J. Hara, K. Suto, and C. Inoue. 2008. Trichloroethylene transformation by natural mineral pyrite: The deciding role of oxygen. *Environ. Sci. Technol.* 42 no. 19: 7470-7475 10.1021/es801310y.

Pugnetti, M. 2018. Trichloroethene and Trichlorofluoroethene Equilibrium Competitive Sorption to Sedimentary Rock from the Newark Basin, New Jersey, Geological Sciences, Thesis (M.S.)--University at Buffalo, State University of New York, Buffalo, NY, pp.

Quinn, P., J.A. Cherry, and B.L. Parker, 2012, Hydraulic testing using a versatile straddle packer system for improved transmissivity estimation in fractured-rock boreholes: *Hydrogeol. J.* 20:1529-1547 https://doi.org/10.1007/s10040-012-0893-8.

Révész, K.M., B.S. Lollar, J.D. Kirshtein, C.R. Tiedeman, T.E. Imbrigiotta, D.J. Goode, A.M. Shapiro, M.A. Voytek, P.J. Lacombe, and E. Busenberg. 2014. Integration of stable carbon isotope, microbial community, dissolved hydrogen gas, and H-2(H2O) tracer data to assess bioaugmentation for chlorinated ethene degradation in fractured rocks. *J. Contamin. Hydrol.* 156: 62-77 10.1016/j.jconhyd.2013.10.004.

Rossi, F., R. Cucciniello, A. Intiso, A. Proto, O. Motta, and N. Marchettini. 2015. Determination of the trichloroethylene diffusion coefficient in water. *AIChE Journal* 61 no. 10: 3511-3515 10.1002/aic.14861.

Schaefer, C.E., R.M. Towne, D.R. Lippincott, V. Lazouskaya, T.B. Fischer, M.E. Bishop, and H.L. Dong. 2013. Coupled Diffusion and Abiotic Reaction of Trichlorethene in Minimally Disturbed Rock Matrices. *Environ. Sci. Technol.* 47 no. 9: 4291-4298 10.1021/es400457s.

Schloss, P.D. 2015. "MiSeq SOP.", accessed 12/3 at http://www.mothur.org/MiSeq_SOP.

Schloss, P.D., S.L. Westcott, J.W. Sahl, B. Stres, G.G. Thallinger, D.J. Van Horn, C.F. Weber, T. Ryabin, J.R. Hall, M. Hartmann, E.B. Hollister, R.A. Lesniewski, B.B. Oakley, D.H. Parks, and C.J. Robinson. 2009. Introducing mothur: Open-Source, Platform-Independent, Community-Supported Software for Describing and Comparing Microbial Communities. *Appl. Environ. Microbiol.* 75 no. 23: 7537-7541 10.1128/AEM.01541-09.

Shapiro, A.M. 2007. Characterizing hydraulic properties and ground-water chemistry in fractured-rock aquifers: A user's manual for the multifunction Bedrock-Aquifer Transportable Testing Tool (BAT3). U. S. G. Survey Open-File Report 2007-1134, 127 pp.

Shapiro, A.M., 2001, Effective matrix diffusion in kilometer-scale transport in fractured crystalline rock, *Water Resour. Res.*, v. 37, no. 3, p. 507-522.

Shapiro, A.M., and P.A. Hsieh. 1998. How Good Are Estimates of Transmissivity from Slug Tests in Fractured Rock? Groundwater 36 no. 1: 37-48 10.1111/j.1745-6584.1998.tb01063.x.

Shapiro, A.M., and R.J. Brenneis. 2018. Variability of organic carbon content and the retention and release of trichloroethene in the rock matrix of a mudstone aquifer. *J. Contamin. Hydrol.* 217: 32-42 10.1016/j.jconhyd.2018.09.001.

Shapiro, A.M., and R.J. Brenneis. 2018. Variability of organic carbon content and the retention and release of trichloroethene in the rock matrix of a mudstone aquifer. *J. Contamin. Hydrol.* 217: 32-42 10.1016/j.jconhyd.2018.09.001.

Shapiro, A.M., C.E. Evans, and E.C. Hayes. 2017. Porosity and pore size distribution in a sedimentary rock: Implications for the distribution of chlorinated solvents. *J. Contamin. Hydrol.* 203: 70-84 10.1016/j.jconhyd.2017.06.006.

Shapiro, A.M., C.R. Tiedeman, T.E. Imbrigiotta, D.J. Goode, P.A. Hsieh, P.J. Lacombe, M.F. DeFlaun, S.R. Drew, and G.P. Curtis. 2018. Bioremediation in Fractured Rock: 2. Mobilization of Chloroethene Compounds from the Rock Matrix. *Groundwater* 56 no. 2: 317-336 10.1111/gwat.12586.

Shapiro, A.M., R.A. Renken, R.W. Harvey, M.R. Zygnerski, and D.W. Metge, 2008, Pathogen and chemical transport in the karst limestone of the Biscayne aquifer: 2. Chemical retention from diffusion and slow advection, *Water Resour. Res.*, v. 44, no. 8, W08430.

Steimle, R. 2002. The State of the Practice: Characterizing and Remediating Contaminated Groundwater at Fractured Rock Sites. *Rem. J.* 12 no. 2: 23-33 10.1002/rem.10024.

Team, R.C. 2015. R: A language and environment for statistical computing. Vienna, Austria: R Foundation for Statistical Computing.

Tiedeman, C.R., A.M. Shapiro, P.A. Hsieh, T.E. Imbrigiotta, D.J. Goode, P.J. Lacombe, M.F. DeFlaun, S.R. Drew, C.D. Johnson, J.H. Williams, and G.P. Curtis. 2018. Bioremediation

in Fractured Rock: 1. Modeling to Inform Design, Monitoring, and Expectations. *Groundwater* 56 no. 2: 300-316 10.1111/gwat.12585.

Tiedeman, C.R., P.J. Lacombe, and D.J. Goode. 2010. Multiple Well-Shutdown Tests and Site-Scale Flow Simulation in Fractured Rocks. Ground Water 48 no. 3: 401-415 10.1111/j.1745-6584.2009.00651.x.

U.S. Environmental Protection Agency. 2013. Technical Factsheet on: Trichloroethylene, accessed at https://yosemite.epa.gov/r9/sfund/r9sfdocw.nsf/688299b284b16e92882574260073faef/dec46d2e9b7ac79188257af60079c75d/$FILE/EPA%20TCE%20Technical%20Fact%20Sheet%201-10-13.pdf.

U.S. Geological Survey. 2020. USGS GeoLog Locator: U.S. Geological Survey database, accessed August 24, 2020, at https://doi.org/10.5066/F7X63KT0.

Vancheeswaran, S., Hyman, M.R., and Semprini, L., 1999, Anaerobic biotransformation of trichlorofluoroethene in groundwater microcosms: *Environ. Sci. Technol.*, v. 33, p. 2040-2045.

Willmann, M., Lanyon, G. W., Marschall, P., Kinzelbach, W. (2013). A new stochastic particle-tracking approach for fractured sedimentary formations. *Water Resour. Res* 49(1): 352-359.

Young, D.F., and W.P. Ball, 1998, Estimating diffusion coefficients in low-permeability porous media using a macropore column, *Environ. Sci. Technol*., v. 32, no. 17, p. 2578-2584.

Zhou, Quanlin, Liu, H.-H., Molz, F.J., Zhang, Yingqi, and Bodvarsson, G.S., 2007, Field-scale effective matrix diffusion coefficient for fractured rock: Results from literature survey: *J. Contamin. Hydrol.*, v. 93, p. 161-187.

Appendix A. Supporting Data

Include all refined data collected during the research project that warrants archiving in this report. Data in the form of tables, graphs, graphics, plots, and/or datasets that are not provided in the Results and Discussion section above should be included with sufficient detail to reconstruct the experiments or research. As needed for complex datasets, provide a separate “readme.txt” file with a brief description of the file format. In short, the data should be described sufficiently to enable others not familiar with the data to use and understand them.

Appendix A.1: Results of the 07BR-49 test

For the majority of the historical record, borehole 07BR was an open borehole with a total depth of less than 60 feet. CVOC concentration data from 07BR (Figure A1-1) was generally less stable compared to 71BR, possibly due to water table response to precipitation events. The historical averages for 07BR (Table A1-1) were calculated between 2008 and 2017, as this period covered close to a decade of the historical record prior to the diffusion test initiation and concentration records were more stable during this period. The average concentration of TCE was 2800 µg/L and the average concentration of cis-DCE (cDCE) was 330% higher (9300 µg/L), which indicates biodegradation has been ongoing within 07BR or intersecting fractures. (Throughout Appendix A.1, the abbreviation used for *cis*-1,2-dichloroethene is cis-DCE). VC was recorded at an average of 1200 µg/L. The historical average recorded for methane was 70 µg/L, for ethane 3 µg/L, and ethylene 135 µg/L.

Compared to the historical data form 71BR, the concentrations of degradation products are significantly higher in 07BR. This indicates that more biodegradation of TCE has occurred around 07BR compared to 71BR. The presence of a packer system in 71BR kept the zones more isolated from one another and therefore the concentration data is affected only by the fractures and rock surrounding the specific interval. In contrast, 07BR was predominantly open, so the concentrations were possibly affected by precipitation as well as all fractures intersecting 07BR. Samples were analyzed during the pre- and post-test periods for general water chemistry (Table A1-2). The sparging and tracer addition processes did cause the pH to increase due to removal of dissolved carbon dioxide.

A diffusion test was conducted in 07BR at 49 ft bls (07BR-49) for 140 days. Between day 86 and day 93, a heavy precipitation event occurred and the pressure in the upper packer decreased to 39 psi (from 55 psi prior to the decrease). It is assumed there was a leak to the test interval and samples collected after this time are not considered representative of the test.

The bromide concentration decreased throughout the duration of the test due to dilution and diffusion into the rock (Figure A1-2). CVOC concentrations in 07BR for the duration of the test are shown in Figure A1-3. TCFE concentrations decreased throughout the test. The decrease was most likely due to a combination of diffusion into and sorption to the rock matrix and not due to biodegradation, as degradation products of TCFE were not detected. For the first 6 days, the concentration of TCE increased in the borehole due to diffusion from the rock matrix. The concentration of cis-DCE also increased during this period due to the same process. After the first 6 days, the slope of the cis-DCE curve changes, indicating more cis-DCE is accumulating in the borehole. Due to the associated decrease in TCE, biodegradation of TCE was likely occurring in the borehole, though it is possible that back diffusion of cis-DCE into the borehole was a larger contributor to concentration increases due to the high concentrations of cis-DCE in the historical record. VC concentrations increased in the borehole for the duration of the test, but did not exceed the historical average prior to the interval being compromised. The main driver of VC concentration increase was likely back diffusion, not biodegradation of cis-DCE.

Table A.1-1. Historical average and pre-test water chemistry in 07BR. The historical average was taken between 2008 and 2012 for all existing sample records. The pre-test average for each well was the average of the first pumping sample, the last pumping sample, and the first flushing sample. Historical data for 07BR provided by Thomas Imbrigiotta (personal communication, April 11, 2017). Data from Kiekhaefer (2018) used with permission.

Parameter	Units	07BR	
		Historical Average	Pre-Test Average
TCE	µg/L	2600	2900
Cis-DCE	µg/L	10000	5300
VC	µg/L	1300	600
TCFE	µg/L	NS[1]	<25[2]
Methane	µg/L	70	65
Ethylene	µg/L	135	45
Acetylene	µg/L	NS	BDL[3]
Ethane	µg/L	3	<35
Oxygen	mg/L	1.2	<0.05
pH	-	8.02	7.41
Calcium	mg/L	70	NS
Magnesium	mg/L	25	NS
Sodium	mg/L	15	NS
Potassium	mg/L	3	NS
Chloride	mg/L	10	15
Sulfate	mg/L	120	90
Bicarbonate	mg/L	210	210
P_{CO2}[4]	atm	$10^{-2.4}$	$10^{-2.1}$
Iron	mg/L	3.5	3
Bromide	mg/L	NS	0.1
DOC	mg/L	1.5	2
Conductivity	µS/cm	350	550

[1]Not sampled

[2]Below quantification limit (limit listed)

[3]Below detection limit

[4]Calculated from pH and bicarbonate data

Table A.1-2. Pre- and post- test general water chemistry for 07BR-49 for each water sample collected during the pre-test period and an average of two samples collected after the test. The bromide quantification limit is 0.25 mg/L. "First" and "last" refer to the order in which the sample was collected during either the pumping or flushing period of the test. Data from Kiekhaefer (2018) used with permission.

	DOC (mg/L)	Alkalinity as Bicarbonate (mg/L)	Bromide (mg/L)	pH	DO (mg/L)	Ferrous iron (mg/L)	Conductivity (µS/cm)
First Pumping	2.11	214.5	0.1	7.47	<0.05	>3.30	552
Last Pumping	1.89	211.3	0.1	7.35	<0.05	2.78	538
First Flushing	1.83	197.8	18.8	NS[1]	NS	NS	NS
Sparged groundwater	1.88	215.5	0.3	8.52	<0.05	3.06	527
Last Flushing	2.05	210.8	0.1	8.84	<0.05	0.12	515
Post-Test[2]	58.9	318.6[3]	192.0	7.71	0.40	3.11	814

[1]Not sampled

[2]The 07BR-49 test interval was compromised by a packer leak before test conclusion; the post-test samples are not representative (further discussion in the Results and Discussion section).

[3]Protocol dictated that alkalinity samples be filtered in the field; however, the field notes do not state that this sample was filtered.

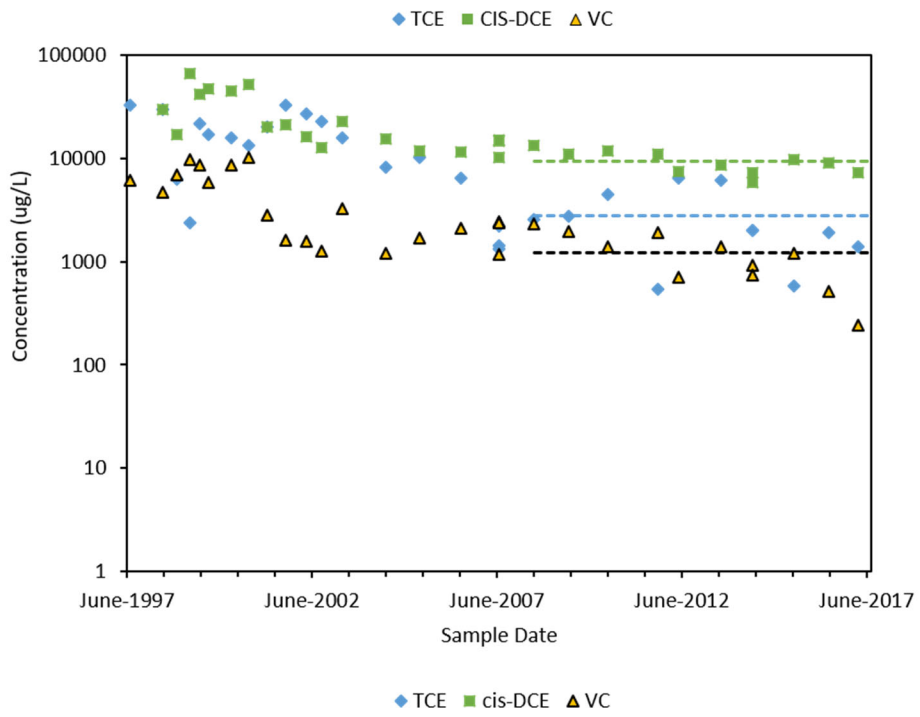

Figure A.1-1. Historical and pre-test CVOC concentrations in 07BR (log scale y-axes). Dashed lines indicate the historical average over the time period the average was taken. Historical data for 07BR provided by Thomas Imbrigiotta (personal communication, April 11, 2017). From Kiekhaefer (2018) used with permission.

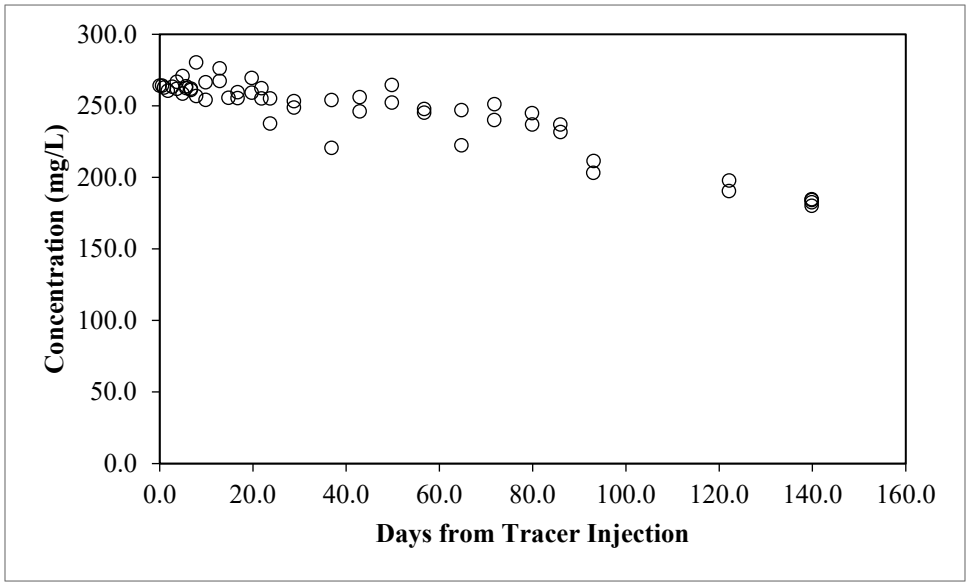

Figure A1-2. Bromide concentration from tracer injection to test conclusion. The samples after 86 days in the 07BR-49 test were not used for interpretation due to the potential that a leak occurred. From Kiekhaefer (2018) used with permission.

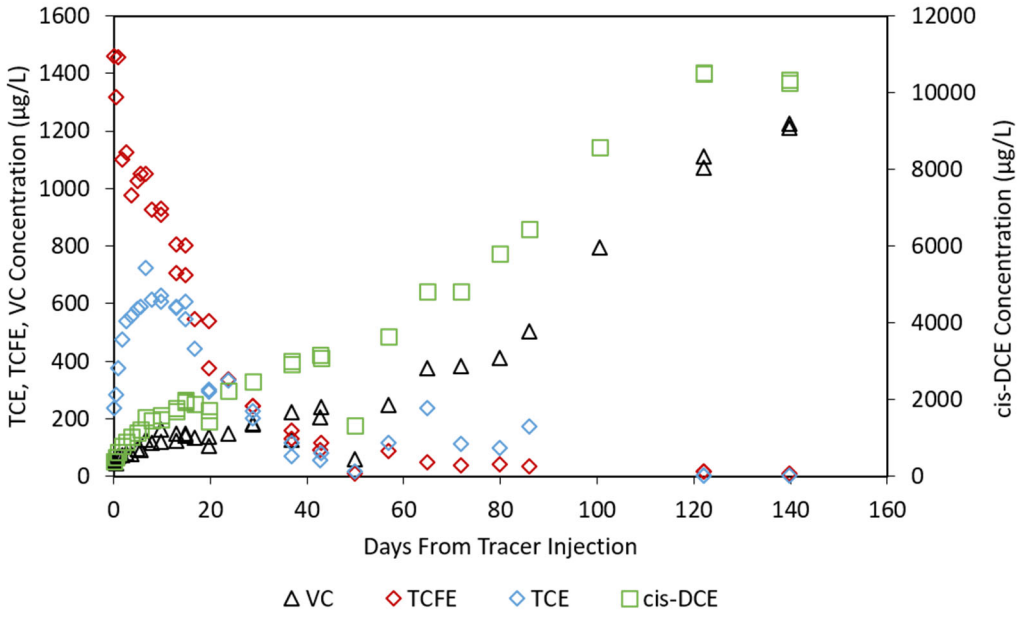

Figure A1-3. CVOC concentrations during the diffusion test in 07BR-49. The samples after 86 days in the 07BR-49 test were not used for interpretation due to the potential that a leak occurred. From Kiekhaefer (2018) used with permission.

Appendix A.2: Data from the 71BR-87 test

Table A.2. 1. Test activity designation for each sample number for pre- and post-test samples

sample #	~ Volume pumped to/from test interval(L)	Narrative
Pre Test		
2	2	pumping existing borehole water to fill sparge vessel, top packer closed and bottom open
4	10-15	"" ""
6	25	"" ""
7	35	"" ""
8	35	"" ""
10	45	"" ""
11	NA	sparge vessel sample while filling sampling manifold, tracer, and replacement water bags
12	NA	"" ""
14	2	flushing test interval with both packers closed, replacing with sparged (low VOC) water, to start test
15	35-40	"" ""
16	35-40	"" ""
Post Test		
98	<2	flushing test interval with both packers closed, replacing with water from above top packer, to remove tracer and end test
100		"" ""

Table A.2. 2. The TCE and DP concentrations for samples collected during the test initiation process.

Sample #	VC (ug/L)	cDCE (ug/L)	TCE (ug/L)
2	32.3	2134.3	8892.5
4	23.4	2168.4	12286.9
6	18.0	2007.2	11263.5
7	9.5	1576.7	8848.1
8	12.5	1859.5	10733.9
10	11.9	1638.8	9588.3
11	0.0	3.7	217.7
12	0.0	70.9	569.5
14	11.9	1673.5	7425.7
15	0.0	118.6	513.0
16	0.0	103.8	497.7

Sample No. 7 not included in average.

Table A.2. 3. The major anion, DO, and total dissolved nitrogen (TN) concentrations observed in pre- and post-test samples.

	Major Anions			Major Cations					
Sample Number	Chloride (mg/L)	Sulfate (mg/L)	Bicarbonate* (mg/L)	Calcium (mg/L)	Magnesium (mg/L)	Sodium (mg/L)	Potassium** (mg/L)	DOC (mg/L)	DN (mg/L)
Pre Test									
2	56.7	29.0	171	55.9	21.5	15.7	2.44	0.67	0.27
10	60.9	30.5	169					0.28	0.23
12	60.3	34.2	170	56.6	22.1	15.1	2.30	0.45	0.26
14	61.5	33.9	169					0.52	0.31
16	59.9	33.8	169	57.0	22.2	14.8	2.26	0.60	0.28
Post Test									
98	63.9	17.8	NA	65.5	25.9	16.0	31.4	0.50	0.18
100	63.9	17.2	NA	67.1	26.0	16.0	30.5	0.46	0.18

*Bicarbonate from alkalinity analysis. Alkalinity analyses were conducted with Hach titrimeter. Titrimeter cartridges supplied for the end of test were not reliable (leaked) and these samples were lost (marked NA). **Potassium increase from bromide tracer addition.

Table A.2. 4. The volatile fatty acid concentrations observed in pre- and post-test samples.

Sample no.	lactate (mg/L)	acetate (mg/L)	propionate (mg/L)	formate (mg/L)	butyrate (mg/L)	pyruvate (mg/L)	benzoate (mg/L)
	Pre Test						
2	<0.009	0.049	0.046	0.043	<0.014	<0.076	<0.010
16	<0.009	0.027	0.045	0.023	<0.014	<0.076	<0.010
	Post Test						
98	<0.009	<0.019	<0.1 BQL	<0.021	<0.014	<0.076	<0.010
100	<0.009	<0.019	<0.1 BQL	<0.021	<0.014	<0.076	<0.010

BQL is below quantitation limit; otherwise <value is detection limit

Table A.2. 5. The Fe(II), sulfide and DO concentrations in pre- and post-test samples.

	Laboratory Analyses			Field Analyses		
Sample No.	Fe^{2+}	Fe total	Fe^{3+}	Fe^{2+}	S^{2-}	DO
	Pre Test					
2	-	-	-	-	-	<0.05
10	0.65	0.73	0.08	0.64	<0.01	0.1
12	1.09	1.08	<0.01	-	-	-
12	1.14	1.15	0.01	-	-	-
14	1.09	1.16	0.07	-	-	-
16	1.15	1.2	0.05	-	-	-
17*	<0.01	0.04	0.04	-	-	-
	Post Test					
98	-	-	-	0.15	<0.01	-
100	-	-	-	0.03	0.02	-

'-' no analysis available

*collected from tracer bag

Appendix B. List of Scientific/Technical Publications

Refereed Journal Articles

1. Allen-King, R.M., et al., *A borehole test for chlorinated solvent diffusion and degradation rates in sedimentary rock.* Ground Water Monitoring and Remediation, In revision.

Technical Reports, including Peer Reviewed Theses and Data Releases

2. Brotsch, J., *Trichloroethylene (TCE) Sorption to Organic Matter in Sedimentary Rocks of the Newark Basin*. Geological Sciences. 2017, Buffalo, NY: Thesis (M.S.)--University at Buffalo, State University of New York.
3. Kiekhaefer, R., *Evaluation of a Field Method for Monitoring the Diffusion of Trichloroethene (TCE) and its Degradation Products in Fractured Sedimentary Rock*. Department of Geosciences. 2018: Thesis (M.S.)--University at Buffalo, State University of New York. 232.
4. Pugnetti, M., *Trichloroethene and Trichlorofluoroethene Equilibrium Competitive Sorption to Sedimentary Rock from the Newark Basin, New Jersey*. Geological Sciences. 2018, Buffalo, NY: Thesis (M.S.)--University at Buffalo, State University of New York.
5. Hsieh, P.A. and D.J. Goode, *A finite-difference algorithm used to simulate radial diffusion, sorption, and reactions of chlorinated ethenes in porous media*, U.S. Geological Survey Data Release, Editor. 2021.
6. Dugan, C.M., et al., *Volatile Organic Compound and Other Analyses Associated with Laboratory Microcosm Experiments to Determine Biodegradation Rates in Fractured Sedimentary Rock at the Former Naval Air Warfare Center in West Trenton, New Jersey, 2016–18*, U.S. Geological Survey data release, Editor. 2021.

Peer-reviewed conference presentations with published abstract

5. Goode, D., T. Imbrigiotta, P. Hsieh, R. Kiekhaefer, M. Masse, R. M. Allen-King. 2019. Prototype field method for diffusion and sorption coefficients and CVOC reaction rates in low-permeability strata. Presented at *2019 NGWA Conference on Fractured Rock and Groundwater*, Burlington, Vermont. September 23-23, 2019.
6. Hsieh, P.A., R.M. Allen-King, T.E. Imbrigiotta, and D.J. Goode, 2019. Simulation of borehole test to estimate in-situ CVOC diffusion, sorption, and reaction coefficients. Presented at *2019 NGWA Conference on Fractured Rock and Groundwater*, Burlington, Vermont. September 23-23, 2019.
7. Allen-King, R.M., M. Buzzeo, R.Dishman, and R. Kiekhaefer. 2019. Comparison of near replicate in-situ trichloroethene diffusion tests in fractured sedimentary rock matrix. Presented at *2019 NGWA Conference on Fractured Rock and Groundwater*, Burlington, Vermont. September 23-23, 2019.
8. Allen-King, R. M., M. Buzzeo, R. Dishman, and R. Kiekhaefer (2019), Development of a downhole trichloroethene diffusion test for fractured sedimentary rock matrix. Paper presented at *6th International Conference Novel Methods for Subsurface Characterization and Monitoring: From Theory to Practice, NovCare 2019,* May 28-31, 2019, Waterloo, Ontario, Canada.
9. Allen-King, R. M., R. L. Kiekhaefer, and J. Brotsch (2019), Field test analysis of trichloroethene abiotic and bio-degradation rates, sorption and diffusion coefficients for low permeability fractured rock. Paper presented at *International Symposium on Bioremediation and Sustainable Environmental Technologies*, April 15-19, 2019, Baltimore, Maryland.

10. Allen-King, R.M., R. L. Kiekhaefer, and R. Dishman. (2019), Field tests yield trichloroethene diffusion and sorption coefficients, & degradation rates for a fractured sedimentary rock aquifer. Paper presented at *Geological Society of America Annual Meeting*, Indianapolis, Indiana.
11. Allen-King, R. M., R. Dishman, and R. Kiekhaefer (2018), A method to determine trichloroethene diffusion and sorption coefficients in the matrix of fractured sedimentary rock. Paper presented at *Strategic Environmental Research and Development Program (SERDP) and Environmental Security Technology Certification Program (ESTCP) Symposium*, Washington, D.C.
12. Allen-King, R. M., R. L. Kiekhaefer, and J. Brotsch (2018), A field method to quantify chlorinated solvent diffusion, retardation and degradation coefficients in fractured sedimentary rock. Paper presented at *Conference on Remediation of Chlorinated and Recalcitrant Compounds*, Battelle, Palm Springs, California.
13. Goode, D. J., T. E. Imbrigiotta, P. A. Hsieh, R. L. Kiekhaefer, M. M. Masse, and R. M. Allen-King (2017), Development of a packer-based tracer-test method for characterization of processes controlling long-term fate of chlorinated volatile organic contaminants in low-permeability zones. Paper presented at *Strategic Environmental Research and Development Program (SERDP) and Environmental Security Technology Certification Program (ESTCP) Symposium*, Washington, D.C.
14. Imbrigiotta, T. E., P. A. Hsieh, D. J. Goode, R. M. Allen-King, and R. L. Kiekhaefer (2017), Modeling approach used in evaluating field measurements of diffusion and sorption coefficients and biotic and abiotic degradation rates in low-permeability rock strata at the former Naval Air Warfare Center, West Trenton, New Jersey. Paper presented at *Strategic Environmental Research and Development Program (SERDP) and Environmental Security Technology Certification Program (ESTCP) Symposium*, Washington, D.C.
15. Kiekhaefer, R. L., and R. M. Allen-King (2017), Field measurements to quantify the fate of trichloroethene (tce) and degradation products in fractured sedimentary rocks. Paper presented at *Strategic Environmental Research and Development Program (SERDP) and Environmental Security Technology Certification Program (ESTCP) Symposium*, Washington, D.C.
16. Allen-King, R.M., R. L. Kiekhaefer, J. Brotsch, and M. Pugnetti (2017), Field measurements to quantify trichloroethene diffusion, degradation, and sorption in fractured sedimentary rock. Paper presented at *Geological Society of America Annual Meeting*, Seattle, Washington.
17. Dishman, R., K. Kimmey, J. Brotsch, and R.M. Allen-King (2017), *Trichloroethylene adsorption in sediments from the New Jersey Naval Air Warfare Center.* Paper presented at Geological Society of America Annual Meeting, Geological Society of America, Seattle, Washington.
18. Cistaro, V. L., Kiekhaefer, R.L., and R.M. Allen-King (2017), Quantifying the relative reaction rates and pathways of trichlorofluoroethene degradation by pyrite in comparison to trichloroethene. Paper presented at *Geological Society of America Annual Meeting*, Seattle, WA.
19. Goode, D. J., T. E. Imbrigiotta, P. A. Hsieh, R. L. Kiekhaefer, M. M. Masse, and R. M. Allen-King (2017), In situ Characterization of Processes Controlling Long-Term Release of CVOCs from Low-Permeability Zones, paper presented at *NGWA Conference on Fractured Rock and Groundwater*, National Groundwater Association, Burlington, VT.
20. Imbrigiotta, T. E., P. A. Hsieh, D. J. Goode, R. M. Allen-King, and R. L. Kiekhaefer (2017), Field measurement of sorption coefficients and rates of diffusion, biodegradation, and abiotic degradation in the rock matrix, paper presented at *NGWA Conference on Fractured Rock and Groundwater*, National Groundwater Association, Burlington, VT.

Appendix C: Interim Review Questions

1. *Can microfractures within the isolated zone confound the test or data analysis, and if so, how will this possibility be addressed?*

Our conceptual model uses one value to represent all of the rock porosity, including fractures, if any, accessed by the field test; in other words, the conceptual model porosity is a *bulk* porosity. Similarly, we estimate one tortuosity factor to represent the indirect transport pathways through the bulk pore space taken by both contaminants and tracers. The actual pore space in the rock is heterogeneous and includes the space between grains and in fracture apertures. The fractures occur at an observable scale in core and potentially at scales much smaller than can be observed with the naked eye. The properties identified by the field method thus should be representative of other locations with similar rock porosity characteristics, including characteristics of the microfractures, if any.

We conduct field tests in borehole sections without observable fracturing and with low permeability. Core observations indicate competent lithologies suitable for testing. We use geophysical logs to ensure that the borehole diameter in the target interval is competent and of consistent diameter as part of standard test preparation (described in the report section entitled *Field Site Description* and shown in Figs. 4 and 5). Additionally, prior to starting a test, we conduct a pumping test on the prospective interval to insure very low permeability (described in the report section titled *Hydraulic test*). The pumping test insures that diffusion is the dominant transport mode within the matrix of the test interval; if "microfractures" (fractures not observed on the geophysical logs) are present, their connectivity does not allow significant advective flow.

2. *Is there a flux from the matrix, or a concentration within the matrix, that is needed to be able to use this test successfully?*

The minimum measurable mass flux will be site specific and depend on the borehole, analysis method, and tool configuration, in addition to the site-specific matrix transport properties and biodegradation rate in the borehole. Therefore, we cannot specify a particular minimum mass flux value that would be broadly applicable. However, it is possible to outline the conditions necessary for a successful test and suggest tool modifications that could be completed with additional experimentation in the future.

The borehole must have been previously drilled and exposed to the contaminant(s) over a period of years. It should have a monitoring history. At the NAWC, we selected our test boreholes from a longer list of candidate boreholes. Boreholes were rejected from the candidate list for the following reasons.

- The borehole must be of a "standard" design similar to the boreholes that we tested. We rejected at least one borehole because the diameter was wider at depth than nearer the surface, which would not allow deployment of our packer tool.
- In boreholes that had only depth integrated sampling for concentration history, we deployed diffusion samplers at the candidate testing depth(s). This was done in conjunction with standard monitoring sample collection. The regular monitoring samples are collected after high flow-rate pumping. We eliminated at least one borehole because the diffusion sampler results were very low compared to the regular monitoring sample. We determined that the competent borehole rock in this borehole was not exposed to the

contaminant (or exposed at a very low concentration) and that the monitoring concentration history characterized contaminant concentrations representative of the fractured zone at the upper part of the open borehole. Hence the monitoring data would not provide a good indication of the test interval concentration history. The unfractured portion of this borehole was deemed not adequate for testing.

In the borehole intervals tested, there was a record of the TCE concentration history that well represented the TCE exposure to the matrix of the test interval. In 71BR, there were packed off intervals that were monitored with lower flow (peristaltic pump) sampling.

The potential for successful flux measurements from a test can be evaluated by forward modeling using the simulation tool developed for this project (Hsieh and Goode 2021). Successful flux measurement depends on properties such as the contaminant concentration to which the borehole is exposed, the borehole diameter (volume to circumference), and the sampling and analytical methods to be used, in addition to matrix transport properties. Forward simulations would use the best available matrix property information to produce back diffusion simulations comparable to those shown for our tests. These forward models could be used to evaluate the potential for successful results from a test.

There are alternative approaches to some aspects of the test that could otherwise limit flux measurement. For example, lower analytical detection limits can accommodate lower fluxes. Lower detection limits for organic contaminants can be achieved with either increased sample size or use of an instrument with a more sensitive detector. However, trade-offs for test operation may be needed. Larger samples lead to more rapid dilution in the test interval, therefore limiting sampling volume and frequency. Alternative nonreactive tracers (e.g. deuterated water, for example) may be necessary to accommodate much slower diffusive uptake by the matrix than we observed. The borehole volume to circumference can be reduced by adding a solid object within the tracer zone. Such modifications were not necessary to attain a successful test at the NAWC and beyond the scope of this project.

3. Can mineral coatings (e.g., oxidized iron) or biological growth at the borehole/matrix interface impact the testing, and if so, how will this be addressed?

We treat the borehole water as if it is a well-mixed reactor. We characterize the biodegradation rate based on the observed concentrations in the bulk fluid although we know this is an oversimplification of the system. From our biodegradation microcosm experiments, we know that the attached organisms are more important than the planktonic organisms to TCE biodegradation. This is consistent with extensive literature on groundwater TCE biodegraders. However, a process-based model of the biodegradation, e.g. of a biofilm active layer at the matrix interface, is not necessary to extract reasonable transport parameters for the matrix and is beyond the scope of this project.

Another way to state our approach is that we neglect skin effects; effects caused by a thin layer with properties different than the matrix at the interface of the matrix. Although biofouling that can reduce permeability is well known, it is not the subject of this test that estimates diffusivity. It would seem unlikely that a thin layer, such as a biofilm, formed within a few years in a monitoring borehole would significantly lower diffusivity to bromide or another nonreactive tracer into the rock matrix.

If a borehole had developed a mineral coating with different composition than the matrix, conditions in which the coating promotes reactions in addition to those modelled are certainly possible. One would want to determine the significance of the coating driven reactions compared to the other processes affecting TCE during a test to evaluate whether the estimated parameters are significantly affected.

We share additional observations from our field site relevant to this question here. Neither the packer tool nor the microbial samplers had observable biofilm when the packer tool was removed to collect the microbial samplers. The sand in the microbial samplers often had observable black particulate or coating. Additionally, the packer tool fits the borehole dimensions relatively snugly even when uninflated. The packer tool may disturb surface films during the set-up process, if they are present.